Am J Transl Res 2015;7(11):2442-2461
www.ajtr.org /ISSN:1943-8141/AJTR0016309

Original Article

A SILAC-based proteomics elicits the molecular interactome of alisertib (MLN8237) in human erythroleukemia K562 cells

Li-Ping Shu[1,2], Zhi-Wei Zhou[2], Dan Zi[1,2], Zhi-Xu He[1], Shu-Feng Zhou[2]

[1]Guizhou Provincial Key Laboratory for Regenerative Medicine, Tissue Engineering and Stem Cell Research Center, Laboratory Animal Center, Department of Immunology, Guiyang Medical University, Guiyang, Guizhou 550004, People's Republic of China; [2]Department of Pharmaceutical Sciences, College of Pharmacy, University of South Florida, Tampa, FL 33612, USA

Received September 16, 2015; Accepted November 4, 2015; Epub November 15, 2015; Published November 30, 2015

Abstract: Alisertib (MLN8237, ALS), an Aurora kinase A (AURKA) inhibitor, exerts potent anti-tumor effects in the treatment of solid tumor and hematologic malignancies in preclinical and clinical studies. However, the fully spectrum of molecular targets of ALS and its anticancer effect in the treatment of chronic myeloid leukemia (CML) are not clear. This study aimed to examine the proteomic responses to ALS treatment and unveil the molecular interactome and possible mechanisms for its anticancer effect in K562 cells using stable-isotope labeling by amino acids in cell culture (SILAC) approach. The proteomic data identified that ALS treatment modulated the expression of 1541 protein molecules (570 up; 971 down). The pathway analysis showed that 299 signaling pathways and 459 cellular functional proteins directly responded to ALS treatment in K562 cells. These targeted molecules and signaling pathways were mainly involved in cell growth and proliferation, cell metabolism, and cell survival and death. Subsequently, the effects of ALS on cell cycle distribution, apoptosis, and autophagy were verified. The flow cytometric analysis showed that ALS significantly induced G_2/M phase arrest and the Western blotting assays showed that ALS induced apoptosis via mitochondria-dependent pathway and promoted autophagy with the involvement of PI3K/Akt/mTOR, p38 MAPK, and AMPK signaling pathways in K562 cells. Collectively, this study provides a clue to quantitatively evaluate the proteomic responses to ALS and assists in globally identifying the potential molecular targets and elucidating the underlying mechanisms of ALS for CML treatment, which may help develop new efficacious and safe therapies for CML treatment.

Keywords: Alisertib, human erythroleukemia cells, cell cycle, apoptosis, autophagy, SILAC

Introduction

Myeloproliferative neoplasms are a group of clonal hematopoietic malignancies that include chronic myeloid leukemia (CML), polycythemia vera, essential thrombocythemia, and primary myelofibrosis, with a characteristics of excessive proliferation of myeloid/erythroid lineage cells [1, 2]. CML accounts for 10-15% among those neoplasms [3, 4]. Almost all CML patients have a chromosomal abnormality known as the Philadelphia chromosome producing an abnormal protein called BCR-ABL that signals the bone marrow to keep generating abnormal white blood cells [3, 4]. Currently, CML therapies include surgery, chemotherapy, radiotherapy, immunotherapy, and target therapy [1]. Imatibnib, a tyrosine kinase inhibitor (TKI), is the first targeted drug approved by FDA in 2001 and has become the "Gold standard" treatment for CML, due to its activity to specifically inhibit BCR-ABL protein. Other targeted therapeutics also included dasatinib, nilotinib, bosutinib, and ponatinib. Although there is great advances been made in the treatment of CML, many patients still develops resistance to TKI (e.g. imatinib) treatment mainly due to the mutations in ABL kinase. The drug resistance substantially compromises the clinical therapeutic outcome in CML treatment. Therefore, it is imperative to develop more efficacious and safe drug for the treatment of CML.

Aurora kinase A (AURKA), a member of a family of serine-threonine kinases, regulates mitosis [5]. The role of AURKA in the pathogenesis of cancer has been attracted increasing attention and AURKA has been proposed to be a therapeutic target in cancer treatment [6, 7]. Currently, the AURKA inhibitor alisertib (MLN8237, ALS, **Figure 1A**) is being tested in various Phase I and Phase II clinical trials for advanced solid tumors and hematologic malignancies [8-13]. ALS selectively inhibits AURKA and has been shown in preclinical studies to induce cell cycle arrest, polyploidy, and mitotic catastrophe in various types of tumour cells and induce tumour regression [14-16]. Notably, it has been reported that aberrant activity and expression of AURKA has been implicated in the pathogenesis of leukemia and that AURKA may function as a target for leukemia targeted therapy [17-20]. In particular, it has been shown that ALS was active in resistant CML and significantly increased the efficacy of nilotinib [21]. However, the molecular interactome of ALS in CML treatment has not been investigated yet.

Due to the lack of comprehensive and global understanding on the proteomic responses to ALS in the treatment of CML, it is challengable to evaluate the anticancer effect of ALS and to explore the underlying mechanism for its cancer cell killing effect. It therefore needs a practical approach to unveil the full spectrum of molecular targets of ALS in CML treatment. Stable-isotope labeling by amino acids in cell culture (SILAC) is a practical and powerful approach to uncover the global proteomic responses to drug treatment and other interventions [22-24]. Particularly, it can be used to systemically and quantitatively evaluate and explore the target network of drugs, assess drug toxicity, and identify new biomarkers for the diagnosis and treatment of important diseases, including cancer [23-25]. In this regard, we evaluated the proteomic responses and validated the molecular targets of ALS in K562 cells using a combination of proteomic and functional approaches, with a focus on the effect of ALS on cell cycle progression, apoptosis, and autophagy.

Materials and methods

Chemicals and reagents

ALS and all cell culture required materials were purchased from Sigma-Aldrich (St. Louis, MO). FASP™ protein digestion kit was purchased from Protein Discovery Inc. (Knoxville, TN). Polyvinylidene difluoride (PVDF) membrane was purchased from Bio-Rad Inc. (Hercules, CA). The proteomic quantitation kit, ionic detergent compatibility reagent (IDCR), Pierce BCA protein assay kit, and Western blotting substrate were obtained from Thermo Scientific Inc. (Hudson, NH). The antibody against human β-actin was obtained from Santa Cruz Biotechnology Inc. (Santa Cruz, CA); and the other primary antibodies were purchased from Cell Signaling Technology Inc. (Beverly, MA).

Cell line and cell culture

The human erythroleukemia cell line K562 was obtained from the American Type Culture Collection (Manassas, VA) and cultured in DMEM/F12 medium supplemented with 10% heat-inactivated FBS. The cells were maintained at 37°C in a 5% CO_2/95% air humidified incubator. ALS was dissolved in DMSO and the final concentration of DMSO was at 0.05% (v/v).

For proteomic analysis, K562 cells were cultured in DMEM/F12 for SILAC with (heavy) or without (light) stable isotope labeled amino acids ($^{13}C_6$ L-lysine and $^{13}C_6$ $^{15}N_4$ L-arginine) and 10% dialyzed FBS. Cells were cultured in SILAC medium for six cell doubling times to achieve a high level (>98%) of labeled amino acid incorporation. Then, the cells were grown in "light" media were treated with 0.05% DMSO for 24 h to function as the negative control; cells grown in "heavy" media were treated with predetermined ALS for 24 h. All the experiments were performed three times independently.

Proteomic response to ALS treatment analyzed by SILAC-based approach

Digestion and desalting SILAC protein samples: Prior to the quantitative proteomic analysis, the protein samples were subject to digestion and desalting which were performed using SILAC-based approach as previously described [24-26]. The desalted samples were concentrated and resuspended in 0.1% formic acid prior to liquid chromatography-tandem mass spectrometry (LC-MS/MS) analysis.

LC-MS/MS and statistical analysis: The concentrated samples (5 μL) were subject to the hybrid linear ion trap-Orbitrap (LTQ Orbitrap XL, Thermo Scientific Inc., Hudson, NH) as previ-

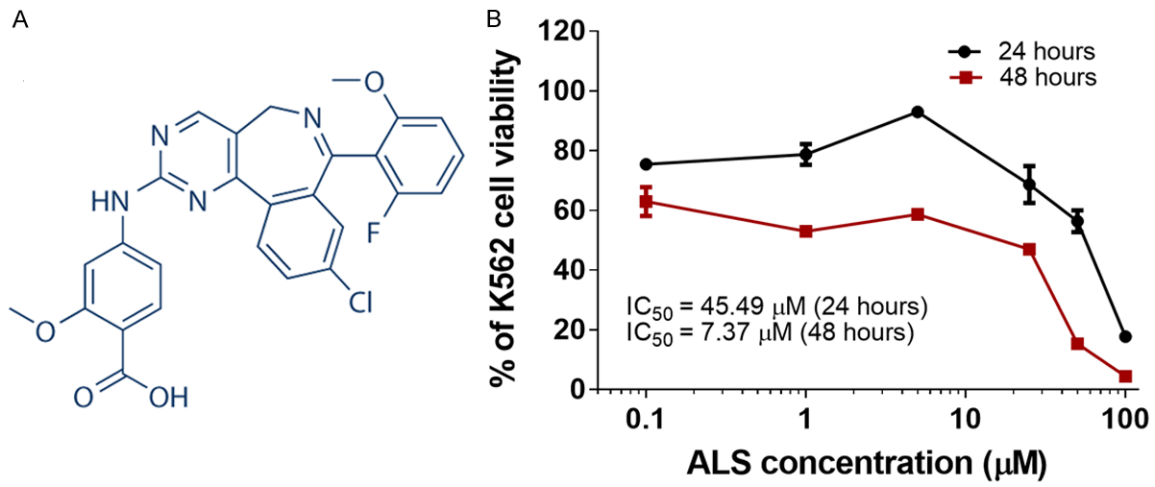

Figure 1. Chemical structure of ALS and the cytotoxic effect of ALS towards to K562 cells. K562 cells were treated with ALS at concentrations ranging from 0.1 to 100 μM for 24 and 48 h and the cell viability was determined using MTT assay. (A) Chemical structure of ALS and (B). The effect of ALS on viability of K562 cells.

ously described [24-26]. Peptide SILAC ratio was calculated using MaxQuant version 1.2.0.13. The SILAC ratio was determined by averaging all peptide SILAC ratios from peptides identified of the same protein.

Pathway and network analysis: The protein IDs were identified using Scaffold 4.3.2 from Proteome Software Inc. (Portland, OR) and the pathway and network were analyzed using Ingenuity Pathway Analysis (IPA) from QIAGEN (www.ingenuity.com, Redwood City, CA). The Database for Annotation, Visualization and Integrated Discovery (DAVID, http://david.abcc.ncifcrf.gov/) was also used to provide biological functional interpretation of the potential targets of ALS derived proteomics [27].

Cell cycle distribution analysis using flow cytometry

The effect of ALS treatment on cell cycle distribution was determined by flow cytometry as previously described [28]. A total number of 1×10^4 cells was subject to cell cycle analysis using a flow cytometer (BD LSR II Analyzer, Becton Dickinson Immunocytometry Systems, San Jose, CA, USA).

Cellular apoptosis and autophagy analysis using flow cytometry

The effect of ALS on apoptosis and autophagy of K562 cells was quantitated using PE Anexin V Apotosis Detction Kit and ENZO Cyto-ID® Autophagy Kit, respectively [28]. The apoptotic and autophagic cells were analyzed using flow cytometry.

Western blotting analysis

The cell lysate was subject to Western blotting assay. Visualization was performed using an enhanced chemiluminescence kit and the blots were analyzed using Image Lab 3.0 (Bio-Rad).

Statistical analysis

The data are presented as the mean ± standard deviation (SD). Comparisons of multiple groups were evaluated by one-way analysis of variance followed by Tukey's multiple comparison procedure. $P<0.05$ was considered to be statistically significant. Assays were performed at least three times independently.

Results

ALS inhibits proliferation and AURKA phosphorylation of K562 cells

We first tested the effect of ALS on the viability of K562 cells using MTT assay. The results showed that ALS markedly inhibited the proliferation of K562 cells (**Figure 1B**). The percentage of viability was 75.4%, 78.7%, 92.9%, 68.6%, 56.4%, and 17.7% for 24 h treatment and 63.0%, 52.9%, 58.7%, 46.9%, 15.4%, and 4.5% for 48 h treatment, when cells were treated with ALS at 0.1, 1, 5, 25, 50, and 100 μM,

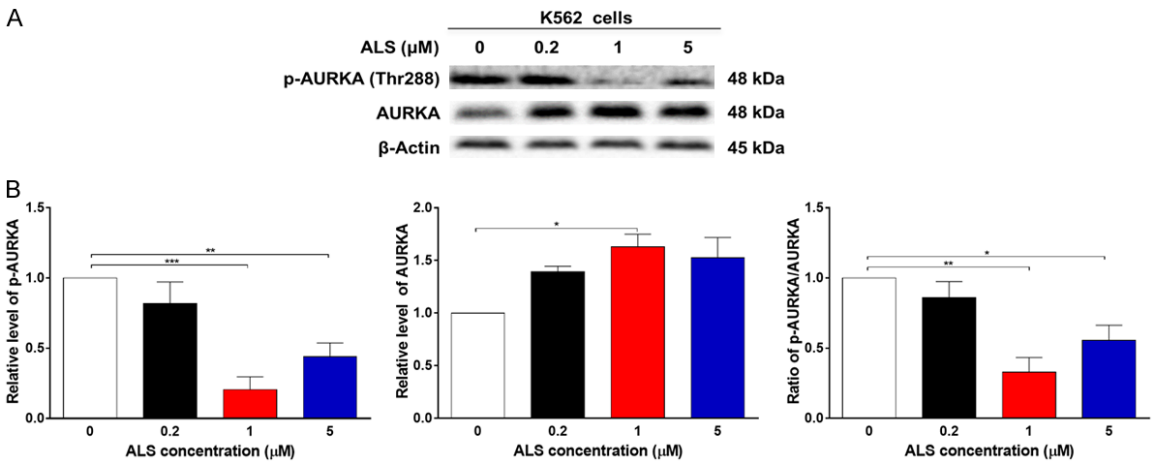

Figure 2. ALS inhibits the phosphorylation of AURKA in K562 cells. K562 cells were treated with ALS at 0.2, 1, and 5 μM for 24 h and the phosphorylation level of AURKA was determined by Western blotting assay. A. Representative blots of p-AURKA, AURKA, and β-actin. B. Relative level of p-AURKA, AURKA, and ratio of p-AURKA/AURKA. β-actin functions as the internal control. Data are expressed as mean ± SD of three independent experiments. **P*<0.05; ***P*<0.01; and ****P*<0.001 by one-way ANOVA.

respectively. The IC_{50} values were 45.49 μM and 7.37 μM for 24 and 48 h incubation, respectively (**Figure 1B**). Taken together, these data suggest that ALS inhibits the growth of K562 cells.

Moreover, the effect of ALS on the phosphorylation of AURKA was determined using Westering botting assay. As shown in **Figure 1A** and **1B**, ALS markedly inhibited the phosphorylation of AURKA at Thr288. Compared to the control, there was a 18.0%, 79.3%, and 55.9% reduction in the level of p-AURKA, whereas there was a 1.4-, 1.6-, and 1.5-fold increase in the level of AURKA when treated with ALS at 0.2, 1, and 5 μM for 24 h, respectively. Consequently, there was a remarkable decrease in the ratio of p-AURKA/AURKA, with a 13.8%, 67.2%, and 44.3% decrease (**Figure 2A** and **2B**). Taken together, ALS inflicts a substantial impact on cellular processes of K562 cells. Following the test of effect of ALS on cell viability and phosphorylation of AURKA, we performed quantitative proteomics to evaluate the proteomic responses to ALS in K562 cells.

Overview of proteomic responses to ALS treatment in K562 cells

To determine the proteomic responses to ALS in K562 cells, we conducted SILAC-based proteomics. There were 1,541 protein molecules which were identified as the potential molecular targets, of which 570 proteins' expression level were increased and 971 proteins' level were decreased (Table S1). Subsequently, these identified proteins were subject to IPA pathway analysis, showing that 299 signaling pathways and 459 cellular functional proteins directly responded to ALS treatment in K562 cells (Tables S2 and S3). These functional proteins were involved in a number of important cellular processes, such as cellular growth and proliferation, protein synthesis, RNA post-transcription modification, cell death and survival, and post-translational modification. The IPA analysis showed that the top five targeted signaling pathways were EIF2 signaling pathway, eIF4 and p70S6K signaling pathway, protein ubiquitination pathway, mTOR signaling pathway, and mitochondrial dysfunction signaling pathway (Table S2) and the top five proteins with increased expression level were DCTN2, NAP1L1, RPLP0, RPL15, and SNW1 (Table S3). In aggregate, ALS modulates various critical singling pathways and molecular proteins in K542 cells, which, eventually, lead to cell proliferation inhibition and cancer cell death.

ALS modulates networked signaling pathways in K562 cells: Further data mining using IPA and KEGG pathway analysis was carried out to determine whether identified proteins could be mapped to a specific functional network (Table S4). The network analysis from KEGG pathway analysis (Figure S1) and IPA (Figure S2) indicated the key functional proteins and signaling

pathways that were involved in cellular growth and proliferation, protein synthesis, and cell survival and death. In Figure S1, the summarized pathways in cancer, including CML, showed the participation of PI3K/Akt, p53, and MAPK signaling pathways in the regulation of cell proliferation and cell death. In Figure S2, the networked signaling pathways revealed a crosstalk among EIF2 signaling pathway, eIF4 and p70S6K signaling pathway, protein ubiquitination pathway, mTOR signaling pathway, and mitochondrial dysfunction, etc. (Figures S3, S4, S5, S6, and S7). These functional proteins and signaling pathways are important in cell cycle regulation, cell survival, cell migration, cell metabolism, and cell autophagy.

ALS regulates cell cycle progression: The proteomic data showed that ALS treatment led to a marked response in cell cycle with the involvement of signaling pathways in G_2/M DNA damage checkpoint regulation and cyclins and cell cycle regulation (Table S2). The functional proteins involved in G_2/M DNA damage checkpoint regulation included YWHAQ, YWHAG, and CDK1; and the functional protein involved in cyclins and cell cycle regulation included PPP2CB, HDAC1, and CDK1. It suggests that ALS possesses a regulatory effect on cell cycle progression in K562 cells.

ALS regulates EIF2 signaling pathways and ribosome network in K562 cells: ALS also induced a marked response with regard to the protein synthesis, which is a complex process that requires cooperation among a large number of polypeptides including ribosomal proteins, modification of enzymes, and ribosome-associated translation factors. ALS showed a potent effect on EIF2 signaling pathway (Figure S3) and ribosome network (Figure S4). The molecules involved in EIF2 signaling pathway included RPL27A, EIF2B4, MAPK1, RPS8, EIF4G1, EIF4E, EIF2A, RPL7, RPL7A, EIF3B, RPS20, RPS13, EIF3D, RPL23A, RPL31, RPL13, RPS24, RPL32, PABPC1, RPL4, RPS2, RPL17, RPL29, RPS10, EIF3J, RPS21, RPL9, RPLP0, RPS6, RPL15, EIF3F, RPS16, RPL28, EIF3L, RPL13A, and RPS14; and the molecules involved in ribosome network included 60S ribosomal subunit, AP-3, CALB1, CNBP, DDOST, DPP3, Fascin, GSR, IGF2BP1, IGF2BP2, LUC7L3, LYAR, NAT10, NF-κB (complex), OTUB1, PHF6, PUF60, RPL4, RPL7, RPL9, RPL13, RPL15, RPL17, RPL28, RPL29, RPL31, RPL32, RPL13A, RPL23A, RPL27A, RPL7A, SRSF11, TROVE2, UBE2, and ZC3H18.

ALS regulates cell death singals: As showed in Figure S1, ALS has been predicted to affect cell death by KEGG pathway analysis in K562 cells. The IPA results further showed that treatment of K562 cells regulated apoptosis signaling pathway (Table S2) and led to mitochondrial dysfunction (Figure S5). MAPK1, LMNA, and CDK1 responded to ALS treatment in apoptosis signaling pathway. ALS-induced mitochondrial dysfunction was one of the top signaling pathways responding to ALS treatment in K562 cells (Table S2 and Figure S5). The molecular proteins included ATP5J, NDUFV1, COX17, PRDX5, ATP5A1, ACO2, VDAC3, CYB5R3, UQCRB, NDUFB10, VDAC2, GSR, NDUFB9, NDUFS8 NDUFV2, ATP5B, COX7A2, NDUFA10, OGDH, and VDAC1. The data suggest that ALS may induce apoptosis of K562 through mitochondria-mediated pathway.

ALS regulates PI3K/Akt/mTOR, ERK/MAPK, and AMPK signaling pathways: Additionally, the proteomics and IPA data showed that there were marked alteration in signal transduction in response to ALS treatment in K562 cells. As shown in Table S2 and Figure S6, treatment of K562 cells with ALS resulted in a remarkable change in PI3K/Akt/mTOR, MAPK, and AMPK signaling pathways. The protein molecules included YWHAQ, PPP2CB, YWHAG, HSP90AA1, MAPK1, RPS2, RPS10, EIF3J, RPS8, FKBP1A, RPS21, EIF4G1, EIF4E, RPS6, PPP2CB, EIF3F, RPS16, EIF3B, RPS20, RPS13, EIF3D, EIF3L, RPS24, RPS14, and EIF4B in PI3K/Akt/mTOR signaling pathway (Table S2). The proteins included RAP1B, YWHAQ, PPP2CB, YWHAG, MAPK1, TLN1, EIF4E, and KSR1 which were involved in ERK/MAPK signaling pathway (Table S2). PPP2CB, SLC2A1, MAPK1, and PFKP were involved in AMPK signaling pathway (Table S2). Moreover, the IPA also showed that ALS regulated PTEN and eIF4 and p70S6K signaling pathways in K562 cells (Table S2 and Figure S7), which were closely orchestrated with PI3K/Akt/mTOR signaling pathway. The proteins included MAPK1, CDC42, and CSNK2B in PTEN signaling pathway (Table S2) and PABPC1, EIF2B4, MAPK1, RPS2, RPS10, EIF3J, RPS8, RPS21, EIF4G1, EIF4E, EIF2A, RPS6, PPP2CB, EIF3F, RPS16, EIF3B, RPS20, RPS13, EIF3D, EIF3L, RPS14, and RPS24 in eIF4 and p70S6K signaling pathway (Figure S7).

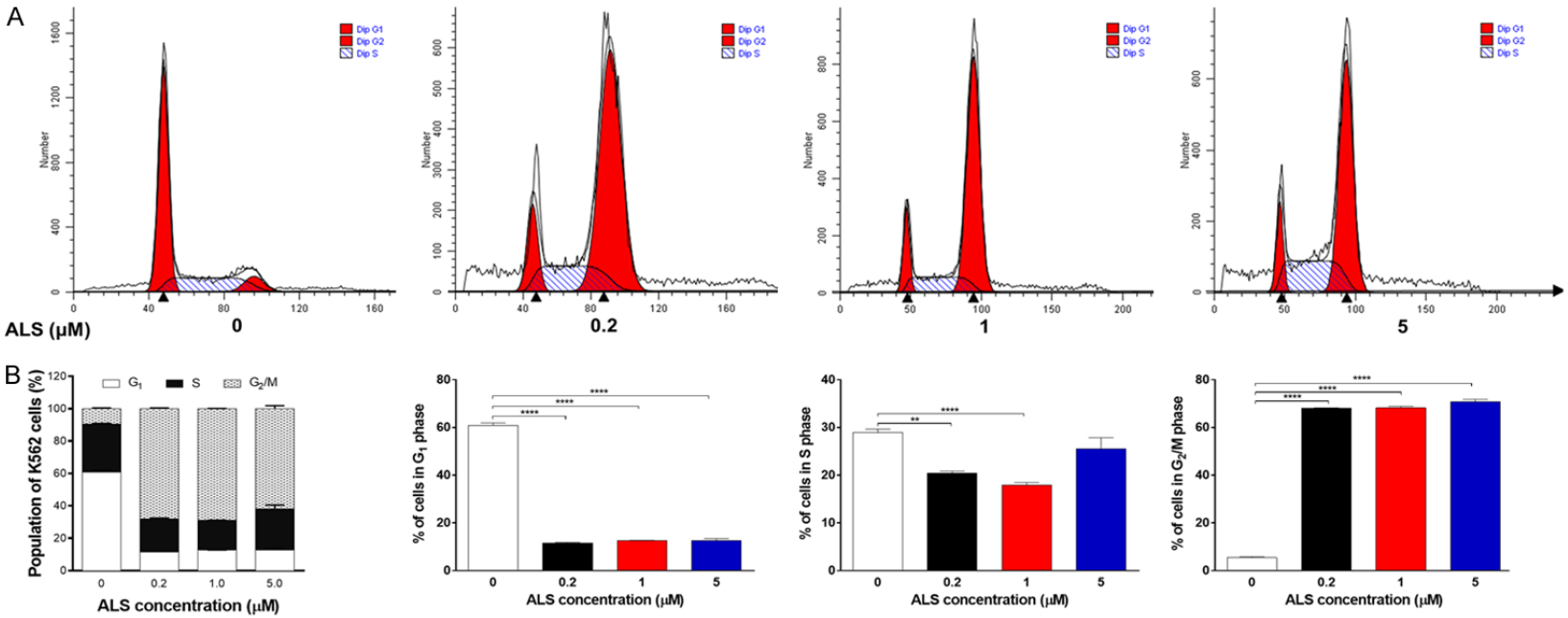

Figure 3. ALS induces cell cycle arrest at G_2/M phase in K562 cells. K562 cells were treated with ALS at 0.2, 1, and 5 μM for 24 h and the cell samples were subject to flow cytometry. (A) Representative plots of cell cycle distribution of K562 cells and (B). The population of K562 cells at G_1, S, and G_2/M phases. Data are expression as mean ± SD of three independent experiments. $^{**}P<0.01$; and $^{****}P<0.0001$ by one-way ANOVA.

Taken together, the data showed that ALS may exert its anticancer effect via the regulation of the multiple functions proteins and signaling pathways in K562 cells. Subsequentially, we verified the effect of ALS on cell cycle distribution and programmed cell death and explored the potential mechanisms in K562 cells.

Verification of reguatory effects and molecular targets of ALS in K562 cells

Our above quantitative proteomic studies have shown that ALS modulated a number of functional proteins and related signaling pathways in cell proliferation, cell invasion and migration, and cell survival and death. In order to verify these effects, we tested how ALS affected the cell cycle distribution, apoptosis, and autophagy in K562 cells.

ALS induces cell cycle arrest in G_2/M phase in K562 cells: First, the cell cycle distribution was determined in K562 cells using flow cytometry. As shown in **Figure 3A** and **3B**, there was a marked alteration in the cell population in cell cycle distribution. Compared to the control cells (9.6%), the percentage of cell population in G_2/M phase was 68.0%, 69.0% and 61.9% when cells were treated with ALS at 0.2, 1, and 5 μM for 24 h, with a 7.1-, 7.2-, and 6.4-fold rise in the number of cells arrested in G_2/M phase, respectively (P<0.0001; **Figure 3B**). In contrast, there was a remarkable decrease in the number of cells in G_1 and S phases in K562 cells when treated with ALS at 0.2, 1, and 5 μM for 24 h (P<0.01 or 0.0001; **Figure 3B**). Taken together, the results show that ALS can regulate the cell cycle distribution, contributing to its anticancer effect in K562 cells. Moreover, the inducing effect of ALS on cell cycle arrest further verifies the regulatory activities of ALS on cell proliferation determined by proteomics.

ALS regulates cell cycle regulators of K562 cells: Following the observations on the cell cycle arrest, we examined the effect of ALS on the expression of several key cell cycle regulators in K562 cells. As shown in **Figure 4A** and **4B**, ALS treatment exhibited a marked regulating effect on the expression of PLK-1, CDK1/CDC2, cyclin B1, p21 Waf1/Cip1, p27 Kip1, and p53. There was a marked decrease in the level of PLK-1, CDK1/CDC2, and cyclin B1 that are the positive regulators of cell cycle progression, whereas there was a remarkable increase in the level of p21 Waf1/Cip1 and p27 Kip1 that exhibit inhibitory effect on cell cycle progression (**Figure 4A** and **4B**). Compared to the control cells, 5 μM ALS decreased 23.9% in the level of PLK-1 in K562 cells (P<0.01; **Figure 4A** and **4B**). Treatment of K562 cells with ALS concentration-dependently reduced the expression level of CDK1/CDC2 and cyclin B1 (**Figure 4A** and **4B**). There was a 24.8% and 28.9% reduction in the level of CDK1/CDC2 and 21.1% and 43.8% decline in the level of cyclin B1 when K562 cells were treated with ALS at 1 and 5 μM for 24 h, respectively (P<0.01, 0.001 or 0.0001; **Figure 4A** and **4B**). On the other hand, treatment of K562 cells with 1 μM ALS led to a 1.5-fold increase in the level of p21 Waf1/Cip1, compared to the control cells (P<0.05; **Figure 4A** and **4B**). Moreover, there was a 1.3-, 1.3-, and 1.4-fold elevation in the level of p27 Kip1 when treated with ALS at 0.2, 1, and 5 μM for 24 h, respectively (P<0.05; **Figure 4A** and **4B**). ALS treatment did not significantly altered the expression of p53 in K562 cells. Taken together, the results suggest that the cell cycle arresting effect of ALS may be attributed to the regulating effect on the key cell cycle modulators in K562 cells, which also further verifies the proteomic data showing the effect of ALS on cell proliferation and cell cycle distribution.

ALS promotes the expression of DCTN2, NAP1L1, RPLP0, and RPL15 in K562 cells

As shown in the proteomic data, treatment of K562 cells with ALS dramatically altered the expression of DCTN2, NAP1L1, RPLP0, and RPL15. DCTN2 modulates cytoplasmic dynein binding to an organelle, plays a role in prometaphase chromosome alignment and spindle organization during mitosis, and is involved in anchoring microtubules to centrosomes [29]. NAP1L1 participates in DNA replication and may play a role in modulating chromatin formation and contribute to the regulation of cell proliferation [30, 31]. RPLP0 and RPL15 are ribosomal proteins involved in protein synthesis [32, 33]. The results showed a promoting effect of ALS on the expression of DCTN2, NAP1L1, RPLP0, and RPL15 in K562 cells (**Figure 5A** and **5B**). Compared to the control cells, there was a 1.7-fold increase in the level of DCTN2 when K562 cells were treated with 1 μM ALS for 24 h (P<0.01; **Figure 5A** and **5B**). There was a concentration-dependent elevation in the

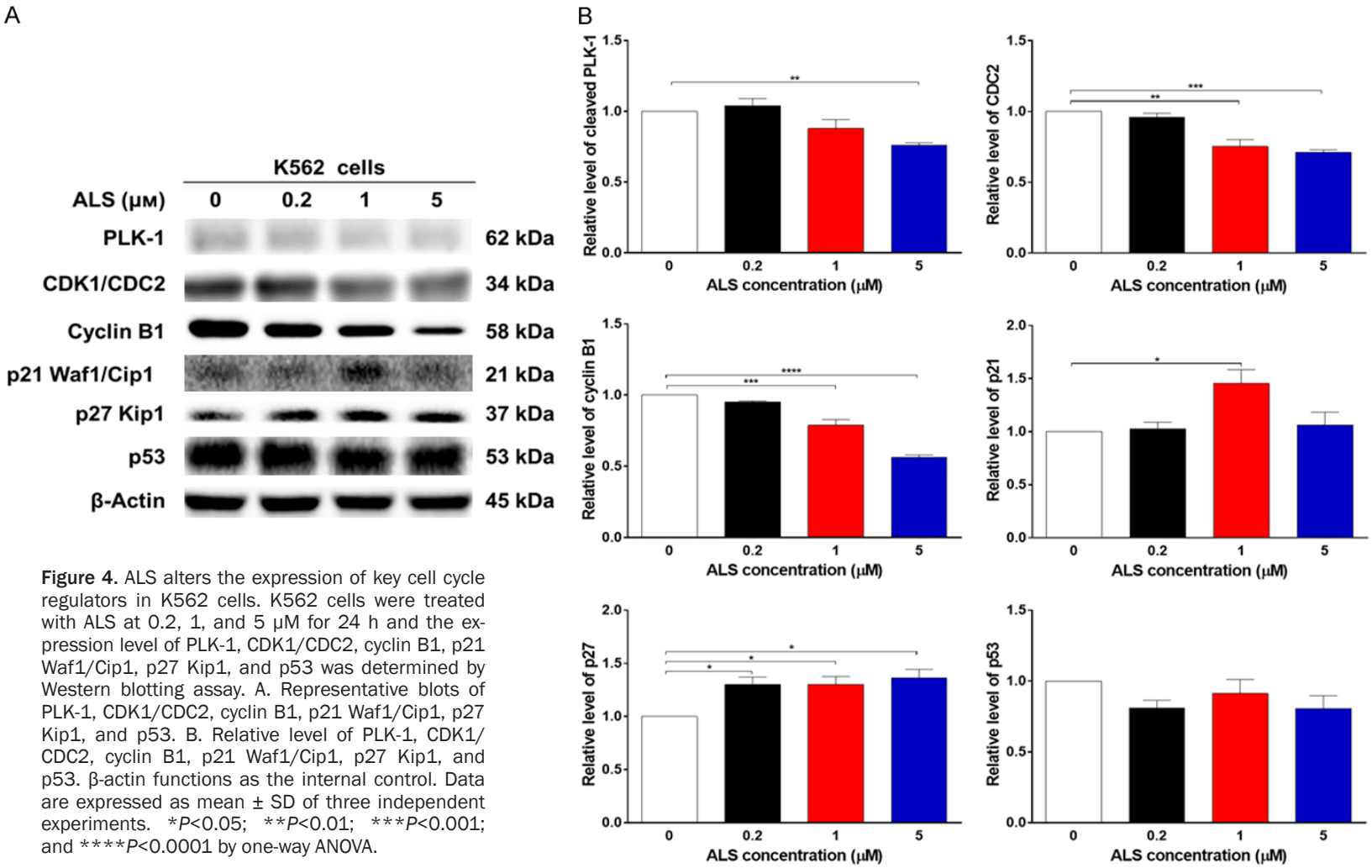

Figure 4. ALS alters the expression of key cell cycle regulators in K562 cells. K562 cells were treated with ALS at 0.2, 1, and 5 μM for 24 h and the expression level of PLK-1, CDK1/CDC2, cyclin B1, p21 Waf1/Cip1, p27 Kip1, and p53 was determined by Western blotting assay. A. Representative blots of PLK-1, CDK1/CDC2, cyclin B1, p21 Waf1/Cip1, p27 Kip1, and p53. B. Relative level of PLK-1, CDK1/CDC2, cyclin B1, p21 Waf1/Cip1, p27 Kip1, and p53. β-actin functions as the internal control. Data are expressed as mean ± SD of three independent experiments. **P*<0.05; ***P*<0.01; ****P*<0.001; and *****P*<0.0001 by one-way ANOVA.

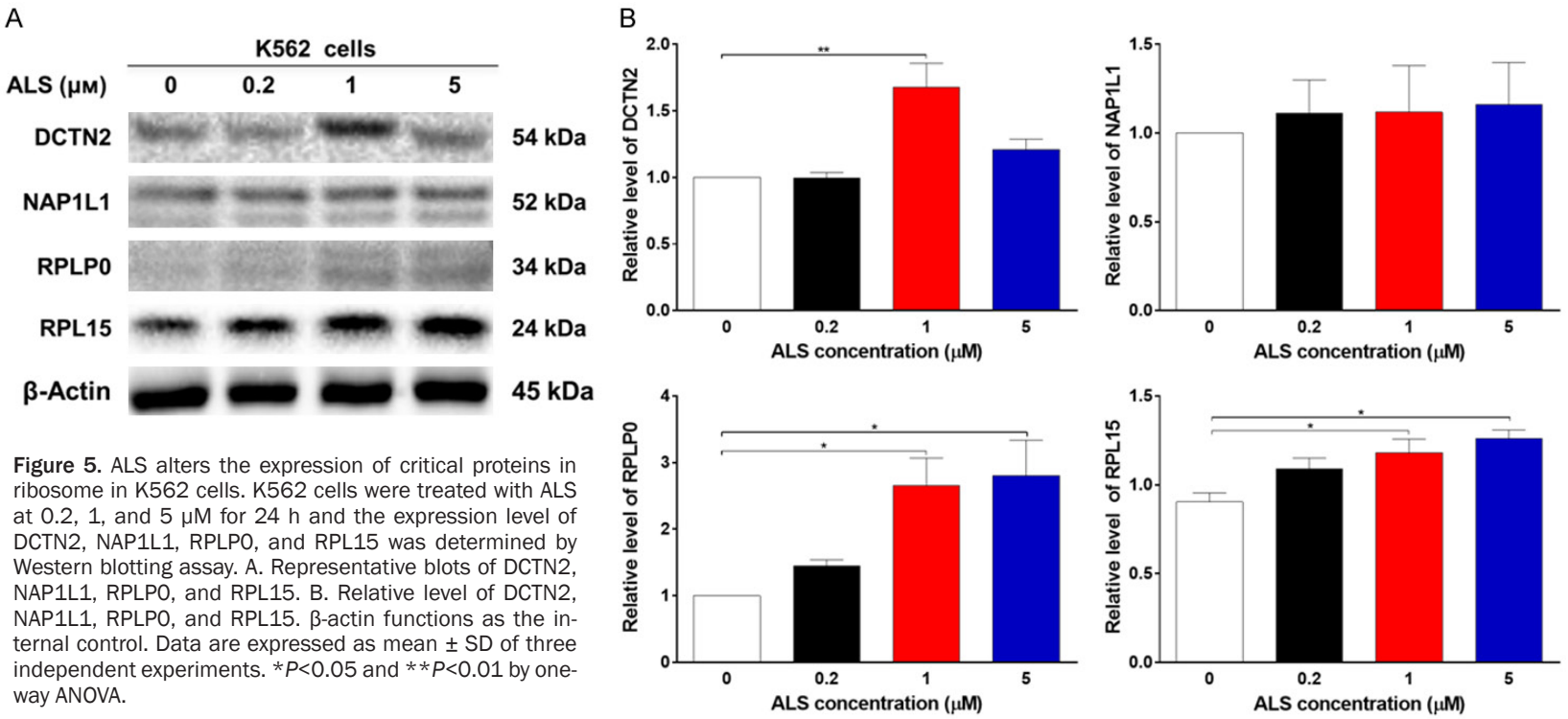

Figure 5. ALS alters the expression of critical proteins in ribosome in K562 cells. K562 cells were treated with ALS at 0.2, 1, and 5 μM for 24 h and the expression level of DCTN2, NAP1L1, RPLP0, and RPL15 was determined by Western blotting assay. A. Representative blots of DCTN2, NAP1L1, RPLP0, and RPL15. B. Relative level of DCTN2, NAP1L1, RPLP0, and RPL15. β-actin functions as the internal control. Data are expressed as mean ± SD of three independent experiments. **P*<0.05 and ***P*<0.01 by one-way ANOVA.

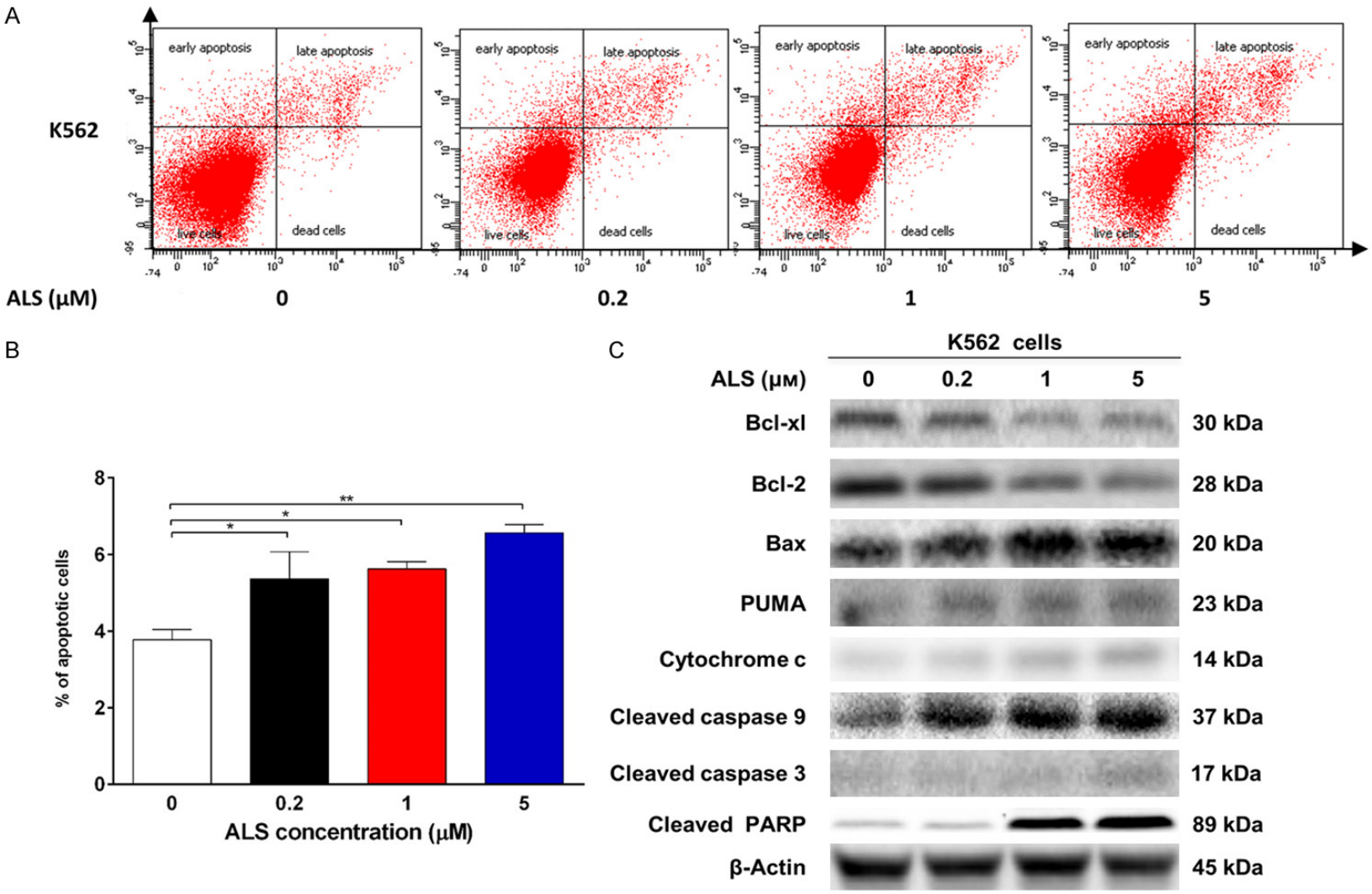

Figure 6. ALS induces apoptosis of K562 cells. K562 cells were treated with ALS at 0.2, 1, and 5 μM for 24 h and the cell samples were subject to flow cytometry and the cell lysates were subject to Western blotting assay. (A) Representative flow cytometric plots of apoptotic K562 cells; (B) Bar graphs showing the percentage of apoptosis of K562 cells and (C). Representative blots of Bcl-xl, Bcl-2, Bax, PUMA, cytochrome c, cleaved caspase 9, cleaved caspase 3, and cleaved PARP. Data are expression as mean ± SD of three independent experiments. **P*<0.05 and ***P*<0.01 by one-way ANOVA.

level of two ribosomal proteins, RPLP0 and RPL15 in K562 cells (**Figure 5A** and **5B**). In comparison to the control cells, there was a 2.7- and 2.8-fold increase in the level of RPLP0 and 1.2- and 1.3-fold rise in the level of RPL15 when cells were treated with ALS at 1 and 5 μM, respectively ($P<0.05$; **Figure 5A** and **5B**). Although there was no significant increase in the level of NAP1L1, there was a 1.1-, 1.1-, and 1.2-fold increase in the level of NAP1L1 when treated with ALS at 0.2, 1, and 5 μM, respectively ($P>0.05$; **Figure 5A** and **5B**). Taken together, the results show that ALS exerts a potent effect on protein synthesis and cell proliferation, which may contribute to the cell cycle arresting and cancer cell killing effect in K562 cells.

ALS induces apoptosis of K562 cells: We further validated apoptosis-inducing effect in K562 cells using flow cytometry and Western blotting assay. As shown in **Figure 6A** and **6B**, ALS induced apoptosis of K562 cells in a concentration-dependent manner. In comparison to the control cells, there was a 1.4-, 1.5-, and 1.7-fold increase in apoptotic K562 cells when treated with ALS at 0.2, 1, and 5 μM, respectively (**Figure 6A** and **6B**). Furthermore, the expression of pro-apoptotic and anti-apoptotic proteins were examined. As shown in **Figure 6C** and Figure S8, treatment of K562 cells markedly increased the level of Bax, while decreasing the level of Bcl-xl and Bcl-2. In comparison to the control cells, there was a 2.1- and 2.3-fold elevation in the level of Bax when treated with 1 and 5 μM ALS, respectively ($P<0.01$; **Figure 6C** and Figure S8); whereas there was a 30.6% and 55.3% reduction in the level of Bcl-2 and 45.6% and 25.6% decline in Bcl-xl when treated with ALS at 1 and 5 μM, respectively ($P<0.05$ or 0.01; **Figure 6C** and Figure S8). The concentration-dependent increase in the level of Bax and the decrease in the level of Bcl-2 consequently resulted in a remarkable increase in the ratio of Bax/Bcl-2, which impaired the mitochondrial function in K562 cells. Indeed, treatment of K562 cells induced an impairment in mitochondrial membrane potential, evident from the release of cytochrome c (**Figure 6C**). There was a 1.9-fold increase the level of cytosolic cytochrome c compared to the control cells, when treated with 5 μM ALS ($P<0.05$; Figure S8). Increased level of cytosolic cytochrome c triggers the activation of caspase cascade. Compared to the control cells, treatment of ALS at 0.2, 1, and 5 μM resulted in a 1.8-, 1.9-, and 1.9-fold rise in the level of cleaved caspase 9 ($P<0.0001$; Figure S8). Also, incubation of 5 μM ALS led to a 1.6-fold increase in the level of caspase 3 ($P<0.01$; Figure S8). Furthermore, there was a 2.4- and 2.5-fold increase in the level of cleaved PARP ($P<0.01$; Figure S8). Additionally, ALS also up-regulated the negative regulator of Bcl-2 family, PUMA, in K562 cells. Treatment of cells with ALS at 0.2, 1, and 5 μM resulted in 1.6-, 1.6-, and 1.6-fold increase in the level of PUMA compared to the control cells, respectively ($P<0.05$; Figure S8). Taken together, the results indicate that ALS exhibits a pro-apoptotic effect in K562 cells.

ALS induces autophagy of K562 cells: Following the findings on the apoptosis-inducing effect of ALS in K562 cells, the effect of ALS on autophagy of K562 cells was also examined. As shown in **Figure 7A**, exposure of K562 cells to ALS concentration-dependently increased the autophagy of K562 cells. There was a 1.2-, 1.6-, and 2.2-fold elevation in the autophagic level of K562 cells when treated with ALS at 0.2, 1, and 5 μM, respectively (**Figure 7B**). Furthermore, the effect of ALS on the autophagy-related signaling pathways was examined (**Figure 7C**, Figures S9 and S10).

We further examined the phosphorylation level of PI3K at Tyr458, AMPK at Thr172, and p38 MAPK at Thr180/Tyr182, which are upstream regulators of Akt/mTOR pathway with important role in the regulation of cell proliferation and death [34, 35]. ALS significantly inhibited the phosphorylation of PI3K at Tyr458 in K562 cells compared to the control cells (**Figure 7C**). Exposure of K562 cells to 5 μM ALS for 24 h decreased the phosphorylation level of PI3K at Tyr458 53.3% ($P<0.05$; Figure S9). However, incubation of K562 cells with ALS did not significantly affect the expression of total PI3K ($P>0.05$; Figure S9). The ratio of p-PI3K/PI3K was concentration-dependently decreased by ALS in K562 cells. Compared to the control cells, the p-PI3K/PI3K ratio was decreased 60.5%, when treated with 5 μM ALS ($P<0.05$; Figure S9).

AMPK plays a crucial role in the regulation of energy homeostasis, cell survival, and cell death [36]. In the present study, ALS exhibited a promoting effect on the phosphorylation of AMPK at Thr172 in K562 cells (**Figure 7C** and

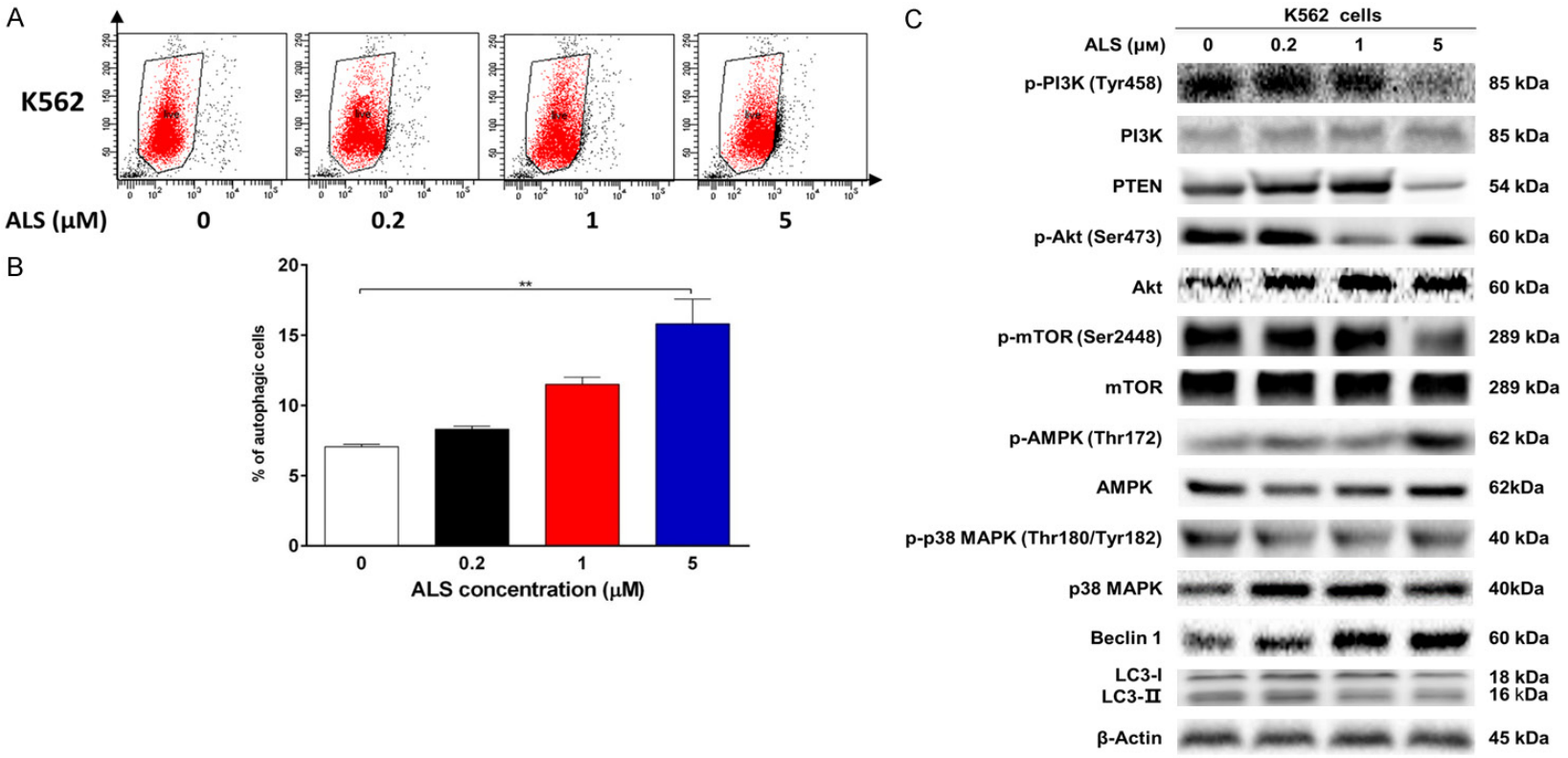

Figure 7. ALS induces autophagy of K562 cells. K562 cells were treated with ALS at 0.2, 1, and 5 μM for 24 h and the cell samples were subject to flow cytometry. (A) Representative flow cytometric plots of autophagic K562 cells and (B). Bar graphs showing the percentage of autophagy of K562 cells. (C) Representative blots of phosphorylated PI3K, Akt, mTOR, AMPK, and p38 MAPK, and the expression of PI3K, PTEN, Akt, mTOR, AMPK, p38 MAPK, beclin 1, LC3-I, and LC3-II. Data are expression as mean ± SD of three independent experiments. $^{**}P<0.01$ by one-way ANOVA.

Figure S10). In comparison to the control cells, there was a 2.7-fold increase in the phosphorylation level of AMPK at Thr172 in K562 cells when treated with 5 μM ALS for 24 h (P<0.01; Figure S10). However, there was no significant change in the expression of total AMPK compared to the control cells. Of note, with increasing concentration of ALS, an increased ratio of p-AMPK/AMPK was observed in K562 cells. Compared to the control cells, the p-AMPK/AMPK ratio was increased 1.9- and 2.2-fold when treated with ALS at 0.2 and 5 μM, respectively (P<0.05 or 0.01; Figure S10).

p38 MAPK exerts a dual role in the regulation of cell death, and it can either promote cell survival or cell death depending not only on the type of stimulus but also in a cell type specific manner [37]. In contrast to the promoting effect on AMPK phosphorylation, we observed an inhibitory effect of ALS on the activation of p38 MAPK at Thr180/Tyr182 in K562 cells (**Figure 7** and Figure S10). In comparison to the control cells, there was a 30.3%, 23.9%, and 7.5% reduction in the phosphorylation of p38 MAPK at Thr180/Tyr182 in K562 cells when treated with0.2, 1, and 5 μM of ALS for 24 h, respectively (Figure S10). Exposure of K562 cells to ALS increased the expression level of total p38 MAPK (P>0.05; Figure S10). Notably, a decreased ratio of p-p38 MAPK/p38 MAPK was observed in both cell lines with increasing concentration of ALS. In comparison to the control cells, the ratio of p-p38 MAPK/p38 MAPK was decreased 33.8%, 37.6%, and 21.8% when K562 cells were treated with ALS at 0.2, 1, and 5 μM, respectively (Figure S10). These findings demonstrate that ALS inhibited the phosphorylation of PI3K Tyr458 and p38 MAPK Thr180/Tyr182 but enhanced the phosphorylation of AMPK Thr172 in K562 cells, contributing to the increase in autophagy flux.

We also examined the regulatory effect of ALS on the phosphorylation of Akt at Ser473 and mTOR at Ser2448 and the expression of PTEN in K562 cells (Figure S10). In comparison to the control cells, the phosphorylation level of Akt at Ser473 was decreased 45.4% and 18.4% in K562 cells with the treatment of ALS at 1 and 5 μM for 24 h, respectively (Figure S10). Notably, there was a significant alteration in the expression of Akt in K562 cells and there was a 1.7-, 2.1-, and 2.1-fold increase in the level of Akt when K562 cells were treated with ALS at 0.2, 1, and 5 μM, compared to the control cells, respectively (P<0.05 or 0.01; Figure S10). Consequently, the ratio of p-Akt/Akt was significantly decreased in K562 cells treated with ALS. In K562 cells, the ratio of p-Akt/Akt was decreased 30.2%, 73.8%, and 59.5% when cells were treated with ALS at 0.2, 1, and 5 μM for 24 h, respectively (Figure S10).

In addition, the expression level of PTEN which is the negative regulator of PI3K/Akt signaling pathway, was significantly increased when K562 cells were treated with 0.2 and 1 μM ALS for 24 h (P<0.01; **Figure 7** and Figure S10). And exposure of K562 cells to 5 μM ALS resulted in a 57.5% decrease in the phosphorylation level of mTOR at Ser2448 (P<0.001; Figure S9). There was no significant change in the expression of total mTOR in K562 cells when treated with ALS for 24 h. However, a decreased ratio of p-mTOR/mTOR was observed in K562 cells when treated with ALS. In K562 cells, the ratio of p-mTOR/mTOR was decreased 56.3% when treated with 5 μM PLB (P<0.05; Figure S9).

Additionally, we examined the effect of PLB on the expression level of beclin 1 and LC3-I/II. Treatment of K562 cells with ALS for 24 h concentration-dependently increased the expression of beclin 1 (**Figure 7** and Figure S10). There was a 1.4 and 1.5-fold increase of beclin 1 in K562 cells when treated with 1 and 5 μM ALS for 24 h (P<0.01; Figure S10). The results showed two bands of LC3-I and II in K562 cells (**Figure 7**). Compared to the control cells, there was a 1.4-fold increase in the LC3-II level in K562 cells treated with 5 μM ALS for 24 h (P<0.001; Figure S10). In addition, treatment of K562 cells with ALS decreased the expression of LC3-I, although which was not significantly different. The ratio of LC3-II/LC3-I was remarkably increased 1.3-, 1.3-, and 1.3-fold in K562 cells with treatment of ALS at 0.2, 1, and 5 μM, respectively (P<0.05 or 0.01; Figure S10). These findings indicate that ALS exhibited a strong autophagy-inducing effect on K562 cells via inhibition of the PI3K/Akt/mTOR pathway.

ALS induces apoptosis of K562 cells involving PI3K/Akt/mTOR and p38 MAPK signaling pathways: To further confirm the role of PI3K/Akt/mTOR and p38 MAPK signaling pathways in ALS-induced apoptosis in K562 cells, we employed the specific chemical inhibitors of

mTOR (0.5 μM rapamycin), PI3K (10 μM wortmannin), Akt (1 μM MK-2206), and p38 MAPK (10 μM SB202190) to examine the apoptosis of K562 cells in the presence and absence of 5 μM ALS using flow cytometry. In the absence of ALS, incubation of 0.5 μM rapamycin, 10 μM wortmannin, 1 μM MK-2206, and 10 μM SB202190 resulted in an increase in the apoptosis of K562 cells (**Figure 8A** and **8B**). In compared to the control cells (DMSO), there were 2.0- and 1.5-flod elevation in the percentage of apoptotic K562 cells when treated with 10 μM wortmannin and 10 μM SB202190, respectively (P<0.05 or 0.001; **Figure 8A** and **8B**). Moreover, although there was no significant inducing effect of 0.5 μM rapamycin and 1 μM MK-2206 on the apoptosis of K562 cells, there was a 1.2- and 1.3-fold increase in the percentage of apoptotic K562 cells compared to DMSO-treated cells, respectively (P>0.05; **Figure 8A** and **8B**). Notably, co-incubation of K562 cells with 0.5 μM rapamycin, 10 μM wortmannin, 1 μM MK-2206, or 10 μM SB202190 and 5 μM ALS remarkably enhanced ALS-induced apoptosis (**Figure 8A** and **8B**). Compared to DMSO-treated cells, ALS induced a 1.6-fold increase in the percentage of apoptotic K562 cells, respectively (P<0.001; **Figure 8A** and **8B**). In comparison to ALS-treated cells, there was a 1.2-, 1.6-, 1.2-, and 1.4-fold elevation in the percentage of apoptotic K562 cells when co-incubated with rapamycin and ALS, wortmannin and ALS, MK-2206 and ALS, or SB202190 and ALS, respectively (P<0.05 or 0.001; **Figure 8A** and **8B**). On the other hand, compared to the mono-treatment of cell with 0.5 μM rapamycin, 10 μM wortmannin, 1 μM MK-2206, or 10 μM SB202190, there was a marked increase in the percentage of apoptotic K562 cells with the co-incubation with rapamycin and ALS, wortmannin and ALS, MK-2206 and ALS, or SB202190 and ALS (P<0.001; **Figure 8A** and **8B**). Taken together, the results further demonstrate the involvement of PI3K/Akt/mTOR and p38 MAPK signaling pathways in ALS-induced apoptosis in K562 cells.

Discussion

Current CML therapies often fail mainly due to the drug resistance, which requires and spurs the development of new therapeutics with novel targets. As stated above, identification of the molecular targets of ALS is critical for CML therapy. With the application of SILAC-based proteomic approach, the present study has evaluated the proteomic responses to ALS treatment in K562 cells, including numerous functional proteins and related signaling pathways. The subsequential validating assays indicated that ALS-regulated proteins and signaling pathways were involved in cell cycle distribution, apoptosis, and autophagy with the participation of PI3K/Akt/mTOR, p38 MAPK, and AMPK signaling pathways in K562 cells.

The SILAC-based proteomics possesses the capability of quantitatively and comprehensively evaluating the effect of a given compound and identify its potential molecular targets and related signaling pathways in vitro or in vivo [38-40]. Our previous studies have unveiled the molecular interactome of plumbagin and 5,6-dimethylxanthenone 4-acetic acid (DMXAA, vadimezan) in several cancer cell lines [41, 42], and explored the potential molecular targets and possible mechanisms for the anticancer effects. In the present study, we employed SILAC-based proteomic approach to evaluate the cellular proteomic responses to ALS treatment in K562 cells, showing that ALS regulated a number of functional proteins and signaling pathways involved in cell cycle progression, apoptosis, and autophagy in K562 cells, such as DCTN2, NAP1L1, RPLP0, RPL15, PI3K/Akt/mTOR, PTEN, ERK/MAKPK, and AMPK and their related signaling pathways. The proteomics results suggest that ALS may target these signaling molecules to elicit its anticancer effects in the treatment of CML. Notably, we further validated the proteomic responses to ALS treatment in K562 cells.

With increasing preclininal and clinical studies focusing on the role of the Aurora kinases in the formation and the treatment of tumours, AURKA becomes an important therapeutic target in cancer therapy [43-45]. Accumulating evidence shows that abberation in the activity and expression of AURKA leads to tumor development and progression [46]. Recent reports have shown that AURKA can induce drug resistance and regulate several key signaling pathways related to cell cycle progression, cell migration and invision, and programmed cell death in cancer cells [46-48], suggesting a pivotal role in cancer cell signaling [49]. Our recent studies showed that inhibition of AURKA/B led to a marked cancer cell death [28, 50-53]. In

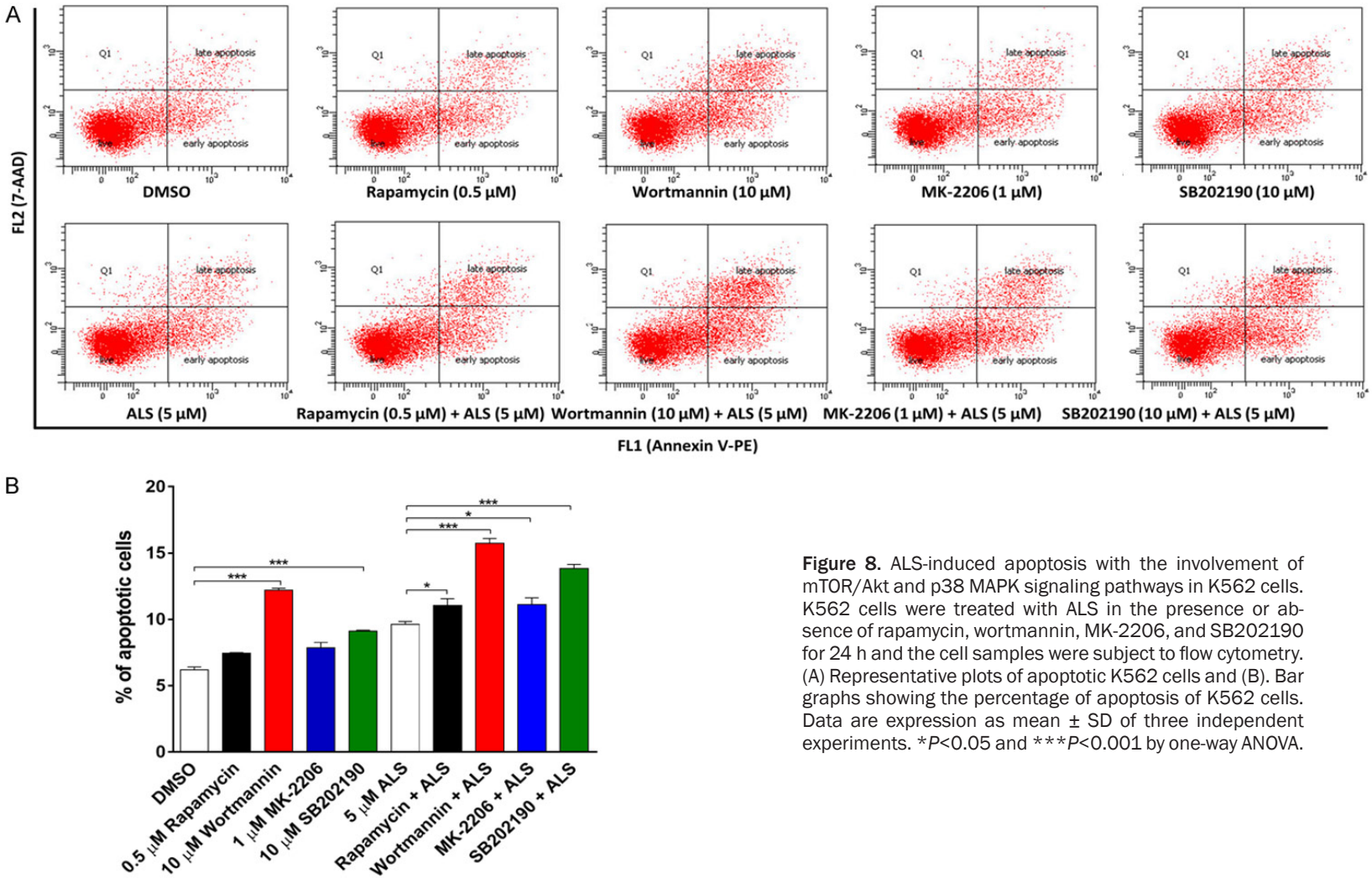

Figure 8. ALS-induced apoptosis with the involvement of mTOR/Akt and p38 MAPK signaling pathways in K562 cells. K562 cells were treated with ALS in the presence or absence of rapamycin, wortmannin, MK-2206, and SB202190 for 24 h and the cell samples were subject to flow cytometry. (A) Representative plots of apoptotic K562 cells and (B). Bar graphs showing the percentage of apoptosis of K562 cells. Data are expression as mean ± SD of three independent experiments. $*P<0.05$ and $***P<0.001$ by one-way ANOVA.

the present study, we found that ALS significantly inhibited the phosphorylation of ARUKA and induced cell death in K562 cells, suggesting an anticancer potential in CML treatment.

Due to the central role of AURKA in mitosis, we examined the effect of ALS on cell cycle distribution and found that ALS dramatically arrested K562 cells in G_2/M phase, which also verified the proteomic data. Based on the proteomic and flow cytometric data, we speculated that the possible mechanism of ALS on G_2/M arrest in K562 cells might involve a number of key regulators, such as PLK-1, p21 Waf1/Cip1, p53, cyclins and cyclin-dependent kinases. In our study, the findings of proteomics and Western blotting assays clearly showed a potent regulatory effect of ALS on the expression of PLK-1, p21 Waf1/Cip1, p53, cyclins, and CDKs. Notably, cell cycle progression is tightly regulated by cyclins and CDKs [54]. p21 Waf1/Cip1, a cyclin-dependent kinase inhibitor, is regulated by p53. It binds to CDC2-cyclin B1 complex, inducing cell cycle arrest [55]. The CDC2 and cyclin B1 complex plays a major role in the entry of cells into mitosis, because cyclins have no catalytic activity and CDKs are inactive in the absence of a partner cyclin. Thus, taken the proteomic and validating results into consideration, ALS-induced cell cycle arrest may be through the regulation of key modulators controlling the G_2/M check point in K562 cells.

Notably, the proteomic data showed that ALS regulated ribosomal signal and dramatically altered the expression of DCTN2, NAP1L1, RPLP0, and RPL15 in K562 cells, which have important roles in protein synthesis and cell division. Human *DCTN2* encodes a 50 kD subunit of dynactin, a macromolecular complex consisting of 10-11 subunits ranging in size from 22 to 150 kD. DCTN2 is involved in a diverse array of cellular functions, including endoplasmic reticulum to Golgi transport, the centripetal movement of lysosomes and endosomes, spindle formation, chromosome movement, nuclear positioning, and axonogenesis [29]. Moreover, NAP1L1 participates in DNA replication and may play a role in modulating chromatin formation and contribute to the regulation of cell proliferation [30, 31]; RPLP0 and RPL15 are ribosomal proteins involved in protein synthesis [32, 33]. Thus, we tested the expression level of DCTN2, NAP1L1, RPLP0, and RPL15 in K562 cells when treated with ALS. The findings showed that ALS exhibited a potent promoting effect on the expression of DCTN2, NAP1L1, RPLP0, and RPL15, which may provide further explanation on the cell cycle arresting effect of ALS on K562 cells.

In the present study, the proteomic study also showed that ALS regulated mitochondrial function and cell death. Disruption of mitochondrial function and the resultant cytochrome c release initiate apoptosis process, with the latter being activated caspase cascade [56, 57]. Also, pro-apoptotic members of the Bcl-2 family but antagonized by anti-apoptotic members of this family were highly involved in apoptosis [56, 57]. Anti-apoptotic members of Bcl-2 is suppressed by post-translational modification and/or by increased expression of PUMA, an essential regulator of p53-mediated cell apoptosis [58]. Cytochrome c released from mitochondria to cytosol induces that activation of caspase 9, subsequently activating caspase 3 [59]. In our study, the finding showed that cytosolic level of cytochrome c was significantly increased and that caspase cascade was markedly activated in response to ALS treatment, which contributes to ALS-induced apoptosis of K562 cells. Intriguingly, the specific chemical inhibitors of mTOR (rapamycin), PI3K (wortmannin), Akt (MK-2206), and p38 MAPK (SB202190) enhanced ALS-induced apoptosis of K562 cells, indicating the involvement of PI3K/AKT/mTOR, MAPK, and AMPK signaling pathways in ALS-induced apoptosis. Furthermore, the proteomic results showed that ALS exhibited a modulating effect on PI3K/Akt/mTOR, ERK/MAPK, and AMPK signaling pathways in K562 cells, which play critical role in regulation of cellular process, including autophagy. Autophagy (also known as type II programmed cell death) is extremely important for a variety of human diseases, especially cancers. It affects various stages of initiation and progression of cancer with the participation of overlapped signaling pathways of autophagy and carcinogenesis [35, 60, 61]. Accumulating evidence shows that the PI3K/Akt/mTOR, MAPK, and AMPK signaling pathways have been regarded to be the key regulators of a series of cell processes as they can be deregulated by various genetic and epigenetic mechanisms, in a wide range of cancer cells [60, 62]. PI3K activates the serine/threonine kinase Akt, which in turn through a cascade of regulators results in the phosphoryla-

tion and activation of the serine/threonine kinase mTOR, activated mTORC1 inhibits autophagy by direct phosphorylation of Atg13 and ULK1 at Ser757 [34, 35, 63, 64]. Also, p38 MAPK and AMPK signals were orchestrated with autophagy process [60]. In the present study, ALS induced autophagy in K562 cells as indicated by flow cytometric data and the increase in the expression of beclin 1 and the ratio of LC3-II over LC3-I. Of note, the PI3K/Akt/mTOR, p38 MAPK, and AMPK signaling pathways were altered in response to ALS treatment. Taken together, out findings indicate that PI3K/AKT/mTOR, MAPK, and AMPK signaling pathways contribute to ALS-induced programmed cell death in K562 cells.

In summary, the quantitative SILAC-based proteomic approach showed that ALS inhibited cell proliferation, induced cell cycle arrest, activated mitochondria-dependent apoptotic pathway and induced autophagy in human K562 cells involving a number of key functional proteins and related molecular signaling pathways, such as PI3K/Akt/mTOR, MAPK, and AMPK signaling pathways. This study may provide a clue to fully identify the molecular targets and elucidate the underlying mechanism of ALS in the treatment of CML, resulting in an improved therapeutic effect and reduced side effect in clinical settings.

Acknowledgements

The authors appreciate the financial support from the Startup Fund of the College of Pharmacy, University of South Florida, Tampa, Florida 33612, USA. Dr. Zhi-Wei Zhou is a holder of a postdoctoral scholarship from College of Pharmacy, University of South Florida, Tampa, Florida 33612, USA.

Disclosure of conflict of interest

None.

Authors' contribution

Participated in research design: Li-Ping Shu, Zhi-Wei Zhou, Dan Zi, Zhi-Xu He, and Shu-Feng Zhou. Conducted experiments: Li-Ping Shu and Zhi-Wei Zhou. Contributed new reagents or analytic tools: Zhi-Xu He and Shu-Feng Zhou. Performed data analysis: Li-Ping Shu, Zhi-Wei Zhou and Dan Zi. Wrote or contributed to the writing of the manuscript: Li-Ping Shu, Zhi-Wei Zhou, Zhi-Xu He and Shu-Feng Zhou.

Address correspondence to: Dr. Shu-Feng Zhou, Department of Pharmaceutical Sciences, College of Pharmacy, University of South Florida, 12901 Bruce B. Downs Boulevard, Tampa, FL 33612, USA. Tel: 1 813-974-6276; Fax: 1 813-905-9885; E-mail: szhou@health.usf.edu; Dr. Zhi-Xu He, Tissue Engineering and Stem Cell Research Center, Guiyang Medical University, Beijing Road No. 9, Guiyang, Guizhou 550004, People's Republic of China. Tel: + 86 851 8690 8118; Fax: + 86 851 841 6015; E-mail: hzx@gmc.edu.cn

References

[1] Geyer HL and Mesa RA. Therapy for myeloproliferative neoplasms: when, which agent, and how? Blood 2014; 124: 3529-3537.

[2] Klco JM, Vij R, Kreisel FH, Hassan A and Frater JL. Molecular pathology of myeloproliferative neoplasms. Am J Clin Pathol 2010; 133: 602-615.

[3] O'Hare T, Zabriskie MS, Eiring AM and Deininger MW. Pushing the limits of targeted therapy in chronic myeloid leukaemia. Nat Rev Cancer 2012; 12: 513-526.

[4] Apperley JF. Chronic myeloid leukaemia. Lancet 2015; 385: 1447-1459.

[5] Carmena M and Earnshaw WC. The cellular geography of aurora kinases. Nat Rev Mol Cell Biol 2003; 4: 842-854.

[6] Nikonova AS, Astsaturov I, Serebriiskii IG, Dunbrack RL Jr and Golemis EA. Aurora A kinase (AURKA) in normal and pathological cell division. Cell Mol Life Sci 2013; 70: 661-687.

[7] Dar AA, Goff LW, Majid S, Berlin J and El-Rifai W. Aurora kinase inhibitors--rising stars in cancer therapeutics? Mol Cancer Ther 2010; 9: 268-278.

[8] Cervantes A, Elez E, Roda D, Ecsedy J, Macarulla T, Venkatakrishnan K, Rosello S, Andreu J, Jung J, Sanchis-Garcia JM, Piera A, Blasco I, Manos L, Perez-Fidalgo JA, Fingert H, Baselga J and Tabernero J. Phase I pharmacokinetic/pharmacodynamic study of MLN8237, an investigational, oral, selective aurora a kinase inhibitor, in patients with advanced solid tumors. Clin Cancer Res 2012; 18: 4764-4774.

[9] Dees EC, Cohen RB, von Mehren M, Stinchcombe TE, Liu H, Venkatakrishnan K, Manfredi M, Fingert H, Burris HA 3rd and Infante JR. Phase I study of aurora A kinase inhibitor MLN8237 in advanced solid tumors: safety, pharmacokinetics, pharmacodynamics, and bioavailability of two oral formulations. Clin Cancer Res 2012; 18: 4775-4784.

[10] Matulonis UA, Sharma S, Ghamande S, Gordon MS, Del Prete SA, Ray-Coquard I, Kutarska E,

Liu H, Fingert H, Zhou X, Danaee H and Schilder RJ. Phase II study of MLN8237 (alisertib), an investigational Aurora A kinase inhibitor, in patients with platinum-resistant or -refractory epithelial ovarian, fallopian tube, or primary peritoneal carcinoma. Gynecol Oncol 2012; 127: 63-69.

[11] Friedberg JW, Mahadevan D, Cebula E, Persky D, Lossos I, Agarwal AB, Jung J, Burack R, Zhou X, Leonard EJ, Fingert H, Danaee H and Bernstein SH. Phase II study of alisertib, a selective Aurora A kinase inhibitor, in relapsed and refractory aggressive B- and T-cell non-Hodgkin lymphomas. J Clin Oncol 2014; 32: 44-50.

[12] Goldberg SL, Fenaux P, Craig MD, Gyan E, Lister J, Kassis J, Pigneux A, Schiller GJ, Jung J, Jane Leonard E, Fingert H and Westervelt P. An exploratory phase 2 study of investigational Aurora A kinase inhibitor alisertib (MLN8237) in acute myelogenous leukemia and myelodysplastic syndromes. Leuk Res Rep 2014; 3: 58-61.

[13] Macarulla T, Cervantes A, Elez E, Rodriguez-Braun E, Baselga J, Rosello S, Sala G, Blasco I, Danaee H, Lee Y, Ecsedy J, Shinde V, Chakravarty A, Bowman D, Liu H, Eton O, Fingert H and Tabernero J. Phase I study of the selective Aurora A kinase inhibitor MLN8054 in patients with advanced solid tumors: safety, pharmacokinetics, and pharmacodynamics. Mol Cancer Ther 2010; 9: 2844-2852.

[14] Maris JM, Morton CL, Gorlick R, Kolb EA, Lock R, Carol H, Keir ST, Reynolds CP, Kang MH, Wu J, Smith MA and Houghton PJ. Initial testing of the aurora kinase A inhibitor MLN8237 by the Pediatric Preclinical Testing Program (PPTP). Pediatr Blood Cancer 2010; 55: 26-34.

[15] Tomita M and Mori N. Aurora A selective inhibitor MLN8237 suppresses the growth and survival of HTLV-1-infected T-cells in vitro. Cancer Sci 2010; 101: 1204-1211.

[16] Gorgun G, Calabrese E, Hideshima T, Ecsedy J, Perrone G, Mani M, Ikeda H, Bianchi G, Hu Y, Cirstea D, Santo L, Tai YT, Nahar S, Zheng M, Bandi M, Carrasco RD, Raje N, Munshi N, Richardson P and Anderson KC. A novel Aurora-A kinase inhibitor MLN8237 induces cytotoxicity and cell-cycle arrest in multiple myeloma. Blood 2010; 115: 5202-5213.

[17] Miano M, Micalizzi C, Calvillo M and Dufour C. New targets in pediatric Acute Myeloid Leukemia. Immunol Lett 2013; 155: 47-50.

[18] Goldenson B and Crispino JD. The aurora kinases in cell cycle and leukemia. Oncogene 2015; 34: 537-545.

[19] Yang J, Ikezoe T, Nishioka C, Nobumoto A, Udaka K and Yokoyama A. CD34(+)/CD38(-) acute myelogenous leukemia cells aberrantly express Aurora kinase A. Int J Cancer 2013; 133: 2706-2719.

[20] Krause DS and Crispino JD. Molecular pathways: induction of polyploidy as a novel differentiation therapy for leukemia. Clin Cancer Res 2013; 19: 6084-6088.

[21] Kelly KR, Ecsedy J, Medina E, Mahalingam D, Padmanabhan S, Nawrocki ST, Giles FJ and Carew JS. The novel Aurora A kinase inhibitor MLN8237 is active in resistant chronic myeloid leukaemia and significantly increases the efficacy of nilotinib. J Cell Mol Med 2011; 15: 2057-2070.

[22] Altelaar AF, Frese CK, Preisinger C, Hennrich ML, Schram AW, Timmers HT, Heck AJ and Mohammed S. Benchmarking stable isotope labeling based quantitative proteomics. J Proteomics 2013; 88: 14-26.

[23] Ong SE. The expanding field of SILAC. Anal Bioanal Chem 2012; 404: 967-976.

[24] Ong SE and Mann M. Stable isotope labeling by amino acids in cell culture for quantitative proteomics. Methods Mol Biol 2007; 359: 37-52.

[25] Mann M. Functional and quantitative proteomics using SILAC. Nat Rev Mol Cell Biol 2006; 7: 952-958.

[26] Ong SE and Mann M. A practical recipe for stable isotope labeling by amino acids in cell culture (SILAC). Nat Protoc 2006; 1: 2650-2660.

[27] Huang da W, Sherman BT and Lempicki RA. Systematic and integrative analysis of large gene lists using DAVID bioinformatics resources. Nat Protoc 2009; 4: 44-57.

[28] Yuan CX, Zhou ZW, Yang YX, He ZX, Zhang X, Wang D, Yang T, Wang NJ, Zhao RJ and Zhou SF. Inhibition of mitotic Aurora kinase A by alisertib induces apoptosis and autophagy of human gastric cancer AGS and NCI-N78 cells. Drug Des Devel Ther 2015; 9: 487-508.

[29] Jacquot G, Maidou-Peindara P and Benichou S. Molecular and functional basis for the scaffolding role of the p50/dynamitin subunit of the microtubule-associated dynactin complex. J Biol Chem 2010; 285: 23019-23031.

[30] Rehtanz M, Schmidt HM, Warthorst U and Steger G. Direct interaction between nucleosome assembly protein 1 and the papillomavirus E2 proteins involved in activation of transcription. Mol Cell Biol 2004; 24: 2153-2168.

[31] Okuwaki M, Kato K and Nagata K. Functional characterization of human nucleosome assembly protein 1-like proteins as histone chaperones. Genes Cells 2010; 15: 13-27.

[32] Chang TW, Chen CC, Chen KY, Su JH, Chang JH and Chang MC. Ribosomal phosphoprotein P0 interacts with GCIP and overexpression of P0 is associated with cellular proliferation in breast

and liver carcinoma cells. Oncogene 2008; 27: 332-338.
[33] Wang H, Zhao LN, Li KZ, Ling R, Li XJ and Wang L. Overexpression of ribosomal protein L15 is associated with cell proliferation in gastric cancer. BMC Cancer 2006; 6: 91.
[34] Klionsky DJ and Emr SD. Autophagy as a regulated pathway of cellular degradation. Science 2000; 290: 1717-1721.
[35] Denton D, Nicolson S and Kumar S. Cell death by autophagy: facts and apparent artefacts. Cell Death Differ 2012; 19: 87-95.
[36] Dunlop EA and Tee AR. The kinase triad, AMPK, mTORC1 and ULK1, maintains energy and nutrient homoeostasis. Biochem Soc Trans 2013; 41: 939-943.
[37] Koul HK, Pal M and Koul S. Role of p38 MAP Kinase Signal Transduction in Solid Tumors. Genes Cancer 2013; 4: 342-359.
[38] Dolai S, Xu Q, Liu F and Molloy MP. Quantitative chemical proteomics in small-scale culture of phorbol ester stimulated basal breast cancer cells. Proteomics 2011; 11: 2683-2692.
[39] Geiger T, Cox J, Ostasiewicz P, Wisniewski JR and Mann M. Super-SILAC mix for quantitative proteomics of human tumor tissue. Nat Methods 2010; 7: 383-385.
[40] Everley PA, Krijgsveld J, Zetter BR and Gygi SP. Quantitative cancer proteomics: stable isotope labeling with amino acids in cell culture (SILAC) as a tool for prostate cancer research. Mol Cell Proteomics 2004; 3: 729-735.
[41] Qiu JX, Zhou ZW, He ZX, Zhao RJ, Zhang X, Yang L, Zhou SF and Mao ZF. Plumbagin elicits differential proteomic responses mainly involving cell cycle, apoptosis, autophagy, and epithelial-to-mesenchymal transition pathways in human prostate cancer PC-3 and DU145 cells. Drug Des Devel Ther 2015; 9: 349-417.
[42] Pan ST, Zhou ZW, He ZX, Zhang X, Yang T, Yang YX, Wang D, Qiu JX and Zhou SF. Proteomic response to 5,6-dimethylxanthenone 4-acetic acid (DMXAA, vadimezan) in human non-small cell lung cancer A549 cells determined by the stable-isotope labeling by amino acids in cell culture (SILAC) approach. Drug Des Devel Ther 2015; 9: 937-968.
[43] Mountzios G, Terpos E and Dimopoulos MA. Aurora kinases as targets for cancer therapy. Cancer Treat Rev 2008; 34: 175-182.
[44] Gautschi O, Heighway J, Mack PC, Purnell PR, Lara PN Jr and Gandara DR. Aurora kinases as anticancer drug targets. Clin Cancer Res 2008; 14: 1639-1648.
[45] Keen N and Taylor S. Aurora-kinase inhibitors as anticancer agents. Nat Rev Cancer 2004; 4: 927-936.
[46] Zhou N, Singh K, Mir MC, Parker Y, Lindner D, Dreicer R, Ecsedy JA, Zhang Z, Teh BT, Almasan A and Hansel DE. The investigational Aurora kinase A inhibitor MLN8237 induces defects in cell viability and cell-cycle progression in malignant bladder cancer cells *in vitro* and *in vivo*. Clin Cancer Res 2013; 19: 1717-1728.
[47] Do TV, Xiao F, Bickel LE, Klein-Szanto AJ, Pathak HB, Hua X, Howe C, O'Brien SW, Maglaty M, Ecsedy JA, Litwin S, Golemis EA, Schilder RJ, Godwin AK and Connolly DC. Aurora kinase A mediates epithelial ovarian cancer cell migration and adhesion. Oncogene 2014; 33: 539-549.
[48] D'Assoro AB, Liu T, Quatraro C, Amato A, Opyrchal M, Leontovich A, Ikeda Y, Ohmine S, Lingle W, Suman V, Ecsedy J, Iankov I, Di Leonardo A, Ayers-Inglers J, Degnim A, Billadeau D, McCubrey J, Ingle J, Salisbury JL and Galanis E. The mitotic kinase Aurora - a promotes distant metastases by inducing epithelial-to-mesenchymal transition in ERa$^+$ breast cancer cells. Oncogene 2014; 33: 599-610.
[49] Melaiu O, Cristaudo A, Melissari E, Di Russo M, Bonotti A, Bruno R, Foddis R, Gemignani F, Pellegrini S and Landi S. A review of transcriptome studies combined with data mining reveals novel potential markers of malignant pleural mesothelioma. Mutat Res 2012; 750: 132-140.
[50] Ding YH, Zhou ZW, Ha CF, Zhang XY, Pan ST, He ZX, Edelman JL, Wang D, Yang YX, Zhang X, Duan W, Yang T, Qiu JX and Zhou SF. Alisertib, an Aurora kinase A inhibitor, induces apoptosis and autophagy but inhibits epithelial to mesenchymal transition in human epithelial ovarian cancer cells. Drug Des Devel Ther 2015; 9: 425-464.
[51] Wang F, Li H, Yan XG, Zhou ZW, Yi ZG, He ZX, Pan ST, Yang YX, Wang ZZ, Zhang X, Yang T, Qiu JX and Zhou SF. Alisertib induces cell cycle arrest and autophagy and suppresses epithelial-to-mesenchymal transition involving PI3K/Akt/mTOR and sirtuin 1-mediated signaling pathways in human pancreatic cancer cells. Drug Des Devel Ther 2015; 9: 575-601.
[52] Niu NK, Wang ZL, Pan ST, Ding HQ, Au GH, He ZX, Zhou ZW, Xiao G, Yang YX, Zhang X, Yang T, Chen XW, Qiu JX and Zhou SF. Pro-apoptotic and pro-autophagic effects of the Aurora kinase A inhibitor alisertib (MLN8237) on human osteosarcoma U-2 OS and MG-63 cells through the activation of mitochondria-mediated pathway and inhibition of p38 MAPK/PI3K/Akt/mTOR signaling pathway. Drug Des Devel Ther 2015; 9: 1555-1584.
[53] Li JP, Yang YX, Liu QL, Pan ST, He ZX, Zhang X, Yang T, Chen XW, Wang D, Qiu JX and Zhou SF. The investigational Aurora kinase A inhibitor alisertib (MLN8237) induces cell cycle G2/M

arrest, apoptosis, and autophagy via p38 MAPK and Akt/mTOR signaling pathways in human breast cancer cells. Drug Des Devel Ther 2015; 9: 1627-1652.
[54] Hunter T. Protein kinases and phosphatases: the yin and yang of protein phosphorylation and signaling. Cell 1995; 80: 225-236.
[55] Bunz F, Dutriaux A, Lengauer C, Waldman T, Zhou S, Brown JP, Sedivy JM, Kinzler KW and Vogelstein B. Requirement for p53 and p21 to sustain G2 arrest after DNA damage. Science 1998; 282: 1497-1501.
[56] Boehning D, Patterson RL, Sedaghat L, Glebova NO, Kurosaki T and Snyder SH. Cytochrome c binds to inositol (1,4,5) trisphosphate receptors, amplifying calcium-dependent apoptosis. Nat Cell Biol 2003; 5: 1051-1061.
[57] Yang J, Liu X, Bhalla K, Kim CN, Ibrado AM, Cai J, Peng TI, Jones DP and Wang X. Prevention of apoptosis by Bcl-2: release of cytochrome c from mitochondria blocked. Science 1997; 275: 1129-1132.
[58] Jeffers JR, Parganas E, Lee Y, Yang C, Wang J, Brennan J, MacLean KH, Han J, Chittenden T, Ihle JN, McKinnon PJ, Cleveland JL and Zambetti GP. Puma is an essential mediator of p53-dependent and -independent apoptotic pathways. Cancer Cell 2003; 4: 321-328.
[59] Fesik SW and Shi Y. Structural biology. Controlling the caspases. Science 2001; 294: 1477-1478.
[60] Wang X, Wang XL, Chen HL, Wu D, Chen JX, Wang XX, Li RL, He JH, Mo L, Cen X, Wei YQ and Jiang W. Ghrelin inhibits doxorubicin cardiotoxicity by inhibiting excessive autophagy through AMPK and p38-MAPK. Biochem Pharmacol 2014; 88: 334-350.
[61] Rabinowitz JD and White E. Autophagy and metabolism. Science 2010; 330: 1344-1348.
[62] Ouyang L, Shi Z, Zhao S, Wang FT, Zhou TT, Liu B and Bao JK. Programmed cell death pathways in cancer: a review of apoptosis, autophagy and programmed necrosis. Cell Prolif 2012; 45: 487-498.
[63] Chen Y and Yu L. Autophagic lysosome reformation. Exp Cell Res 2013; 319: 142-146.
[64] Rodon J, Dienstmann R, Serra V and Tabernero J. Development of PI3K inhibitors: lessons learned from early clinical trials. Nat Rev Clin Oncol 2013; 10: 143-153.

Table S1. The 1541 protein molecules regulated by ALS in K562 cells

	Protein ID/symbol	Molecularweight (kDa)	Normalized heavy/light ratio
1	VPS28	3.9415	28.071
2	KCRU	47.036	11.507
3	ERAP1	107.23	9.292
4	OPLA	137.46	4.6511
5	RIR1	52.005	4.4349
6	TYSY	35.716	3.5194
7	PTRF	33.362	3.23
8	NUCKS	27.296	2.5992
9	B1AR80	57.028	2.5236
10	METK2	32.964	2.3111
11	BOLA2	6.8417	2.3053
12	RIF1	271.69	2.1958
13	ABCF2	71.289	2.1923
14	TIM8B	3.4488	2.1714
15	DNJA1	44.868	2.165
16	MLEC	16.729	2.1519
17	HTF4	48.157	2.1159
18	E9PR17	11.985	2.0893
19	B7Z8D3	29.506	2.0681
20	C9JIM8	47.819	2.0052
21	BZW2	18.71	1.9856
22	F6SH78	9.5799	1.9408
23	B4DJ87	40.548	1.9347
24	F2Z3D7	92.115	1.8986
25	RL37A	6.5677	1.8527
26	ROA0	30.84	1.8512
27	AMPM2	17.068	1.8509
28	G3V153	19.381	1.8146
29	GRSF1	36.613	1.8144
30	NTM1A	25.387	1.8125
31	PR40A	95.096	1.7938
32	EIF3A	162.63	1.7831
33	IMA2	57.861	1.7671
34	PNO1	15.175	1.7514
35	NUDC1	56.613	1.7513
36	B4DNJ6	28.506	1.7472
37	E9PJF4	18.259	1.7416
38	YTHD2	56.877	1.7289
39	B4DXI4	16.268	1.7286
40	DDX50	87.343	1.7247
41	F5H0D4	273.42	1.7238
42	DSRAD	103.64	1.7231
43	F8W026	83.263	1.7103
44	F8VZG8	109.3	1.7086
45	DEST	15.397	1.6941
46	STAU1	54.708	1.6863
47	EPS15	64.375	1.6845
48	E9PNV3	68.563	1.6841

49	F6U211	18.898	1.667
50	E9PSH5	70.897	1.6553
51	CHM1A	19.531	1.6389
52	EIF3I	36.501	1.6315
53	4EBP2	12.939	1.6299
54	WDR61	33.58	1.6268
55	PCNA	28.768	1.6243
56	PAIRB	42.426	1.6234
57	B4DMC6	95.337	1.6226
58	G3V5T9	34.095	1.6174
59	COX41	19.576	1.5727
60	B4DG39	63.146	1.5708
61	HSB11	16.297	1.5688
62	C9JZG1	92.48	1.5654
63	UBP2L	29.16	1.5548
64	RBM4	16.264	1.554
65	RS28	7.8409	1.5533
66	DUT	17.748	1.553
67	THIC	41.35	1.5525
68	GEMI5	168.59	1.5519
69	PPP5	56.878	1.5511
70	RAB8A	23.668	1.5493
71	CDK6	36.938	1.5456
72	9-Sep	47.501	1.544
73	NPM3	19.343	1.5423
74	MTA2	75.022	1.5352
75	B4E3C4	71.354	1.5312
76	RS11	18.431	1.524
77	RL35	10.645	1.5113
78	Q9BYK1	8.85	1.509
79	F5GXU1	36.688	1.503
80	RL19	23.466	1.5019
81	SH3L3	9.3804	1.4997
82	RS7	22.127	1.4936
83	UBP7	128.3	1.4927
84	B7Z4C8	8.9876	1.4924
85	E9PDR7	17.692	1.4906
86	RPAB1	24.551	1.4897
87	RS12	14.515	1.4887
88	PAP1L	61.18	1.4849
89	STAT1	21.776	1.4845
90	MMAB	18.342	1.4842
91	PPID	40.763	1.4812
92	E7ETL9	69.147	1.4803
93	G3V1K0	32.251	1.4626
94	IPO5	109.36	1.4588
95	F8W118	27.724	1.4581
96	ANK1	166.45	1.4564
97	B7Z6F8	68.166	1.4557
98	RL22	14.787	1.4532

99	DNMT1	183.16	1.4525
100	E5RJU8	52.164	1.4431
101	SSRA	29.573	1.441
102	DHSB	31.629	1.4391
103	AQR	171.29	1.4382
104	PP6R3	4.6822	1.435
105	F8WBE5	84.87	1.4338
106	EIF3G	35.611	1.4307
107	DDX18	75.406	1.428
108	B8ZZ09	21.372	1.4244
109	Q3KQS4	88.972	1.4232
110	E7EPK6	15.069	1.4231
111	RL35A	6.4725	1.422
112	B4DNC8	23.577	1.4172
113	C9JSY4	12.701	1.4158
114	F8WE11	46.153	1.4143
115	E9PC97	36.43	1.4141
116	F8W646	29.386	1.414
117	F8WE04	18.536	1.4136
118	Q5JR95	24.205	1.413
119	RL30	12.656	1.41
120	Q5QP23	57.089	1.4098
121	GALT7	75.388	1.4076
122	F5GYQ2	11.972	1.4038
123	RL18A	18.11	1.4016
124	B4DZP5	112.15	1.4004
125	MEP50	29.651	1.3972
126	RHOA	21.768	1.3949
127	PESC	51.464	1.3945
128	C9JQ55	29.597	1.3911
129	LDHC	36.638	1.391
130	BCLF1	52.917	1.391
131	E9PAV3	7.813	1.3867
132	CSTF1	15.594	1.3864
133	CKAP5	218.52	1.3862
134	NAA15	61.602	1.3854
135	C9JCU7	12.958	1.3848
136	B4DDC6	16.476	1.3818
137	RS5	22.876	1.3811
138	G3V2S9	12.349	1.38
139	E7ETK5	55.804	1.3763
140	A6NF51	27.543	1.3758
141	EI2BA	24.617	1.3755
142	E9PPT4	13.742	1.3714
143	SH3G1	41.489	1.37
144	GATA1	34.232	1.3667
145	F8W9G7	49.512	1.3656
146	Q5SQT6	32.66	1.364
147	ERF1	45.462	1.3635
148	PIN1	16.132	1.363

149	SELR1	25.709	1.3557
150	F8WCR1	31.243	1.3548
151	A2A3R5	28.68	1.3534
152	MTND	21.498	1.3527
153	Q68CS0	48.534	1.3517
154	TAGL3	22.391	1.3514
155	B4DRZ7	50.489	1.3487
156	B7WPD3	12.527	1.3465
157	D6RDI0	35.076	1.344
158	HMOX2	36.032	1.342
159	RS19	16.06	1.3415
160	RL27	15.798	1.3402
161	SK2L2	117.8	1.3356
162	RS26L	12.985	1.3341
163	C9J3L7	16.14	1.333
164	B7Z1K2	56.961	1.3327
165	Q5T8U3	29.995	1.3309
166	Q5JP00	46.938	1.3303
167	RREB1	51.609	1.3301
168	TIM13	10.5	1.3289
169	BTF3	17.699	1.325
170	SRS10	20.117	1.3248
171	G3V2I9	36.051	1.3242
172	RB11B	24.393	1.322
173	F5H1S2	24.261	1.3211
174	B3KXF2	204.29	1.3201
175	NU205	23.547	1.3201
176	F8WBH7	30.288	1.3176
177	Q86U51	107.97	1.3174
178	FABP5	15.164	1.3167
179	E9PJD0	28.821	1.3165
180	F8WCK5	17.718	1.3153
181	RL24	14.369	1.3136
182	CHRD1	37.489	1.3115
183	Q5T7N0	28.044	1.3108
184	F8W9D6	50.097	1.3091
185	HS904	84.659	1.303
186	D3DU83	31.324	1.3016
187	PDLI1	36.071	1.3012
188	F8WCH0	41.792	1.2953
189	B9EGQ7	154.8	1.2941
190	D6RDI2	27.017	1.2843
191	E7EX53	20.51	1.2843
192	MLTK	91.154	1.2834
193	B0QY89	55.161	1.2832
194	HEM3	6.9278	1.283
195	IMA4	57.886	1.2824
196	RS15A	14.839	1.2821
197	UB2V2	12.017	1.2814
198	F8WEU3	46.513	1.2798

199	F8WDK9	96.022	1.2737
200	C9K028	17.149	1.272
201	Q5T3N0	38.714	1.2713
202	E9PS50	17.222	1.2709
203	F5GY56	55.18	1.2685
204	S29A2	32.506	1.2651
205	B7Z514	40.349	1.262
206	B5ME19	84.966	1.2614
207	TOP1	90.725	1.2596
208	ASF1A	22.968	1.2591
209	F8W727	15.616	1.258
210	IFM3	12.255	1.2572
211	F5H737	47.716	1.2569
212	S2539	38.564	1.2558
213	B3KRQ1	38.604	1.2557
214	D6R9B6	11.572	1.2557
215	F6Q0E3	30.628	1.2552
216	Q5W012	24.176	1.255
217	F5H5A9	37.804	1.255
218	RL10	18.592	1.2522
219	TIA1	15.821	1.2497
220	MYL3	21.564	1.2484
221	RAB2B	20.847	1.2477
222	E9PCS5	20.811	1.242
223	PSB2	22.836	1.2388
224	CPSF4	23.653	1.2386
225	IF2P	138.83	1.2368
226	C9JQR9	29.505	1.2354
227	B4DX20	54.867	1.235
228	E7EX17	64.805	1.2333
229	A6NIB2	11.665	1.2332
230	NUDC	38.242	1.2324
231	CKAP2	10.865	1.2319
232	E7EU54	31.548	1.2317
233	JIP4	6.8529	1.2316
234	G3V438	32.339	1.2305
235	F5GZ39	17.965	1.2303
236	EFGM	83.471	1.2293
237	KI67	319.44	1.2262
238	FACE1	54.812	1.2244
239	S38A2	10.027	1.2244
240	E7EW92	18.091	1.224
241	B4DF96	62.288	1.2232
242	VTA1	24.553	1.2221
243	D6RBQ9	27.191	1.2218
244	RL36	12.254	1.2215
245	PFD6	14.582	1.2184
246	ZC3HF	44.891	1.2182
247	DYL1	4.7714	1.2164
248	Q6IPX4	16.445	1.2161

249	RL14	14.558	1.2159
250	RL10A	24.831	1.2157
251	DPOE3	16.859	1.2152
252	E9PG15	27.764	1.2144
253	MSH2	54.777	1.2135
254	C9JRT2	7.4894	1.213
255	F5H1H8	14.395	1.2123
256	F5H7Y1	60.343	1.2101
257	F8WC10	113.08	1.2094
258	B3KTM9	54.529	1.2086
259	B7Z2F4	57.924	1.2084
260	RNPS1	30.354	1.2059
261	B4DQH4	57.645	1.2047
262	F8W7I9	63.541	1.2041
263	F8W084	52.269	1.2038
264	ADDA	44.02	1.2024
265	RL8	18.169	1.2017
266	F8WAM2	54.772	1.2016
267	RUXF	9.7251	1.1985
268	F2Z2G2	24.763	1.1977
269	SFR15	124.01	1.1974
270	RS9	22.591	1.1966
271	ACL6A	5.5142	1.1961
272	E9PQX2	26.688	1.1957
273	E7ESE0	20.874	1.1941
274	F5GXM1	55.102	1.1935
275	Q5SX86	50.663	1.1934
276	BACH	27.041	1.1932
277	RL12	17.818	1.193
278	SRPK1	62.032	1.1929
279	RANB3	46.949	1.1913
280	UB2D3	8.2133	1.1888
281	PROF1	15.054	1.1879
282	CUL1	69.885	1.187
283	GET4	36.504	1.187
284	E5RJ94	47.087	1.1866
285	PIN4	13.81	1.1863
286	Q8IWY7	53.704	1.1857
287	B7Z4N8	52.385	1.1849
288	E7ENZ3	55.348	1.1845
289	PAL4A	18.012	1.1842
290	TOM34	20.292	1.1822
291	OLA1	44.743	1.1817
292	A2IDB1	28.218	1.1806
293	WAC	12.834	1.1806
294	F8W6I0	50.184	1.1802
295	F5H281	66.107	1.1773
296	E9PPK9	19.819	1.1751
297	E7ES32	49.611	1.1744
298	UT14A	69.263	1.1744

299	A4D1G5	7.3564	1.1722
300	PHF5A	12.405	1.1716
301	RMXL3	42.141	1.1709
302	RL11	20.252	1.1691
303	F5H2M7	206.64	1.1689
304	B4E2Q4	42.502	1.1683
305	COX5A	16.762	1.1679
306	Q5SZX9	55.674	1.1672
307	HYPK	14.665	1.167
308	CPNS1	28.315	1.1668
309	E9PQY2	15.314	1.1644
310	HN1	11.626	1.1633
311	SSRP1	81.074	1.1632
312	PYR1	236.02	1.1631
313	H31	15.404	1.1628
314	RLA1	11.514	1.1623
315	CYBP	26.21	1.1616
316	A8K854	50.432	1.1609
317	NUDC2	14.745	1.1606
318	RAB14	23.897	1.1602
319	B8ZWD6	10.044	1.1585
320	D6RIA2	94.622	1.1582
321	SRSF3	14.203	1.1582
322	B4DP82	45.498	1.156
323	B4E2I7	138.93	1.1554
324	ROD1	49.539	1.154
325	F5GWZ7	256.64	1.1531
326	E9PL19	54.024	1.1519
327	B4DUI3	23.026	1.1515
328	SCAM3	35.201	1.151
329	TM165	28.432	1.151
330	Q5JR89	75.561	1.1509
331	DFFA	29.41	1.1508
332	E7ESG8	35.594	1.1508
333	XPO2	107.78	1.1502
334	D6RGF4	67.314	1.1489
335	G3V4M8	27.821	1.1477
336	E9PGT0	358.2	1.1475
337	F8VQ14	57.488	1.1468
338	Q5T0S3	51.83	1.1453
339	WDR36	105.32	1.1448
340	DESP	331.77	1.1444
341	ZRAB2	36.318	1.1443
342	E9PCT1	36.739	1.1435
343	UBA6	65.756	1.1429
344	E9PLJ0	119.52	1.1407
345	Q5H918	82.021	1.1402
346	RAB35	21.214	1.1398
347	G3XAN0	13.373	1.1373
348	E5RJ89	9.9601	1.1357

349	G3V3U4	22.842	1.1351
350	B4DDM6	36.954	1.1347
351	Q5SRQ6	24.942	1.1335
352	E5RH77	16.273	1.1322
353	GLRX3	37.432	1.1315
354	RL23	9.6694	1.1314
355	CD63	14.265	1.1311
356	RAB5A	23.482	1.1306
357	Q71RF1	27.882	1.1305
358	E7EVU8	480.19	1.1302
359	C9JIJ5	29.225	1.129
360	C9JF79	23.038	1.1286
361	ELAV1	36.091	1.1284
362	B0QYA7	31.729	1.1259
363	CAB39	39.869	1.1256
364	AFAD	28.908	1.1233
365	B4E3P0	119.77	1.1226
366	TXND5	36.177	1.122
367	Q9BQ02	65.881	1.1219
368	F5GZS2	606.13	1.1216
369	E9PGR9	43.171	1.1213
370	GRPE1	24.279	1.1203
371	F6UXX1	62.656	1.1191
372	C9JCA9	157.9	1.1189
373	G3V2L6	67.673	1.1187
374	EXOSX	77.769	1.1184
375	E5RFP9	51.998	1.1181
376	1433B	27.85	1.1161
377	Q96II6	20.776	1.1156
378	DCNL1	14.665	1.1146
379	F8VZ45	25.892	1.114
380	SNAA	33.232	1.1137
381	D6RDJ1	43.614	1.1131
382	RIM3C	169.91	1.1125
383	F5H4R7	97.169	1.1117
384	G3V2F7	11.842	1.1114
385	E7EQY1	15.641	1.1098
386	PSA3	27.647	1.1091
387	MRP	19.529	1.1091
388	A8MUS3	17.695	1.1077
389	SPTA1	279.67	1.1072
390	B4DP62	34.012	1.1067
391	CATA	59.755	1.1064
392	RS17	15.55	1.1062
393	EIF3K	24.484	1.1056
394	NFH	53.651	1.1054
395	ISOC1	20.239	1.1045
396	G3V3W7	48.46	1.1034
397	YBOX2	35.924	1.1025
398	DCTP1	18.681	1.101

399	MTPN	5.7044	1.099
400	F5GXS4	107.47	1.099
401	E9PNS6	46.158	1.0985
402	SPTB2	80.939	1.0979
403	COF2	18.502	1.0972
404	CAZA1	32.922	1.0967
405	DHX15	89.502	1.0954
406	B4DGZ4	145.83	1.0942
407	SRSF8	23.195	1.0942
408	E7EQZ3	55.755	1.0935
409	B3KPQ8	93.487	1.0926
410	E9PN81	8.9569	1.0926
411	B4DKT0	39.768	1.0922
412	KTN1	18.469	1.092
413	G3V4T5	36.112	1.0917
414	SAR1A	13.265	1.0912
415	NSUN2	59.383	1.091
416	MT1G	6.1103	1.0903
417	ARP5L	16.941	1.0903
418	F8VV04	59.557	1.0902
419	TBL3	89.034	1.0877
420	E7ESY9	58.494	1.0861
421	GRB2	25.206	1.0848
422	F8VZY9	48.057	1.0845
423	B3KS31	46.701	1.0822
424	F8VZ69	41.746	1.081
425	PWP2	102.45	1.0799
426	E9PB61	26.888	1.0792
427	B7Z2F6	102.64	1.0789
428	Q9BUK9	94.33	1.0785
429	SRSF1	22.46	1.0771
430	TRM1L	81.746	1.0771
431	PSB7	29.965	1.077
432	B3KSH1	33.24	1.0768
433	F8W0F6	50.151	1.0761
434	SRSF4	56.678	1.076
435	SF3B4	44.385	1.0755
436	DLG1	97.075	1.0753
437	1433S	27.745	1.0751
438	CHCH8	10.134	1.0748
439	OBRG	14.254	1.0743
440	COX2	25.565	1.074
441	GUAA	65.928	1.0734
442	SNAG	25.662	1.0729
443	F5GZE5	44.644	1.0725
444	PRKRA	10.414	1.072
445	F8VVB7	53.248	1.071
446	DDX46	117.36	1.07
447	C9JTX5	41.736	1.0697
448	SRP09	10.112	1.0664

449	CX6B1	10.192	1.0652
450	G5EA30	6.5312	1.0633
451	AKP8L	71.648	1.063
452	SMN	24.38	1.0627
453	TR150	108.66	1.0626
454	PGAM5	28.02	1.0623
455	F8VTL3	229	1.0616
456	Q8N274	629.09	1.0608
457	B4DUP0	50.118	1.0602
458	CB029	55.215	1.0599
459	SMD3	13.291	1.0595
460	B0LM41	69.491	1.0595
461	ROA2	37.429	1.0583
462	CHM4B	24.95	1.0582
463	GBB4	37.331	1.0568
464	NIPA	5.0796	1.0561
465	CHCH9	15.512	1.056
466	Q5W0X3	11.951	1.0555
467	G3V461	42.644	1.0544
468	EIF1B	12.732	1.0537
469	Q5SWX9	267.29	1.0534
470	D6RDY6	67.879	1.0504
471	SNP29	17.963	1.0501
472	C9JSZ1	66.231	1.0498
473	HBAZ	15.637	1.0496
474	TADBP	44.739	1.0496
475	E9PRM1	81.889	1.0491
476	NOMO2	122.06	1.0482
477	RCC1	24.465	1.0466
478	VAPA	27.893	1.046
479	THOP1	78.839	1.0456
480	B1APP6	85.595	1.0427
481	B4DK71	19.309	1.0413
482	ARL15	22.876	1.0412
483	ALDOA	39.42	1.0411
484	B4DT72	59.767	1.0406
485	DNJB4	27.016	1.0405
486	ERAL1	48.349	1.0401
487	B4DRT2	22.008	1.0393
488	F6QR24	153.94	1.0387
489	SGTA	31.455	1.0375
490	EXOS7	31.821	1.0372
491	A6NHU0	52.228	1.0363
492	CIAO1	37.84	1.036
493	PCBP1	37.497	1.0357
494	F5H4J1	236.51	1.0346
495	PDCD4	50.576	1.0324
496	Q9C083	17.328	1.0322
497	H32	15.388	1.0314
498	A6NEC0	17.163	1.0307

499	E7EQS9	52.478	1.0307
500	Q4VY19	28.302	1.0298
501	B4DV51	24.423	1.0288
502	F6UVQ4	42.051	1.0285
503	RRMJ3	96.557	1.0285
504	SMC2	17.257	1.0278
505	TOP2B	174.38	1.0266
506	E7ETK2	22.677	1.0256
507	1433E	29.174	1.025
508	ZCCHV	77.902	1.0248
509	SKP1	18.72	1.0245
510	TRM1	69.305	1.0245
511	E3W975	17.506	1.024
512	A7YIK0	67.819	1.0227
513	GCN1L	292.75	1.0216
514	RU17	50.617	1.021
515	IF4A3	46.871	1.0209
516	B3KQ59	51.156	1.0209
517	E9PRB9	17.027	1.0206
518	SYUG	13.331	1.0204
519	IF2GL	51.109	1.0203
520	SF3A2	49.255	1.0198
521	F5GY66	37.621	1.0196
522	TOM70	56.93	1.0194
523	H14	21.865	1.019
524	G3V226	16.837	1.0181
525	NAMPT	55.52	1.0176
526	F5H063	119.91	1.0172
527	G3V5M2	32.118	1.0169
528	LAGE3	10.42	1.0166
529	E5RGZ4	47.168	1.0163
530	IR3IP	8.9687	1.0157
531	MYH14	226.53	1.0154
532	TXD17	13.941	1.015
533	A8MXH2	42.823	1.0148
534	MAGB2	35.277	1.0143
535	RU2B	25.486	1.0136
536	PUR1	7.8269	1.0129
537	PSA7L	27.887	1.0128
538	HPRT	24.579	1.0125
539	E5RI98	29.464	1.0125
540	PSB4	29.204	1.0123
541	CY1	35.422	1.0115
542	E9PIL8	98.169	1.0096
543	PSMD4	40.736	1.0093
544	F5GXA5	140.96	1.0091
545	RAP1A	17.682	1.0089
546	PPIF	16.541	1.0088
547	F8VZQ7	25.092	1.0088
548	D6RF62	45.651	1.0083

549	SLTM	61.413	1.0081
550	Q5STZ7	91.679	1.0075
551	E5RJD8	10.08	1.0074
552	STAT3	87.98	1.0071
553	GGCT	18.398	1.0069
554	PSD11	47.463	1.0065
555	E9PDU1	68.047	1.0059
556	A6NFX8	19.961	1.0059
557	C9J4X2	54.231	1.0046
558	C9JVV6	86.948	1.0045
559	VINC	116.72	1.0044
560	F8WEI7	14.716	1.0041
561	PPIB	23.742	1.0034
562	SDF2L	23.598	1.003
563	EIF2D	64.706	1.0028
564	HEMGN	55.34	1.0027
565	HNRH3	31.525	1.0022
566	DRG1	40.542	1.0017
567	B7Z9U9	29.116	1.0016
568	TPMT	28.18	1.0014
569	PRDX1	22.11	1.0007
570	E9PMN9	107.3	1.0006
571	IF5A2	16.832	0.99999
572	MYPT1	105.64	0.99977
573	T106B	11.652	0.99956
574	SNUT2	53.51	0.9992
575	E7EW37	101.31	0.99908
576	B4E2P2	20.161	0.9989
577	E7ESC6	123.91	0.99759
578	DNJC7	50.096	0.99719
579	B4E3C2	21.397	0.99702
580	INO1	44.786	0.99695
581	SMRC1	122.87	0.99653
582	B0QZ36	24.061	0.99585
583	IF1AY	14.455	0.99564
584	C9JKM9	123.38	0.99534
585	C9JGV6	23.31	0.99348
586	TLN2	269.76	0.99333
587	PGAM2	28.85	0.99185
588	AMPL	52.771	0.99118
589	E9PDP1	19.588	0.99014
590	B4E2V4	26.411	0.99009
591	C9JLK0	64.523	0.98957
592	F5H1U3	51.804	0.98888
593	A6NLN1	57.221	0.98852
594	F5H048	77.477	0.98847
595	Q8IV96	54.416	0.98836
596	G3V1V4	19.266	0.98812
597	C9JIG9	58.022	0.98736
598	TBA4B	48.328	0.98707

599	PYRG1	41.22	0.98705
600	CA031	9.4275	0.98703
601	PTTG	11.598	0.9868
602	B4DHP5	70.051	0.98646
603	Q9UQL5	80.272	0.98629
604	F5H3M7	41.331	0.98583
605	UBQL1	52.909	0.98558
606	IF4G2	98.149	0.98426
607	IPP2	8.9811	0.98371
608	SET	32.103	0.98371
609	F8WAR4	26.152	0.98359
610	Q5T6W1	48.562	0.98168
611	F5GXD8	62.639	0.9809
612	SRSF7	15.257	0.98081
613	PSB5	28.48	0.98043
614	D6RE09	60.67	0.98034
615	A8MXW0	23.207	0.97885
616	CDC5L	89.167	0.9781
617	RRP1	52.985	0.97655
618	B1AHD1	14.173	0.97511
619	PSD12	50.578	0.97452
620	PRP8	273.6	0.97443
621	B4DXP9	42.613	0.97438
622	D6RC54	69.007	0.97418
623	E5RH18	15.179	0.97399
624	GDIR2	9.792	0.97377
625	PPCE	80.699	0.97351
626	TRRAP	8.0471	0.97315
627	B4DV68	51.872	0.97233
628	CYTB	11.139	0.97231
629	NEUL	68.867	0.97223
630	ARC1B	40.949	0.97163
631	SRP14	14.57	0.971
632	LSM2	10.834	0.97097
633	E9PRB8	15.584	0.9705
634	TDIF2	17.215	0.96858
635	ADT1	32.866	0.96843
636	RBX1	12.274	0.96835
637	F8WB66	88.885	0.96823
638	KINH	109.68	0.96702
639	MARE1	29.999	0.96701
640	CNDP2	43.833	0.96666
641	E9PEF8	63.566	0.96599
642	G3V2N5	102.71	0.96586
643	LRC59	34.93	0.96483
644	NU155	148.09	0.96466
645	DDX27	15.024	0.96386
646	G5E975	38.77	0.96296
647	SMCA5	116.78	0.9626
648	B4DJ58	54.972	0.96202

649	B0UYU4	61.68	0.96112
650	NTF2	14.478	0.961
651	UCHL3	26.182	0.95936
652	TRA2B	21.935	0.95933
653	ORN	13.151	0.95878
654	LSM12	21.701	0.95729
655	F8VSH0	109.73	0.95643
656	ABL1	122.87	0.9556
657	Q5JUL1	11.777	0.95459
658	FIP1	40.834	0.95441
659	SMU1	39.343	0.95254
660	LRRF1	82.688	0.95192
661	AP2A1	105.36	0.95181
662	SNX3	14.766	0.95163
663	B4DPN6	82.431	0.95081
664	WDR1	66.193	0.95029
665	STRBP	95.337	0.95029
666	F8WED3	16.698	0.94951
667	E5RH09	75.378	0.94938
668	T126A	13.844	0.94758
669	ERH	8.2033	0.94658
670	AN32D	28.585	0.94612
671	CUTA	14.401	0.94607
672	TIM10	10.333	0.94607
673	PPM1G	57.342	0.94557
674	E9PND2	16.94	0.94552
675	PSDE	34.577	0.94519
676	NAA10	24.783	0.94373
677	RC0R3	53.027	0.94342
678	B1AMU3	16.79	0.94052
679	PSB1	26.489	0.93967
680	Q5RI18	88.979	0.93878
681	CHMP5	19.52	0.93873
682	F8VTZ0	29.737	0.93847
683	E9PFH4	97.371	0.9382
684	E7EM57	59.256	0.93819
685	B3KXH8	66.591	0.93815
686	PGK2	44.614	0.93793
687	EDC4	151.66	0.93723
688	E9PMI1	49.973	0.93607
689	SNX1	46.097	0.93499
690	AT5F1	22.275	0.93492
691	PPCE	80.699	0.93492
692	A8MU27	8.1111	0.93471
693	PPIL1	18.237	0.93399
694	Q5T7C0	18.311	0.93391
695	Q6UV22	45.531	0.93212
696	TIM50	39.646	0.93192
697	THIO	9.4519	0.93009
698	API5	37.507	0.93004

699	D6RDJ6	83.434	0.92995
700	E7EPI6	143.23	0.92703
701	E9PLX7	10.127	0.92673
702	SFPQ	76.149	0.92599
703	A8MWR8	35.54	0.92508
704	PAK3	58.042	0.92476
705	C9J165	82.245	0.92422
706	ROA3	34.102	0.92413
707	B4E0P5	244.5	0.92394
708	HACD3	36.43	0.92342
709	F8WDS6	23.735	0.92298
710	VASP	39.829	0.92294
711	Q8N5M0	49.129	0.92196
712	E9PRS3	44.204	0.92173
713	F8WEJ5	62.168	0.92147
714	SMC4	100.95	0.92123
715	D6RCF4	15.278	0.91928
716	Q567Q5	29.483	0.91876
717	RU1C	17.394	0.91854
718	LAP2A	75.491	0.91759
719	NDUA2	10.921	0.91758
720	CXCR3	45.522	0.91673
721	TMSL3	5.1127	0.91653
722	E7ETU3	21.258	0.91619
723	MYADM	15.935	0.91571
724	B7Z5D8	26.669	0.91544
725	B4E363	57.563	0.91503
726	B7Z5E2	48.633	0.91489
727	SURF6	41.45	0.91455
728	RBM25	100.18	0.91307
729	PARK7	19.891	0.91304
730	H2B1A	13.952	0.91272
731	ATG9A	87.378	0.91265
732	E9PPQ8	85.237	0.91234
733	PSD13	29.755	0.9121
734	B1Q2N1	48.991	0.91205
735	E7EWA5	22.171	0.91174
736	F184A	13.936	0.91159
737	F8WBW6	20.63	0.91139
738	C9J7D1	23.489	0.91103
739	E9PF41	44.76	0.90863
740	ATPD	17.49	0.90861
741	F8W791	148.4	0.90856
742	F5H673	41.824	0.90723
743	E9PEG8	55.224	0.90718
744	F5H8C9	49.906	0.90689
745	F5H5E4	36.297	0.90538
746	UBC12	20.9	0.9052
747	E7EQR4	69.412	0.90517
748	K1751	86.955	0.90482

749	B4DJ93	107.77	0.90471
750	CN142	10.859	0.90462
751	SF3A3	52.454	0.9043
752	F5H1I8	69.842	0.90402
753	D6RCQ0	15.548	0.90172
754	UBQL1	62.518	0.90109
755	B4DPJ6	19.901	0.9008
756	TTL12	73.547	0.9008
757	C9J8F3	39.455	0.90068
758	NXF1	13.25	0.89988
759	B4DJC3	39.183	0.89877
760	SSRD	18.998	0.89873
761	NADC	17.02	0.8981
762	KDM1A	92.902	0.89807
763	H4	11.367	0.89784
764	CALB2	30.025	0.89755
765	E7EW44	54.234	0.89705
766	PLRG1	23.52	0.89498
767	ASH2L	55.324	0.89469
768	ARP19	12.975	0.8945
769	CPSF7	26.148	0.89443
770	RENT1	123.03	0.89425
771	ANXA7	37.805	0.89276
772	E9PEC0	42.153	0.89255
773	B4E1K5	54.489	0.89244
774	RS15	17.04	0.89235
775	PSA	29.925	0.89217
776	PSB6	25.357	0.89211
777	Q5T446	40.786	0.89164
778	E9PB24	7.888	0.89102
779	ATP4A	113	0.89095
780	Q5HY57	28.994	0.89047
781	RFA2	19.433	0.88975
782	ADT2	32.852	0.88934
783	D6RGV5	9.3878	0.88911
784	CAND1	117.89	0.88905
785	O95485	28.415	0.88839
786	A8K0C0	21.892	0.8883
787	CLH2	187.89	0.88585
788	A8MX94	23.356	0.88567
789	CMBL	28.048	0.88532
790	DNJC9	29.909	0.88515
791	SRSF9	25.542	0.88512
792	B1AJY6	20.808	0.88493
793	CDC37	44.468	0.88316
794	PP1R8	22.71	0.88258
795	SMD2	13.527	0.88251
796	H2B2C	13.908	0.88093
797	XRCC5	82.704	0.88081
798	A2A3S1	31.566	0.88071

799	D6R9L5	38.704	0.87916
800	LRC47	63.472	0.87885
801	U2AF2	53.12	0.87857
802	E7ETR0	50.227	0.87844
803	HDDC2	8.1635	0.87811
804	B0YIW6	47.204	0.87794
805	FAF1	55.998	0.87784
806	E7EUJ4	57.936	0.87774
807	K1967	31.09	0.87701
808	DHX30	129.44	0.87685
809	ROMO1	5.8998	0.87664
810	LIS1	23.417	0.87638
811	B4DKS8	45.671	0.87592
812	GLRX5	16.628	0.87575
813	OGFR	52.43	0.87564
814	CRKL	33.777	0.87533
815	F5H503	15.936	0.87312
816	HEBP2	12.649	0.87309
817	B4DXW1	47.371	0.87297
818	F8WDB3	19.565	0.87275
819	F5H2F4	69.485	0.87241
820	F5H7A1	189.25	0.87225
821	E9PD07	42.621	0.87172
822	DYL2	10.35	0.86923
823	C9J0F2	20.683	0.86865
824	B4DEB1	15.43	0.86813
825	UBQL4	63.852	0.86772
826	Q5BJH1	50.435	0.86766
827	FPPS	40.532	0.8673
828	F5GX11	29.555	0.86664
829	KATL2	89.321	0.86648
830	C9JPC0	99.271	0.86552
831	LSM3	11.845	0.86529
832	DYHC1	532.4	0.86524
833	MYL9	19.794	0.86498
834	VATE1	22.706	0.86478
835	B4DDG1	17.861	0.86465
836	F8WF69	17.687	0.86418
837	NQO1	22.793	0.86413
838	TRAP1	74.267	0.86412
839	DOCK8	48.812	0.86376
840	ILF2	43.062	0.86331
841	IF2B	38.388	0.86293
842	PGM2	50.743	0.86287
843	F5HE57	53.928	0.86175
844	B4DNT0	42.741	0.86151
845	A8K092	59.75	0.86121
846	PGP	34.006	0.86096
847	B7Z8G2	51.212	0.86071
848	OTUB1	31.284	0.86041

849	FHL3	31.192	0.85967
850	SMD1	13.281	0.85918
851	PITH1	24.121	0.85916
852	MPCP	36.161	0.85909
853	SPEE	33.824	0.85891
854	NOL9	79.322	0.85791
855	F8W813	49.83	0.85758
856	USMG5	6.4575	0.85721
857	SODM	12.13	0.85597
858	E9PKD5	44.323	0.85587
859	F8VWV4	34.273	0.85503
860	HINT1	7.3235	0.85377
861	UBR4	571.85	0.85194
862	F110B	40.727	0.85187
863	RECQ1	73.457	0.8517
864	Q5TCU8	27.174	0.85157
865	B4E1Q0	56.849	0.8514
866	CLIC1	26.922	0.85026
867	ACPM	17.417	0.8493
868	PRS10	44.172	0.8487
869	E9PQI8	90.254	0.84826
870	PRC2A	145.94	0.84776
871	G3V110	17.302	0.84748
872	B4DZ61	140.46	0.84714
873	B4DRT4	21.057	0.84709
874	TSNAX	33.112	0.84665
875	RAC1	16.797	0.84638
876	F5H4U5	40.532	0.84525
877	ERP44	46.971	0.84416
878	PLIN3	46.946	0.84409
879	B7Z977	108.24	0.84394
880	Q5TCI8	74.139	0.84336
881	NUP53	11.723	0.84307
882	E7ERS3	39.064	0.84266
883	FBLL1	33.784	0.84208
884	G3V2X9	104.85	0.84186
885	MK03	36.432	0.84158
886	PRP4	58.32	0.84124
887	E7EU01	68.297	0.83993
888	DNJC8	29.841	0.83983
889	F5GXQ6	51.129	0.83941
890	DBPA	31.947	0.83929
891	G3XAH0	34.672	0.8387
892	LAS1L	81.242	0.83821
893	CISD1	12.199	0.83763
894	PNPT1	85.95	0.83749
895	ARMC1	11.335	0.83703
896	NDUS4	20.108	0.83582
897	NFYA	33.939	0.83531
898	B4DIC4	29.717	0.83525

899	F8WE98	280.01	0.83481
900	SMRD2	55.238	0.83463
901	HAUS5	32.638	0.83432
902	HPBP1	27.91	0.83365
903	HMG3M	24.033	0.83359
904	PA1B3	25.734	0.83199
905	E9PFW3	42.701	0.83141
906	C9J4N8	136.31	0.83122
907	RL21	18.565	0.83107
908	PSMD5	51.311	0.83069
909	F5H7Z1	73.62	0.83032
910	E9PBC7	26.304	0.82915
911	F5H456	132.71	0.82858
912	C9JQM9	57.136	0.82855
913	NUBP1	33.412	0.82854
914	F8VRV7	41.694	0.82769
915	A4D198	25.2	0.82762
916	A4D286	23.671	0.82663
917	VATL	15.736	0.82648
918	F5GXQ0	42.871	0.82563
919	F8VPP1	17.499	0.82547
920	EXOS3	17.247	0.82528
921	C1QBP	31.362	0.82499
922	UBP5	93.307	0.8247
923	F8WDZ1	119.7	0.82402
924	EI2BB	38.989	0.82397
925	UGPA	4.3668	0.82382
926	E9PDI8	66.049	0.82299
927	C9JAK5	14.553	0.82286
928	RAB4B	22.541	0.82238
929	A8K3Z3	45.626	0.82124
930	STT3A	69.588	0.82091
931	LSM5	7.0202	0.82075
932	UE2NL	17.138	0.82074
933	E5RFL1	30.658	0.82036
934	F2Z2K0	40.572	0.82003
935	F8W4S1	50.431	0.81991
936	MIRO2	68.117	0.81954
937	PRDX6	25.035	0.81949
938	VAPB	16.633	0.81877
939	COX5B	13.696	0.81825
940	KAD3	18.192	0.81778
941	G3V3T3	147.36	0.81742
942	PRS6B	43.507	0.81717
943	ARF5	17.107	0.81702
944	G3V4X1	41.167	0.81696
945	ATX10	14.209	0.81684
946	COPB2	99.045	0.81661
947	B1AKR6	10.921	0.81631
948	SIN3A	145.17	0.81611

949	F8W888	62.878	0.81575
950	FUMH	50.212	0.81573
951	B5MEG9	121	0.81571
952	11-Sep	49.005	0.81571
953	C9IYI4	17.752	0.81541
954	C9JT33	63.48	0.81507
955	E9PGI8	18.979	0.81466
956	ERO1A	19.154	0.81432
957	CT072	28.839	0.81402
958	PDS5A	150.83	0.81389
959	F5H1Y3	42.592	0.81373
960	RCC2	56.084	0.81277
961	CDV3	27.335	0.81216
962	B7Z2R2	13.53	0.8117
963	B4DNK3	34.352	0.81113
964	B4DQJ1	39.31	0.81113
965	A6NJ37	61.64	0.81112
966	KCC2B	33.295	0.81103
967	CLPP	30.18	0.81051
968	E9PBF6	66.408	0.81042
969	CCHL	30.601	0.80953
970	C9J2Q4	36.94	0.80953
971	E7EWT1	50.8	0.80935
972	E5RI06	50.496	0.80928
973	H33	15.328	0.80899
974	ATD3B	66.217	0.80863
975	B7Z8J4	48.14	0.80831
976	IDI1	26.319	0.80748
977	E7EQZ9	59.177	0.80652
978	ANM6	41.937	0.80567
979	RRS1	41.193	0.80548
980	TRI25	70.973	0.80485
981	LARP7	34.448	0.8046
982	E9PLC4	30.692	0.80377
983	F8VV40	59.732	0.80375
984	PRKDC	465.38	0.80161
985	E7EN38	138.43	0.80136
986	SPCS3	20.313	0.80103
987	FKBP8	44.561	0.80102
988	A8MUF7	16.203	0.80082
989	C9J363	15.59	0.80078
990	IGBP1	39.221	0.79955
991	GCSH	18.884	0.79931
992	A6NEL0	9.5355	0.7992
993	F8VVL1	22.092	0.79882
994	E9PMX3	14.763	0.79866
995	SRPRB	29.702	0.79823
996	MTX2	23.643	0.79748
997	NOP58	59.578	0.79543
998	TIM16	13.825	0.79379

999	E9PBP3	148.74	0.79376
1000	C9J1E7	98.117	0.79279
1001	E7ERW2	47.517	0.79262
1002	VPS35	76.211	0.79206
1003	D6RA36	16.156	0.79109
1004	E7ETM7	70.942	0.79059
1005	F5H6R6	23.076	0.79046
1006	UBAC1	45.338	0.79025
1007	B4E0P8	32.611	0.78957
1008	VATA	37.751	0.78947
1009	LYRIC	63.836	0.78855
1010	C9J2F8	11.216	0.78838
1011	E7ER14	30.772	0.7883
1012	EFHD2	26.697	0.78826
1013	F5H131	212.57	0.7876
1014	B4DL85	18.416	0.78544
1015	C9K0U8	15.713	0.78542
1016	LMNB2	67.688	0.78479
1017	MCM6	92.888	0.78471
1018	F5H4B2	14.095	0.78325
1019	CSN1	55.092	0.78313
1020	PDIP3	20.574	0.78312
1021	PI42B	46.224	0.78308
1022	F5GZ76	107.89	0.78304
1023	F8WDC9	35.243	0.78178
1024	GOGA2	70.472	0.78056
1025	F8WDM3	101.89	0.77983
1026	TOM40	37.893	0.77981
1027	E9PKI8	37.54	0.77981
1028	A6NMX6	44.812	0.7796
1029	Q1L6K6	66.294	0.77942
1030	E9PFP4	27.99	0.77929
1031	IDH3A	28.134	0.77675
1032	SNP23	23.354	0.77613
1033	PRDX4	29.353	0.77566
1034	BID	21.994	0.7751
1035	ZFR	115.15	0.77509
1036	B4DF41	17.308	0.77418
1037	TIF1B	88.549	0.77397
1038	E7ETI0	13.057	0.7736
1039	Q5JYR7	56.36	0.77282
1040	B8ZZ54	10.689	0.772
1041	C9K0M0	48.879	0.77026
1042	PEBB	21.508	0.76958
1043	RBM28	22.737	0.76934
1044	PTH2	19.193	0.76882
1045	F8VXU5	20.505	0.76805
1046	MK67I	19.553	0.76623
1047	F8WF32	65.89	0.7645
1048	E9PQM1	30.781	0.76444

1049	Q5T0G9	45.728	0.76444
1050	E5RI16	36.748	0.76444
1051	SMHD1	215.74	0.76415
1052	SRRT	96.221	0.76348
1053	RBM8A	19.76	0.76245
1054	CYFP1	51.533	0.76226
1055	C9J0S9	61.054	0.76122
1056	PPAC	18.042	0.76045
1057	TOM22	15.521	0.7604
1058	CAN2	71.475	0.76035
1059	C9JSW4	41.293	0.7599
1060	ECH1	35.816	0.75909
1061	CT011	17.563	0.75834
1062	G3V1N8	28.938	0.75813
1063	DIC	48.099	0.75793
1064	RPB1	217.17	0.75771
1065	ROAA	30.302	0.75683
1066	E9PIE4	17.641	0.75584
1067	C9JAM8	70.288	0.75546
1068	SC61G	7.7412	0.75538
1069	DHR11	12.585	0.75393
1070	B7WNL4	89.42	0.75367
1071	F5H1C6	75.429	0.75309
1072	F8WCA0	11.309	0.75278
1073	CAPG	36.248	0.75277
1074	TYB10	5.0256	0.75262
1075	F5H5C4	76.868	0.75253
1076	F8VQY0	56.559	0.75248
1077	E7EP96	73.114	0.75232
1078	AAAT	33.709	0.75225
1079	F5H1N1	57.196	0.7519
1080	B4DP75	29.723	0.75135
1081	PARN	52.988	0.75108
1082	B4DYP2	82.999	0.75088
1083	D6RBK0	29.804	0.75004
1084	SF3B3	135.58	0.74838
1085	SF01	59.711	0.74789
1086	F8W950	26.76	0.74752
1087	VATH	51.57	0.74717
1088	RHOG	21.308	0.74645
1089	H15	22.58	0.7462
1090	A4D1J9	287.28	0.7446
1091	B4DPK8	64.132	0.74409
1092	PRP6	102.43	0.74393
1093	LETM1	83.353	0.74382
1094	VPS25	20.747	0.74316
1095	G3V138	398.96	0.74273
1096	WIBG	22.704	0.74259
1097	G3V3F0	48.755	0.74258
1098	SERC	35.188	0.74228

1099	A8MUH2	12.587	0.74182
1100	RM49	19.198	0.74111
1101	E7EQD5	64.705	0.74094
1102	C9JNV2	11.905	0.74051
1103	RM41	15.383	0.73993
1104	F8WFD7	82.285	0.73954
1105	G3XAL0	35.503	0.73911
1106	EDF1	15.48	0.73866
1107	PCNP	18.925	0.73859
1108	FLII	130.7	0.73838
1109	Q5T0H9	22.949	0.738
1110	FIS1	16.937	0.73778
1111	GAR1	20.834	0.73775
1112	Q8WXC9	40.836	0.73702
1113	PTN1	41.26	0.73633
1114	KS6A1	72.697	0.73611
1115	PREB	38.939	0.73558
1116	CHTOP	21.918	0.73492
1117	NDUS1	66.921	0.73489
1118	A8MUW5	37.19	0.73458
1119	CHD4	215.31	0.73323
1120	HNRL2	85.104	0.73242
1121	CCNY	24.152	0.73239
1122	ACSL4	80.419	0.73148
1123	COPA	138.34	0.73069
1124	F5H4L5	60.838	0.73064
1125	Q5T5C7	58.777	0.73054
1126	Q5JRS0	117.85	0.72998
1127	B4DZT4	106.62	0.72958
1128	APT	14.557	0.72864
1129	UK114	11.825	0.72823
1130	C9JIF9	5.4681	0.72789
1131	E9PF11	90.98	0.72633
1132	TP4A2	2.63	0.72587
1133	F5GWQ7	61.557	0.72583
1134	F5H2L4	14.96	0.7256
1135	ATP5H	11.448	0.724
1136	F2Z2I8	33.337	0.72374
1137	ZW10	88.828	0.72199
1138	F5GZI0	55.939	0.72162
1139	Q5T6H2	62.138	0.72153
1140	TRA2A	12.951	0.72076
1141	IPO9	115.96	0.71936
1142	E9PKH6	20.656	0.7178
1143	CSTF3	75.108	0.71732
1144	QCR2	48.442	0.71721
1145	TTC1	33.526	0.71706
1146	DBNL	37.1	0.71687
1147	F2Z2W7	22.104	0.71557
1148	Q1W5D8	8.5076	0.71319

1149	TPM4	28.521	0.71301
1150	HNRL1	84.499	0.7126
1151	D6RD16	67.567	0.71176
1152	TEX10	90.716	0.71076
1153	LMAN1	57.548	0.71064
1154	C9IZ08	157.46	0.71037
1155	U5S1	105.38	0.70922
1156	Q5QPP2	26.391	0.70916
1157	A6NFY0	49.853	0.70896
1158	C9JMA6	55.874	0.70774
1159	ISOC2	14.765	0.70707
1160	IF2M	51.736	0.7066
1161	PDIA4	72.932	0.70605
1162	SMC3	141.54	0.70549
1163	F5H434	144.5	0.70548
1164	B4DW08	83.415	0.70354
1165	CA055	39.367	0.70225
1166	B4DHQ6	17.605	0.70219
1167	BAF	10.058	0.70153
1168	BCAT2	33.776	0.70151
1169	Q9BWA2	62.507	0.7015
1170	B1AKQ7	37.377	0.70081
1171	A8MRB2	29.096	0.7004
1172	CMC1	74.175	0.70024
1173	E7EN15	131.47	0.70017
1174	F5H015	62.942	0.69929
1175	F5H119	54.102	0.69918
1176	WASH6	47.989	0.69787
1177	C9IYT0	57.644	0.69778
1178	PPIG	40.299	0.6975
1179	BAX	18.129	0.69734
1180	C9J8M6	81.307	0.69704
1181	E9PGU4	41.887	0.69655
1182	TIM44	51.355	0.69622
1183	B9A067	83.677	0.69608
1184	Q6NX52	98.767	0.69456
1185	B2BCH7	21.445	0.69402
1186	UBE2K	14.035	0.69397
1187	B3KVK7	101.11	0.69344
1188	NFU1	10.443	0.6931
1189	D6RAE9	35.619	0.69273
1190	SRP54	48.67	0.69228
1191	NSF	71.583	0.69191
1192	SL9A6	74.161	0.69133
1193	FHOD1	81.333	0.69128
1194	CBX5	10.857	0.68998
1195	GLYC	53.454	0.68973
1196	B4DTC1	42.316	0.68938
1197	PRPK	13.659	0.68852
1198	ATPO	23.277	0.68784

1199	F8W1G0	28.993	0.68779
1200	ABCB7	77.12	0.68727
1201	MTDC	26.849	0.68713
1202	M2OM	28.494	0.68636
1203	E7EPW6	21.664	0.68616
1204	CYC	11.333	0.68571
1205	D6RJI2	72.4	0.68545
1206	E7EMY5	32.046	0.68419
1207	NDUA5	13.563	0.68396
1208	F8VXC8	124.84	0.68378
1209	TRXR1	50.666	0.68334
1210	TBCD	110.42	0.6833
1211	SBP1	9.1504	0.6829
1212	C9J386	13.509	0.68271
1213	G3V2K7	24.976	0.68244
1214	RN126	33.861	0.68117
1215	E9PF31	53.059	0.68
1216	RAC3	16.775	0.67989
1217	COTL1	15.945	0.67954
1218	PRP31	28.915	0.67883
1219	B4DUA5	55.395	0.67825
1220	SCOT1	56.157	0.67797
1221	GMFG	16.801	0.67708
1222	B4DDX8	20.198	0.67651
1223	PRDX3	25.838	0.67627
1224	FAF2	52.623	0.67623
1225	F5H8B1	43.835	0.67493
1226	TM214	17.61	0.67435
1227	DAZP1	40.529	0.6728
1228	B4DMN9	113.89	0.67263
1229	WDR46	68.04	0.67248
1230	KAT3	18.352	0.67243
1231	HCD2	17.224	0.67232
1232	RIR2	33.789	0.67192
1233	F5H218	64.033	0.67174
1234	6PGL	27.547	0.67166
1235	F8WB96	16.126	0.66951
1236	PDIA6	47.837	0.66899
1237	QCR1	52.645	0.66857
1238	E9PNH1	96.215	0.66674
1239	B0QYN7	18.007	0.66662
1240	E9PS48	30.241	0.66649
1241	KITH	25.468	0.66494
1242	D6RA32	270.63	0.66453
1243	G5E9U5	50.582	0.66289
1244	TRXR2	53.406	0.66247
1245	SMAP2	37.697	0.66162
1246	G5E977	57.578	0.66112
1247	VRK1	45.476	0.66066
1248	F5H4S7	46.51	0.66024

1249	E7EPT4	27.391	0.65852
1250	C9JXK0	70.702	0.65816
1251	E7ERK9	57.495	0.6579
1252	NHP2	15.017	0.6576
1253	B7Z1I2	46.247	0.65712
1254	C9J9M4	105.84	0.65691
1255	PO210	205.11	0.6561
1256	E7EMN0	170.59	0.65592
1257	F2Z2E3	48.881	0.65418
1258	TRIP6	50.287	0.65244
1259	G3V5D9	17.765	0.65222
1260	EFTU	49.541	0.65208
1261	TWF2	28.882	0.65154
1262	TM109	24.983	0.6513
1263	MISSL	24.269	0.65079
1264	SND1	101.21	0.65046
1265	ES1	24.757	0.6493
1266	ERLN2	37.725	0.64924
1267	B4DTQ6	123.28	0.64915
1268	GSTK1	20.538	0.64909
1269	E9PLP0	82.845	0.64859
1270	B4DDC7	31.279	0.64801
1271	F8WE76	19.88	0.64747
1272	BIEA	33.428	0.64729
1273	DDAH2	23.512	0.647
1274	ARI2	57.818	0.64695
1275	PA1B2	14.888	0.64437
1276	SC23A	86.478	0.64356
1277	E9PKF3	45.199	0.64329
1278	B3KY56	122.85	0.64272
1279	E9PBB7	26.761	0.64225
1280	NPL4	51.549	0.64216
1281	VATB1	56.5	0.6421
1282	NDUS2	26.97	0.64184
1283	B8ZZ75	37.765	0.64168
1284	LAP2B	46.306	0.64165
1285	ENPLL	92.468	0.64078
1286	RDH13	28.793	0.6388
1287	E9PPU0	555.61	0.63739
1288	B8ZZN6	6.6846	0.6352
1289	SYG	83.165	0.63478
1290	Q5T621	36.573	0.63423
1291	RBM42	47.025	0.6328
1292	UBP48	112.96	0.63223
1293	ARP19	12.323	0.63207
1294	IPYR2	21.39	0.63147
1295	F8WDU6	109.96	0.6308
1296	F5GYP4	68.058	0.62914
1297	HYES	42.102	0.62814
1298	Q5T946	35.668	0.62753

1299	GGEE3	10.42	0.62715
1300	FAH2B	34.596	0.62617
1301	B4E0Y9	39.657	0.62616
1302	SC61B	9.9743	0.62583
1303	CN166	22.703	0.62533
1304	E9PPD9	104.36	0.62423
1305	B4DT43	35.079	0.62259
1306	DECR	15.898	0.62221
1307	SPB9	42.403	0.62188
1308	EBP2	34.852	0.62162
1309	E9PPN1	18.641	0.62019
1310	ESTD	31.462	0.61952
1311	E5RFJ8	92.803	0.61941
1312	IDHP	45.179	0.61885
1313	PSPC1	45.57	0.61748
1314	AIBP	20.43	0.61656
1315	RSMB	23.656	0.61618
1316	E7EVD1	77.528	0.61555
1317	KIFC1	73.747	0.6147
1318	B7Z525	26.788	0.61438
1319	H1T	21.364	0.614
1320	C9J4N6	46.659	0.61368
1321	TRPV2	85.98	0.6132
1322	A8MX97	59.918	0.61299
1323	PEX14	34.216	0.61294
1324	SF3B5	10.135	0.61231
1325	E9PJM9	42.426	0.61179
1326	HBXIP	9.5279	0.61119
1327	F5H1F8	28.772	0.61037
1328	MBB1A	67.539	0.60987
1329	S10AB	11.74	0.60853
1330	GCP60	60.593	0.60756
1331	BLVRB	22.119	0.60625
1332	AP3D1	136.65	0.6054
1333	FLNB	256.28	0.60524
1334	ACTBL	42.003	0.6044
1335	C9JMZ3	68.168	0.60278
1336	D6R9G2	39.724	0.60273
1337	GLPC	11.499	0.60183
1338	JIP4	101.41	0.60091
1339	E9PP90	57.466	0.60017
1340	CNNM3	68.648	0.59864
1341	SC22B	24.593	0.59646
1342	DCXR	25.913	0.59604
1343	C9JA91	90.359	0.59453
1344	G3V3A4	61.494	0.59301
1345	Q5QPH3	45.545	0.59206
1346	SFR19	139.27	0.59142
1347	GOLP3	32.223	0.59117
1348	CPT2	73.776	0.59099

1349	C9JZI1	39.681	0.59078
1350	RT05	48.006	0.59041
1351	G3V1N2	15.257	0.58975
1352	F8WD96	44.552	0.58971
1353	Q5TBR1	40.307	0.58952
1354	MVD1	43.404	0.58863
1355	A8MTM1	30.375	0.58592
1356	CS010	18.795	0.58504
1357	RAVR1	77.859	0.58437
1358	NHRF1	29.44	0.58345
1359	PEA15	12.53	0.58301
1360	UFM1	9.1175	0.58281
1361	NDUV3	50.982	0.58224
1362	DHE4	54.286	0.58011
1363	UBXN4	55.055	0.57867
1364	LYPL1	24.476	0.57776
1365	RM55	15.128	0.57696
1366	E9PCR7	99.015	0.57689
1367	IF2B3	63.704	0.5758
1368	CSN3	45.726	0.57577
1369	F8WEA9	97.114	0.57517
1370	TF65	20.838	0.5749
1371	F8W180	15.021	0.57168
1372	PURA	34.91	0.57113
1373	NNMT	29.574	0.57112
1374	NECP2	11.325	0.5689
1375	ZN512	44.133	0.56879
1376	GFPT2	76.758	0.56844
1377	DJB11	40.513	0.56823
1378	RT31	45.318	0.56709
1379	PLCA	18.756	0.56276
1380	DHSO	38.324	0.56219
1381	TPM3	32.818	0.56156
1382	TMED4	27.277	0.55912
1383	E9PKQ1	107.14	0.55745
1384	A8MZ77	22.764	0.55648
1385	Q5TD05	21.537	0.55642
1386	Q9P0H9	18.388	0.55303
1387	CD11B	18.11	0.55299
1388	TCEA2	31.664	0.55264
1389	CEP41	14.384	0.54911
1390	DTD1	23.423	0.54743
1391	GSH0	30.727	0.54729
1392	HP1B3	61.206	0.54516
1393	PSIP1	37.725	0.54509
1394	PSMD9	9.4303	0.5449
1395	FKBP3	25.177	0.54483
1396	E9PF49	20.383	0.54314
1397	C9JTY3	40.691	0.54269
1398	GAG2E	12.763	0.54018

1399	BAZ1B	170.45	0.5396
1400	D6REQ8	38.258	0.53911
1401	RFC5	11.9	0.53868
1402	TOM6	8.0019	0.53838
1403	F5H0X9	68.996	0.53741
1404	DYN3	97.553	0.53647
1405	RM04	29.502	0.53637
1406	E9PHT9	24.698	0.53422
1407	C9JGM7	43.193	0.534
1408	STX7	24.554	0.53379
1409	E2QRB3	33.36	0.53366
1410	MAGD2	55.795	0.5307
1411	B2CL2	31.496	0.52883
1412	ALDH2	40.793	0.52822
1413	LAT1	55.01	0.52697
1414	3HIDH	35.329	0.52587
1415	D3DRA3	23.708	0.52535
1416	SATT	24.619	0.52512
1417	HMGA1	11.676	0.52502
1418	TXLNA	61.89	0.52489
1419	COPE	28.772	0.51992
1420	NDUB7	16.402	0.51949
1421	E9PSI5	104.78	0.5192
1422	NDUBB	17.316	0.51758
1423	A2AB10	31.789	0.51756
1424	SCMC1	51.354	0.51744
1425	NDUB8	12.323	0.51607
1426	E9PEW9	63.254	0.51571
1427	EI2BE	11.243	0.51326
1428	ETFB	27.843	0.51271
1429	K6PL	85.018	0.51241
1430	F5H1Q9	37.106	0.5122
1431	F8W031	11.662	0.5117
1432	IN35	31.546	0.51074
1433	NEUA	48.379	0.5075
1434	MBOA7	44.732	0.50698
1435	ODC	33.116	0.5063
1436	Q5T8R5	53.944	0.50523
1437	A8MX49	49.83	0.50343
1438	E7EUD8	33.637	0.5014
1439	PGRC2	23.818	0.50108
1440	ATRAP	16.669	0.50068
1441	ACAD9	53.933	0.49795
1442	RAD21	7.77	0.49728
1443	SUCA	36.249	0.49364
1444	NOL6	77.637	0.49056
1445	E7ETK8	106.81	0.49052
1446	D6RDU5	42.894	0.48905
1447	DHB11	28.074	0.48664
1448	PSB3	22.949	0.48545

1449	SPT5H	96.913	0.48378
1450	B4E2Y9	48.141	0.47943
1451	MANF	20.7	0.47784
1452	A6PVS0	28.356	0.47716
1453	A8MV58	40.372	0.47473
1454	D6RG17	97.717	0.47447
1455	HEMH	47.862	0.47352
1456	PCKGM	70.729	0.4721
1457	C9JMV9	37.596	0.47178
1458	E9PF86	59.851	0.46927
1459	ATP5L	8.4518	0.46664
1460	CORO7	76.604	0.46654
1461	HMGB3	17.522	0.4664
1462	NIT1	31.858	0.46093
1463	E9PDV0	44.508	0.45894
1464	SYYC	59.143	0.45702
1465	G3V0F2	48.056	0.45684
1466	E7ETR5	49.485	0.45672
1467	NDUB4	8.0551	0.4527
1468	PYGL	93.133	0.45206
1469	A6NC19	17.031	0.45115
1470	F5GYN9	56.65	0.44942
1471	ACOT9	43.206	0.44871
1472	UBFD1	33.382	0.44628
1473	ST1A3	22.069	0.44437
1474	B0AZP7	41.92	0.44342
1475	AGK	43.796	0.44278
1476	MDC1	178.87	0.44276
1477	LARP1	69.902	0.44192
1478	KAP0	42.981	0.44016
1479	SERB	20.745	0.43716
1480	ECI1	30.895	0.43178
1481	G3XAE1	109.03	0.43086
1482	ARMX3	42.5	0.42992
1483	ECHM	31.387	0.42943
1484	E7EWR4	46.665	0.4267
1485	G3V2Y7	48.179	0.42466
1486	B4DEF7	72.332	0.41846
1487	CLIP1	54.165	0.41338
1488	INCE	104.99	0.41336
1489	A6NJD0	42.272	0.41164
1490	RTN4	40.317	0.41125
1491	BT3L4	10.905	0.40613
1492	G3V3D1	13.078	0.40435
1493	NUDT4	20.306	0.40378
1494	FRIH	12.876	0.40291
1495	ZN326	65.653	0.40094
1496	B7Z7L3	13.675	0.40091
1497	CT47B	30.1	0.40077
1498	LONM	85.64	0.39983

1499	C9J8T6	6.9151	0.39901
1500	B7Z3I2	65.565	0.3951
1501	THUM1	39.315	0.39134
1502	B2L13	34.6	0.38716
1503	D6RBW1	25.097	0.38481
1504	MECP2	53.323	0.38069
1505	TOPK	36.085	0.37935
1506	SNF8	11.602	0.37044
1507	B7Z6L5	46.91	0.36868
1508	MARE3	24.582	0.36594
1509	E9PHK9	144.31	0.36565
1510	A6NJG9	28.723	0.36244
1511	GOGA3	167.35	0.36153
1512	NUDT3	19.471	0.35655
1513	SON	73.883	0.34934
1514	HIG2A	11.528	0.34559
1515	H1X	22.487	0.3451
1516	E9PCI5	17.135	0.33
1517	CSTFT	64.436	0.32306
1518	C9JRJ8	41.013	0.32071
1519	F8W930	54.721	0.3067
1520	ROA3	39.594	0.30428
1521	PGRC1	15.879	0.29636
1522	PDXK	29.245	0.28711
1523	GAGE1	12.978	0.2832
1524	NIBAN	103.13	0.27827
1525	F107B	6.2011	0.2752
1526	E9PBU9	82.98	0.27087
1527	RENBP	47.065	0.25065
1528	COR1A	51.026	0.24923
1529	HCLS1	49.704	0.24227
1530	UTP15	7.4134	0.20757
1531	RTN3	12.747	0.20322
1532	K1C9	62.064	0.17342
1533	SPR2G	7.9053	0.14774
1534	K22E	65.432	0.14256
1535	S100P	10.4	0.12833
1536	T2FA	14.685	0.11412
1537	DHRS2	23.818	0.10367
1538	K2C1B	66.038	0.093844
1539	K1C24	58.826	0.091785
1540	PTPC1	84.456	0.029713
1541	B7WNR0	69.366	0.028723

Table S2. Signaling pathways for the target proteins regulated by ALS in K562 cells

Ingenuity canonical pathways	-Log*P*	Molecules
EIF2 signaling	2.29E01	RPL27A, EIF2B4, MAPK1, RPS8, EIF4G1, EIF4E, EIF2A, RPL7, RPL7A, EIF3B, RPS20, RPS13, EIF3D, RPL23A, RPL31, RPL13, RPS24, RPL32, PABPC1, RPL4, RPS2, RPL17, RPL29, RPS10, EIF3J, RPS21, RPL9, RPLP0, RPS6, RPL15, EIF3F, RPS16, RPL28, EIF3L, RPL13A, RPS14
Regulation of eIF4 and p70S6K signaling	1.18E01	PABPC1, EIF2B4, MAPK1, RPS2, RPS10, EIF3J, RPS8, RPS21, EIF4G1, EIF4E, EIF2A, RPS6, PPP2CB, EIF3F, RPS16, EIF3B, RPS20, RPS13, EIF3D, EIF3L, RPS14, RPS24
Protein ubiquitination pathway	1.14E01	USP14, HSPA5, TCEB2, PSMC5, PSMD10, HSPE1, UCHL5, SUGT1, PSMC2, PSMA6, USP15, USP19, PSMD6, PSMA1, PSMD3, DNAJC11, HSPA8, PSMC1, PSME1, UBE2L3, PSMD2, PSMA5, PSMA4, HSP90AA1, PSMD4, UBC, PSMC3, UBE2I
mTOR signaling	8.82E00	MAPK1, RPS2, RPS10, EIF3J, RPS8, FKBP1A, RPS21, EIF4G1, EIF4E, RPS6, PPP2CB, EIF3F, RPS16, EIF3B, RPS20, RPS13, EIF3D, EIF3L, RPS24, RPS14, EIF4B
Mitochondrial dysfunction	8.74E00	ATP5J, NDUFV1, COX17, PRDX5, ATP5A1, ACO2, VDAC3, CYB5R3, UQCRB, NDUFB10, VDAC2, GSR, NDUFB9, NDUFS8, NDUFV2, ATP5B, COX7A2, NDUFA10, OGDH, VDAC1
Signaling by Rho family GTPases	6.48E00	ACTR2, SEPT5, CFL1, MAPK1, ACTB, SEPT7, GNB2L1, RDX, VIM, ARHGEF1, SEPT11, STMN1, ACTA2, CDC42, EZR, GNB2, ARHGEF2, PIP4K2A, ARPC4, SEPT2
RhoGDI signaling	5.75E00	GDI1, ACTR2, CFL1, ACTB, GNB2L1, RDX, GDI2, ARHGEF1, ACTA2, CDC42, EZR, GNB2, ARHGEF2, ARHGDIA, PIP4K2A, ARPC4
tRNA charging	5.71E00	NARS, LARS, CARS, DARS, TARS, SARS, MARS, FARSA
RhoA signaling	5.46E00	ACTR2, SEPT5, CFL1, ACTB, SEPT7, RDX, ARHGEF1, SEPT11, ACTA2, EZR, PIP4K2A, SEPT2, ARPC4
Superpathway of methionine degradation	5.36E00	CBS/LOC102724560, PRMT5, DLD, GOT1, CTH, GOT2, AHCY
Oxidative phosphorylation	5.19E00	ATP5J, NDUFV1, NDUFB9, COX17, ATP5B, NDUFV2, NDUFS8, ATP5A1, COX7A2, NDUFA10, NDUFB10, UQCRB
Aspartate degradation II	5.09E00	GOT1, MDH1, MDH2, GOT2
Actin cytoskeleton signaling	5.09E00	MYH10, ACTR2, CFL1, MAPK1, ACTB, RDX, ARHGEF1, TLN1, GSN, DIAPH1, ACTA2, CDC42, FLNA, EZR, PIP4K2A, ARPC4, ACTN1
TCA cycle II (eukaryotic)	5.06E00	ACO2, DLST, DLD, MDH1, MDH2, OGDH
Nrf2-mediated oxidative stress response	4.87E00	USP14, MAPK1, ACTB, NQO2, GSTO1, DNAJC11, GSR, ERP29, ACTA2, STIP1, CCT7, DNAJA3, FKBP5, CBR1, GSTP1
Gluconeogenesis I	4.83E00	PGK1, GPI, GAPDH, MDH1, MDH2, ALDOC
Clathrin-mediated endocytosis signaling	4.73E00	ACTR2, AP2M1, RAB5C, ACTB, RAB7A, HSPA8, SNX9, ACTA2, CDC42, CLTA, TFRC, CSNK2B, UBC, CTTN, ARPC4
Remodeling of epithelial adherens junctions	4.71E00	ACTR2, TUBB3, RAB5C, TUBB6, ACTA2, ACTB, RAB7A, ACTN1, ARPC4
RAN signaling	4.57E00	KPNB1, TNPO1, RANGAP1, RAN, RANBP1
2-Ketoglutarate dehydrogenase complex	4.36E00	DLST, DLD, OGDH
Huntington's disease signaling	4.19E00	ATP5J, MAPK1, HDAC1, GNB2L1, HSPA5, PSME3, TGM2, HSPA8, CTSD, DYNC1I2, PSME1, ATP5B, CLTA, GNB2, POLR2H, UBC
Regulation of actin-based motility by Rho	3.7E00	ACTR2, CFL1, ACTA2, CDC42, ACTB, ARHGDIA, GSN, PIP4K2A, ARPC4
Caveolar-mediated endocytosis signaling	3.7E00	COPZ1, ARCN1, RAB5C, ACTA2, FLNA, ACTB, FLOT1, COPB1
Glycolysis I	3.7E00	PGK1, GPI, GAPDH, PFKP, ALDOC
Ephrin B signaling	3.66E00	MAPK1, CFL1, CDC42, GNB2L1, GNB2, CAP1, ACP1, HNRNPK
Epithelial adherens junction signaling	3.35E00	RAP1B, MYH10, ACTR2, TUBB3, TUBB6, ACTA2, CDC42, ACTB, CLINT1, ACTN1, ARPC4
Cysteine biosynthesis/homocysteine degradation	3.3E00	CBS/LOC102724560, CTH
Cysteine biosynthesis III (mammalian)	3.23E00	CBS/LOC102724560, PRMT5, CTH, AHCY
ILK signaling	3E00	PPP2CB, MYH10, MAPK1, CFL1, ACTA2, FLNA, CDC42, ACTB, VIM, KRT18, ACTN1, NACA
Hereditary breast cancer signaling	2.95E00	NPM1, RFC4, HDAC1, MSH6, RFC2, POLR2H, UBC, CDK1, RAD50
FcγReceptor-mediated phagocytosis in macrophages and monocytes	2.95E00	ACTR2, MAPK1, ACTA2, CDC42, EZR, ACTB, TLN1, ARPC4
Aryl hydrocarbon receptor signaling	2.92E00	TGM2, CTSD, MAPK1, NQO2, ALDH1A2, HSP90AA1, GSTP1, PTGES3, GSTO1, MCM7
Unfolded protein response	2.9E00	HSPA8, CALR, P4HB, CANX, HSPA5, EIF2A

Breast cancer regulation by stathmin1	2.9E00	PPP2CB, CALM1 (includes others), STMN1, TUBB3, TUBB6, MAPK1, CDC42, GNB2L1, GNB2, ARHGEF1, ARHGEF2, CDK1
Inosine-5'-phosphate biosynthesis II	2.83E00	PAICS, ATIC
Oxidized GTP and dGTP detoxification	2.83E00	DDX6, RUVBL2
Glutamate degradation II	2.83E00	GOT1, GOT2
Aspartate biosynthesis	2.83E00	GOT1, GOT2
Purine nucleotides de novo biosynthesis II	2.68E00	PAICS, ATIC, GART
Lipid antigen presentation by CD1	2.6E00	CALR, AP2M1, PSAP, CANX
L-cysteine degradation I	2.54E00	GOT1, GOT2
Germ cell-sertoli cell junction signaling	2.49E00	TUBB3, TUBB6, MAPK1, CFL1, ACTA2, CDC42, ACTB, CLINT1, GSN, ACTN1
Isoleucine degradation I	2.47E00	HADHB, BCAT1, DLD
Virus entry via endocytic pathways	2.42E00	AP2M1, ACTA2, FLNA, CDC42, CLTA, ACTB, TFRC
Tetrahydrofolate salvage from 5,10-methenyltet-rahydrofolate	2.32E00	MTHFD1, GART
Folate polyglutamylation	2.32E00	MTHFD1, SHMT2
Mismatch repair in eukaryotes	2.3E00	RFC4, MSH6, RFC2
Integrin signaling	2.23E00	RAP1B, ACTR2, MAPK1, ACTA2, ARF3, CDC42, ACTB, TLN1, CTTN, ACTN1, ARPC4
Pentose phosphate pathway (non-oxidative branch)	2.15E00	TKT, TALDO1
Valine degradation I	2.15E00	HADHB, BCAT1, DLD
Role of CHK proteins in cell cycle Checkpoint control	2.12E00	PPP2CB, RFC4, RFC2, CDK1, RAD50
Regulation of cellular mechanics by calpain protease	2.06E00	MAPK1, EZR, TLN1, CDK1, ACTN1
Acetyl-CoA biosynthesis (pyruvate dehydrogenase complex)	2.01E00	DLAT, DLD
fMLP signaling in neutrophils	1.97E00	CALM1 (includes others), ACTR2, MAPK1, CDC42, GNB2L1, GNB2, ARPC4
Androgen signaling	1.91E00	CALM1 (includes others), CALR, MAPK1, GNB2L1, GNB2, HSP90AA1, POLR2H
Tight junction signaling	1.89E00	PPP2CB, MYH10, EPB41, ACTA2, CDC42, ACTB, CSTF2, ARHGEF2, SAFB
Mechanisms of viral exit from host cells	1.89E00	ACTA2, ACTB, PDCD6IP, LMNB1
Hypoxia signaling in the cardiovascular system	1.82E00	P4HB, UBE2L3, SUMO1, HSP90AA1, UBE2I
14-3-3-Mediated signaling	1.79E00	YWHAQ, TUBB3, YWHAG, TUBB6, MAPK1, VIM, PDCD6IP
Sucrose degradation V (mammalian)	1.79E00	GALM, ALDOC
Leucine degradation I	1.79E00	BCAT1, ACADM
UDP-*N*-acetyl-D-galactosamine biosynthesis II	1.79E00	GPI, PGM3
Folate transformations I	1.79E00	MTHFD1, SHMT2
Ephrin receptor signaling	1.78E00	RAP1B, ACTR2, MAPK1, CFL1, CDC42, GNB2L1, GNB2, ACP1, ARPC4
Sertoli cell-sertoli cell junction signaling	1.72E00	EPB41, TUBB3, TUBB6, MAPK1, ACTA2, CDC42, ACTB, CLINT1, ACTN1
Agrin interactions at neuromuscular junction	1.72E00	MAPK1, ACTA2, CDC42, ACTB, CTTN
Aldosterone signaling in epithelial cells	1.68E00	HSPA8, MAPK1, HSPE1, HSP90AA1, HSPA5, PIP4K2A, DNAJC11, AHCY
Renal cell carcinoma signaling	1.67E00	SLC2A1, MAPK1, CDC42, UBC, TCEB2
Acetyl-CoA biosynthesis III (from citrate)	1.65E00	ACLY
L-cysteine degradation II	1.65E00	CTH

Asparagine biosynthesis I	1.65E00	ASNS
Glutaryl-CoA degradation	1.62E00	HADHB, HSD17B4
Pentose phosphate pathway	1.62E00	TKT, TALDO1
HIF1αsignaling	1.57E00	SLC2A1, MAPK1, HSP90AA1, TCEB2, APEX1, LDHB
Paxillin signaling	1.57E00	MAPK1, ACTA2, CDC42, ACTB, TLN1, ACTN1
Fatty acidβ-oxidation I	1.54E00	HADHB, HSD17B4, ACADM
Rac signaling	1.53E00	ACTR2, MAPK1, CFL1, CDC42, PIP4K2A, ARPC4
NAD phosphorylation and dephosphorylation	1.48E00	NNT, ACP1
Leukocyte extravasation signaling	1.47E00	RAP1B, MAPK1, ACTA2, CDC42, EZR, ACTB, RDX, CTTN, ACTN1
DNA double-strand break repair by non-homologous end joining	1.42E00	XRCC6, RAD50
Phenylalanine degradation IV (mammalian, via side chain)	1.42E00	GOT1, GOT2
Vitamin-C transport	1.42E00	SLC2A1, GSTO1
Phospholipase C signaling	1.37E00	RAP1B, TGM2, PEBP1, CALM1 (includes others), MAPK1, GNB2L1, HDAC1, GNB2, ARHGEF1, ARHGEF2
Telomere extension by telomerase	1.37E00	XRCC6, RAD50
L-cysteine degradation III	1.35E00	GOT1
Glycine biosynthesis I	1.35E00	SHMT2
Calcium signaling	1.33E00	RAP1B, CALM1 (includes others), MYH10, CALR, MAPK1, ACTA2, HDAC1, TPM3
Granzyme B signaling	1.31E00	NUMA1, LMNB1
Oxidative ethanol degradation III	1.31E00	ALDH1A2, ACSS2
Methionine degradation I (to homocysteine)	1.31E00	PRMT5, AHCY
Parkinson's signaling	1.31E00	SEPT5, MAPK1
Antiproliferative role of somatostatin Receptor 2	1.28E00	RAP1B, MAPK1, GNB2L1, GNB2
VEGF signaling	1.27E00	EIF2B4, MAPK1, ACTA2, ACTB, ACTN1
Role of BRCA1 in DNA damage response	1.26E00	RFC4, MSH6, RFC2, RAD50
PI3K/AKT signaling	1.24E00	YWHAQ, PPP2CB, YWHAG, MAPK1, HSP90AA1, EIF4E
ERK/MAPK signaling	1.23E00	RAP1B, YWHAQ, PPP2CB, YWHAG, MAPK1, TLN1, EIF4E, KSR1
Systemic lupus erythematosus signaling	1.23E00	SNRPA, PRPF19, MAPK1, PRPF3, LSM1, NHP2L1, HNRNPC, SNRPA1, SNRNP40
Glutathione redox reactions I	1.22E00	GSR, CLIC2
Ethanol degradation IV	1.22E00	ALDH1A2, ACSS2
NADH repair	1.18E00	GAPDH
Glutathione biosynthesis	1.18E00	GSS
Ascorbate recycling (cytosolic)	1.18E00	GSTO1
Glutathione redox reactions II	1.18E00	GSR
Thyroid hormone biosynthesis	1.18E00	CTSD
Estrogen receptor signaling	1.18E00	DDX5, PELP1, MAPK1, PHB2, POLR2H, HNRNPD
CCR5 signaling in macrophages	1.16E00	CALM1 (includes others), MAPK1, GNB2L1, GNB2
Glucocorticoid receptor signaling	1.16E00	HSPA8, MAPK1, SUMO1, ANXA1, HSP90AA1, POLR2H, FKBP5, HSPA5, PTGES3, UBE2I
Telomerase signaling	1.15E00	PPP2CB, MAPK1, HDAC1, HSP90AA1, PTGES3
DNA methylation and transcriptional repression signaling	1.14E00	HDAC1, RBBP7

Granzyme A signaling	1.14E00	HMGB2, APEX1
Tryptophan degradation III (eukaryotic)	1.14E00	HADHB, HSD17B4
Endoplasmic reticulum stress pathway	1.1E00	CALR, HSPA5
Polyamine regulation in colon cancer	1.07E00	PSME1, PSME3
Arsenate detoxification I (glutaredoxin)	1.06E00	GSTO1
Creatine-phosphate biosynthesis	1.06E00	CKB
Branched-chain α-keto acid dehydrogenase complex	1.06E00	DLD
Heme biosynthesis from uroporphyrinogen-III	1.06E00	UROD
5-aminoimidazole ribonucleotide Biosynthesis I	1.06E00	GART
Proline biosynthesis I	1.06E00	PYCR1
Cell cycle: G_2/M DNA damage checkpoint regulation	1.02E00	YWHAQ, YWHAG, CDK1
Role of tissue factor in cancer	9.99E-01	P4HB, MAPK1, CFL1, CDC42, EIF4E
2-Oxobutanoate degradation I	9.71E-01	DLD
Galactose degradation I (leloir pathway)	9.71E-01	GALM
dTMP de novo biosynthesis	9.71E-01	SHMT2
Acetate conversion to acetyl-CoA	9.71E-01	ACSS2
Antiproliferative role of TOB in T cell signaling	9.43E-01	PABPC1, MAPK1
CCR3 signaling in eosinophils	9.15E-01	CALM1 (includes others), MAPK1, CFL1, GNB2L1, GNB2
Proline biosynthesis II (from arginine)	8.97E-01	PYCR1
Pyruvate fermentation to lactate	8.97E-01	LDHB
Arginine degradation VI (arginase 2 pathway)	8.97E-01	PYCR1
Glycine cleavage complex	8.97E-01	DLD
Selenocysteine biosynthesis II (archaea and eukaryotes)	8.97E-01	SARS
UDP-*N*-acetyl-D-glucosamine biosynthesis II	8.97E-01	PGM3
GDP-mannose biosynthesis	8.97E-01	GPI
p70S6K signaling	8.93E-01	YWHAQ, RPS6, PPP2CB, YWHAG, MAPK1
Glutathione-mediated detoxification	8.9E-01	GSTP1, GSTO1
Superpathway of cholesterol biosynthesis	8.9E-01	HADHB, DHCR7
Actin nucleation by ARP-WASP complex	8.88E-01	ACTR2, CDC42, ARPC4
α-Adrenergic signaling	8.85E-01	CALM1 (includes others), MAPK1, GNB2L1, GNB2
FAK signaling	8.85E-01	MAPK1, ACTA2, ACTB, TLN1
Gβγ signaling	8.72E-01	MAPK1, CDC42, GNB2L1, GNB2
Gap junction signaling	8.72E-01	DBN1, TUBB3, TUBB6, MAPK1, ACTA2, ACTB
Role of p14/p19ARF in tumor suppression	8.41E-01	NPM1, SF3A1
Superpathway of serine and glycine biosynthesis I	8.35E-01	SHMT2
GDP-glucose biosynthesis	8.35E-01	PGM3
Xenobiotic metabolism signaling	8.18E-01	PPP2CB, MAPK1, NQO2, SUMO1, ALDH1A2, HSP90AA1, GSTP1, PTGES3, GSTO1
Glucose and glucose-1-phosphate degradation	7.82E-01	PGM3

Histidine degradation III	7.82E-01	MTHFD1
ERK5 signaling	7.79E-01	YWHAQ, YWHAG, WNK1
G protein signaling mediated by tubby	7.76E-01	GNB2L1, GNB2
Ethanol degradation II	7.76E-01	ALDH1A2, ACSS2
Cdc42 signaling	7.66E-01	ACTR2, DIAPH1, MAPK1, CFL1, CDC42, ARPC4
IGF-1 signaling	7.65E-01	YWHAQ, YWHAG, MAPK1, CSNK2B
Insulin receptor signaling	7.42E-01	EIF2B4, MAPK1, ACLY, VAMP2, EIF4E
Mitotic roles of polo-like kinase	7.38E-01	PPP2CB, HSP90AA1, CDK1
tRNA splicing	7.36E-01	TSEN15, APEX1
Nucleotide excision repair pathway	7.36E-01	POLR2H, RAD23B
Prostanoid biosynthesis	7.35E-01	PTGES3
Phosphatidylethanolamine biosynthesis II	7.35E-01	PCYT2
Heme biosynthesis II	7.35E-01	UROD
Ketolysis	7.35E-01	HADHB
Relaxin signaling	7.33E-01	RAP1B, MAPK1, GNB2L1, GNB2, APEX1
Antigen presentation pathway	6.99E-01	CALR, CANX
RAR activation	6.96E-01	RPL7A, MAPK1, ALDH1A2, SNW1, CSNK2B, PSMC5
Ketogenesis	6.94E-01	HADHB
Glycogen degradation II	6.94E-01	PGM3
Glycine betaine degradation	6.94E-01	SHMT2
Chemokine signaling	6.75E-01	CALM1 (includes others), MAPK1, CFL1
D-myo-inositol-5-phosphate metabolism	6.65E-01	NUDT5, ACP1, PPM1F, PIP4K2A, SACM1L
Cleavage and polyadenylation of Pre-mRNA	6.24E-01	CSTF2
Glycogen degradation III	6.24E-01	PGM3
BER pathway	6.24E-01	APEX1
Protein kinase A signaling	6.17E-01	RAP1B, YWHAQ, CALM1 (includes others), MYH10, YWHAG, MAPK1, FLNA, GNB2L1, GNB2, ACP1, APEX1
PDGF signaling	6.07E-01	MAPK1, ACP1, CSNK2B
VDR/RXR activation	5.97E-01	SERPINB1, CALB1, PSMC5
Cyclins and cell cycle regulation	5.97E-01	PPP2CB, HDAC1, CDK1
Assembly of RNA polymerase III complex	5.94E-01	SF3A1
Cholesterol biosynthesis I	5.94E-01	DHCR7
Mevalonate pathway I	5.94E-01	HADHB
Cholesterol biosynthesis II (via 24, 25-dihydrolanosterol)	5.94E-01	DHCR7
Histamine degradation	5.94E-01	ALDH1A2
Cholesterol biosynthesis III (via Desmosterol)	5.94E-01	DHCR7
iNOS signaling	5.89E-01	CALM1 (includes others), MAPK1
Axonal guidance signaling	5.8E-01	RAP1B, ACTR2, TUBB3, TUBB6, MAPK1, CFL1, CDC42, GNB2L1, RTN4, GNB2, ARPC4, EIF4E
Ceramide signaling	5.77E-01	CTSD, PPP2CB, KSR1
3-phosphoinositide biosynthesis	5.75E-01	NUDT5, ACP1, PPM1F, PIP4K2A, SACM1L
CD28 signaling in T helper cells	5.68E-01	CALM1 (includes others), ACTR2, CDC42, ARPC4

DNA double-strand break repair by homologous recombination	5.67E-01	RAD50
Leukotriene biosynthesis	5.67E-01	LTA4H
Colanic acid building blocks biosynthesis	5.67E-01	GPI
γ-glutamyl cycle	5.67E-01	GSS
Role of Oct 4 in mammalian embryonic stem cell pluripotency	5.62E-01	PHB, IGF2BP1
MSP-RON signaling pathway	5.62E-01	ACTA2, ACTB
Prostate cancer signaling	5.57E-01	MAPK1, HSP90AA1, GSTP1
Tec kinase signaling	5.55E-01	ACTA2, GTF2I, ACTB, GNB2L1, GNB2
nNOS signaling in skeletal muscle cells	5.41E-01	CALM1 (includes others)
Chondroitin sulfate degradation (metazoa)	5.41E-01	HEXB
Ephrin A signaling	5.36E-01	CFL1, CDC42
HIPPO signaling	5.21E-01	YWHAQ, PPP2CB, YWHAG
Dermatan sulfate degradation (metazoa)	5.18E-01	HEXB
Fatty acid α-oxidation	5.18E-01	ALDH1A2
TGF-β signaling	5.12E-01	MAPK1, CDC42, HDAC1
Neuregulin signaling	5.03E-01	RPS6, MAPK1, HSP90AA1
CTLA4 signaling in cytotoxic T lymphocytes	5.03E-01	PPP2CB, AP2M1, CLTA
RANK signaling in osteoclasts	5.03E-01	CALM1 (includes others), MAPK1, GSN
D-myo-inositol (1,4,5,6)-tetrakisphosphate biosynthesis	5.01E-01	NUDT5, ACP1, PPM1F, SACM1L
D-myo-inositol (3,4,5,6)-tetrakisphosphate biosynthesis	5.01E-01	NUDT5, ACP1, PPM1F, SACM1L
Amyloid processing	5.01E-01	MAPK1, CSNK2B
γ-linolenate biosynthesis II (Animals)	4.96E-01	CYB5R3
Putrescine degradation III	4.96E-01	ALDH1A2
Superpathway of geranylgeranyldiphosphate biosynthesis I (via mevalonate)	4.96E-01	HADHB
Crosstalk between dendritic cells and natural killer cells	4.95E-01	ACTA2, ACTB, TLN1
PAK signaling	4.95E-01	MAPK1, CFL1, CDC42
Apoptosis signaling	4.95E-01	MAPK1, LMNA, CDK1
Cellular effects of sildenafil (viagra)	4.87E-01	CALM1 (includes others), MYH10, ACTA2, ACTB
Wnt/β-catenin signaling	4.86E-01	PPP2CB, HDAC1, RUVBL2, CSNK2B, UBC
IL-1 signaling	4.79E-01	MAPK1, GNB2L1, GNB2
Semaphorin signaling in neurons	4.78E-01	MAPK1, CFL1
UVB-Induced MAPK signaling	4.78E-01	MAPK1, EIF4E
IL-2 signaling	4.78E-01	MAPK1, CSNK2B
Tryptophan degradation X (mammalian, via tryptamine)	4.76E-01	ALDH1A2
D-myo-inositol (1,4,5)-trisphosphate degradation	4.76E-01	BPNT1

CREB signaling in neurons	4.75E-01	CALM1 (includes others), MAPK1, GNB2L1, GNB2, POLR2H
Death receptor signaling	4.71E-01	ACTA2, ACTB, LMNA
Cardiac β-adrenergic signaling	4.61E-01	PPP2CB, GNB2L1, GNB2, APEX1
GADD45 signaling	4.57E-01	CDK1
DNA damage-induced 14-3-3σ signaling	4.57E-01	CDK1
AMPK signaling	4.55E-01	PPP2CB, SLC2A1, MAPK1, PFKP
EGF signaling	4.48E-01	MAPK1, CSNK2B
B cell receptor signaling	4.47E-01	RAP1B, CALM1 (includes others), MAPK1, CFL1, CDC42
Nur77 signaling in T lymphocytes	4.38E-01	CALM1 (includes others), HDAC1
Antioxidant action of vitamin C	4.33E-01	SLC2A1, MAPK1, GSTO1
Role of NFAT in cardiac hypertrophy	4.31E-01	CALM1 (includes others), MAPK1, GNB2L1, HDAC1, GNB2
Myc mediated apoptosis signaling	4.28E-01	YWHAQ, YWHAG
Cardiac hypertrophy signaling	4.2E-01	CALM1 (includes others), EIF2B4, MAPK1, GNB2L1, GNB2, EIF4E
ATM signaling	4.19E-01	CDK1, RAD50
Nitric oxide signaling in the cardiovascular system	4.19E-01	CALM1 (includes others), MAPK1, HSP90AA1
eNOS signaling	4.13E-01	HSPA8, CALM1 (includes others), HSP90AA1, HSPA5
Maturity onset diabetes of young (MODY) signaling	4.07E-01	GAPDH
3-phosphoinositide degradation	3.96E-01	NUDT5, ACP1, PPM1F, SACM1L
Estrogen-dependent breast cancer signaling	3.93E-01	MAPK1, HSD17B4
GM-CSF signaling	3.93E-01	MAPK1, GNB2L1
Agranulocyte adhesion and diapedesis	3.82E-01	MYH10, ACTA2, EZR, ACTB, RDX
Gαq signaling	3.8E-01	CALM1 (includes others), MAPK1, GNB2L1, GNB2
HGF signaling	3.8E-01	RAP1B, MAPK1, CDC42
IL-22 signaling	3.78E-01	MAPK1
Estrogen-mediated S-phase entry	3.78E-01	CDK1
Dopamine degradation	3.78E-01	ALDH1A2
Superpathway of D-myo-inositol (1,4,5)-trisphosphate metabolism	3.78E-01	BPNT1
Calcium-induced T lymphocyte apoptosis	3.77E-01	CALM1 (includes others), HDAC1
Pyridoxal 5'-phosphate salvage pathway	3.77E-01	MAPK1, CDK1
Thrombin signaling	3.73E-01	MAPK1, GNB2L1, GNB2, ARHGEF1, ARHGEF2
Superpathway of inositol phosphate compounds	3.68E-01	NUDT5, ACP1, PPM1F, PIP4K2A, SACM1L
NGF signaling	3.68E-01	RAP1B, MAPK1, CDC42
IL-17A signaling in gastric cells	3.65E-01	MAPK1
Role of JAK family kinases in IL-6-type cytokine signaling	3.65E-01	MAPK1
Gαs signaling	3.56E-01	MAPK1, GNB2L1, GNB2
GABA receptor signaling	3.53E-01	AP2M1, UBC
Neurotrophin/TRK signaling	3.53E-01	MAPK1, CDC42
NAD salvage pathway II	3.52E-01	ACP1
GDNF family ligand-receptor interactions	3.46E-01	MAPK1, CDC42

Corticotropin releasing hormone signaling	3.44E-01	RAP1B, CALM1 (includes others), MAPK1
Cell cycle control of chromosomal replication	3.4E-01	MCM7
D-myo-inositol (1,4,5)-trisphosphate biosynthesis	3.4E-01	PIP4K2A
Pyrimidine ribonucleotides interconversion	3.4E-01	NUDT5
Melatonin signaling	3.32E-01	CALM1 (includes others), MAPK1
Pyrimidine ribonucleotides de novo biosynthesis	3.18E-01	NUDT5
Gα12/13 signaling	3.12E-01	MAPK1, CDC42, ARHGEF1
LPS-stimulated MAPK signaling	3.12E-01	MAPK1, CDC42
Sonic hedgehog signaling	3.08E-01	CDK1
PTEN signaling	3.07E-01	MAPK1, CDC42, CSNK2B
FLT3 signaling in hematopoietic progenitor cells	3.06E-01	MAPK1, EIF4E
Toll-like receptor signaling	3.06E-01	MAPK1, UBC
Synaptic long term potentiation	3.03E-01	RAP1B, CALM1 (includes others), MAPK1
P2Y purigenic receptor signaling pathway	3.03E-01	MAPK1, GNB2L1, GNB2
4-1BB signaling in T lymphocytes	2.98E-01	MAPK1
HMGB1 signaling	2.98E-01	MAPK1, CDC42, RBBP7
Gαi signaling	2.98E-01	MAPK1, GNB2L1, GNB2
MIF-mediated glucocorticoid regulation	2.79E-01	MAPK1
Retinoate biosynthesis I	2.79E-01	ALDH1A2
Complement system	2.79E-01	CD59
Reelin signaling in neurons	2.76E-01	ARHGEF1, ARHGEF2
Regulation of IL-2 expression in activated and anergic T lymphocytes	2.76E-01	CALM1 (includes others), MAPK1
Role of NFAT in regulation of the immune response	2.73E-01	CALM1 (includes others), MAPK1, GNB2L1, GNB2
Oncostatin M signaling	2.71E-01	MAPK1
Inhibition of angiogenesis by TSP1	2.71E-01	MAPK1
Cell cycle regulation by BTG family proteins	2.62E-01	PPP2CB
IL-17A signaling in fibroblasts	2.62E-01	MAPK1
Noradrenaline and adrenaline degradation	2.62E-01	ALDH1A2
Estrogen biosynthesis	2.47E-01	HSD17B4
TR/RXR activation	2.45E-01	SLC2A1, PFKP
ErbB signaling	2.4E-01	MAPK1, CDC42
April mediated signaling	2.39E-01	MAPK1
B cell activating factor signaling	2.25E-01	MAPK1
Thyroid cancer signaling	2.25E-01	MAPK1
MIF regulation of innate immunity	2.19E-01	MAPK1
Melanoma signaling	2.12E-01	MAPK1
UVC-induced MAPK signaling	2.12E-01	MAPK1
Role of IL-17F in allergic inflammatory airway diseases	2E-01	MAPK1

Table S3. The 459 direct targets of ALS in k562 cells analyzed by IPA

UniProt	Symbol	Entrez gene name	Fold change	Type(s)	Location
F8W1I6	DCTN2	Dynactin 2 (p50)	38.152	Other	Cytoplasm
F8W118	NAP1L1	Nucleosome assembly protein 1-like 1	24.085	Other	Nucleus
G3V210	RPLP0	Ribosomal protein, large, P0	23.618	Other	Cytoplasm
E7EX53	RPL15	Ribosomal protein L15	22.901	Other	Cytoplasm
G3V3A4	SNW1	SNW domain containing 1	16.919	Transcription regulator	Nucleus
C9J363	PDCD10	Programmed cell death 10	14.869	Other	Cytoplasm
F8WED3	CAPZA2	Capping protein (actin filament) muscle Z-line, α2	3.545	Other	Cytoplasm
E9PR17	CD59	CD59 molecule, complement regulatory protein	2.089	Other	Plasma membrane
B3KQ25	PSME3	Proteasome (prosome, macropain) activator subunit 3 (PA28γ; Ki)	2.068	Peptidase	Cytoplasm
C9JIM8	SLC2A1	Solute carrier family 2 (facilitated glucose transporter), member 1	2.005	Transporter	Plasma membrane
F6SH78	ELOVL5	ELOVL fatty acid elongase 5	1.941	Enzyme	Cytoplasm
G3V153	CAPRIN1	Cell cycle associated protein 1	1.815	Other	Plasma membrane
B4DNJ6	STRAP	Serine/threonine kinase receptor associated protein	1.747	Other	Plasma membrane
E9PJF4	CLNS1A	Chloride channel, nucleotide-sensitive, 1A	1.742	Ion channel	Plasma membrane
B4DXI4	MRPL21	Mitochondrial ribosomal protein L21	1.729	Other	Cytoplasm
Q9H8G9	USP15	Ubiquitin specific peptidase 15	1.709	Peptidase	Cytoplasm
A7YIJ8	RDX	Radixin	1.684	Other	Cytoplasm
F6U211	RPS10	Ribosomal protein S10	1.667	Other	Cytoplasm
E9PN89	HSPA8	Heat shock 70 kDa protein 8	1.655	Enzyme	Cytoplasm
E5RIU6	CDK1	Cyclin-dependent kinase 1	1.617	Kinase	Nucleus
B4DG39	GPI	Glucose-6-phosphate isomerase	1.571	Enzyme	Extracellular space
A4D210	EIF3B	Eukaryotic translation initiation factor 3, subunit B	1.565	Translation regulator	Cytoplasm
B4E132	DDX3Y	DEAD (Asp-Glu-Ala-Asp) box helicase 3, Y-linked	1.531	Enzyme	Other
Q9BYK1	RPS21	Ribosomal protein S21	1.509	Other	Cytoplasm
B7Z4C8	RPL31	Ribosomal protein L31	1.492	Other	Cytoplasm
E9PDR7	CNBP	CCHC-type zinc finger, nucleic acid binding protein	1.491	Transcription regulator	Nucleus
E7ERJ7	PABPC1	Poly(A) binding protein, cytoplasmic 1	1.485	Translation regulator	Cytoplasm
E7ETL9	DDX5	DEAD (Asp-Glu-Ala-Asp) box helicase 5	1.480	Enzyme	Nucleus
B7Z6F8	CLINT1	Clathrin interactor 1	1.456	Other	Cytoplasm
G3V0E5	TFRC	Transferrin receptor	1.434	Transporter	Plasma membrane
B8ZZ09	LUC7L	LUC7-like (S. cerevisiae)	1.424	Other	Nucleus
Q3KQS4	NOP2	NOP2 nucleolar protein	1.423	Other	Nucleus
E7EPK6	RPS24	Ribosomal protein S24	1.423	Other	Cytoplasm
B4DNC8	RPL13A	Ribosomal protein L13a	1.417	Other	Cytoplasm
E9PC97	PHF6	PHD finger protein 6	1.414	Other	Nucleus
Q5JR95	RPS8	Ribosomal protein S8	1.413	Other	Cytoplasm
F5GYQ2	TRMT112	tRNA methyltransferase 11-2 homolog (S. cerevisiae)	1.404	Enzyme	Cytoplasm
B4DZP5	DDB1	Damage-specific DNA binding protein 1, 127 kDa	1.400	Other	Nucleus

A8MW50	LDHB	Lactate dehydrogenase B	1.391	Enzyme	Cytoplasm
E9PAV3	NACA	Nascent polypeptide-associated complex α subunit	1.387	Transcription regulator	Cytoplasm
C9JCU7	POLR2H	-	1.385	Other	Other
B4DP21	PTGES3	Prostaglandin E synthase 3 (cytosolic)	1.382	Enzyme	Cytoplasm
G3V2S9	SLIRP	SRA stem-loop interacting RNA binding protein	1.380	Other	Cytoplasm
A6NF51	BPNT1	3'(2'), 5'-Bisphosphate nucleotidase 1	1.376	Phosphatase	Nucleus
A2A3R5	RPS6	Ribosomal protein S6	1.353	Other	Cytoplasm
B4DRZ7	DDX19A	DEAD (Asp-Glu-Ala-Asp) box polypeptide 19A	1.349	Enzyme	Nucleus
B7WPD3	TCEB2	Transcription elongation factor B (SIII), polypeptide 2 (18 kDa, elongin B)	1.346	Transcription regulator	Nucleus
D6REE5	GNB2L1	Guanine nucleotide binding protein (G protein), β polypeptide 2-like 1	1.344	Enzyme	Cytoplasm
B7Z1K2	HBS1L	HBS1-like translational GTPase	1.333	Translation regulator	Cytoplasm
Q5T8U2	RPL7A	Ribosomal protein L7a	1.331	Other	Cytoplasm
Q5JP00	RBBP7	Retinoblastoma binding protein 7	1.330	Transcription regulator	Nucleus
B4DE86	NDRG2	NDRG family member 2	1.324	Other	Cytoplasm
F5H1S2	RPL13	Ribosomal protein L13	1.321	Other	Cytoplasm
B3KXF2	KIAA0368	KIAA0368	1.320	Other	Cytoplasm
Q86U51	GTF2I	General transcription factor IIi	1.317	Transcription regulator	Nucleus
Q86U12	HSP90AA1	Heat shock protein 90 kDa α (cytosolic), class A member 1	1.303	Enzyme	Cytoplasm
E9PMM9	RPS2	Ribosomal protein S2	1.302	Other	Cytoplasm
C9J6B6	EIF4G1	Eukaryotic translation initiation factor 4 γ, 1	1.294	Translation regulator	Cytoplasm
D6RDI2	LUC7L3	LUC7-like 3 (*S. cerevisiae*)	1.284	Other	Nucleus
B0QY89	EIF3L	Eukaryotic translation initiation factor 3, subunit L	1.283	Other	Cytoplasm
B7Z4Q3	C7orf55	Chromosome 7 open reading frame 55	1.280	Other	Cytoplasm
E9PFU1	PDCD6IP	Programmed cell death 6 interacting protein	1.274	Other	Cytoplasm
Q5T3N0	ANXA1	Annexin A1	1.271	Enzyme	Plasma membrane
E9PS50	RPS13	Ribosomal protein S13	1.271	Other	Other
F5GY56	PRPF19	Pre-mRNA processing factor 19	1.268	Enzyme	Nucleus
B7Z514	GSS	Glutathione synthetase	1.262	Enzyme	Cytoplasm
B5ME19	EIF3CL	Eukaryotic translation initiation factor 3, subunit C-like	1.261	Other	Other
F8W727	RPL32	Ribosomal protein L32	1.258	Other	Cytoplasm
F5H737	AHCY	Adenosylhomocysteinase	1.257	Enzyme	Cytoplasm
F6Q0E3	CAPZB	Capping protein (actin filament) muscle Z-line, β	1.255	Other	Cytoplasm
Q5W012	RBM17	RNA binding motif protein 17	1.255	Other	Nucleus
F5H5A9	SUGT1	SGT1, suppressor of G2 allele of SKP1 (*S. cerevisiae*)	1.255	Other	Nucleus
E9PKL7	RAB2A	RAB2A, member RAS oncogene family	1.248	Enzyme	Cytoplasm
A6NCD2	CCT6A	Chaperonin containing TCP1, subunit 6A (ζ1)	1.235	Other	Cytoplasm
E7EX17	EIF4B	Eukaryotic translation initiation factor 4B	1.233	Translation regulator	Cytoplasm
E7EUT5	GAPDH	Glyceraldehyde-3-phosphate dehydrogenase	1.232	Enzyme	Cytoplasm
G3V438	AHSA1	AHA1, activator of heat shock 90 kDa protein ATPase homolog 1 (yeast)	1.230	Other	Cytoplasm
F5GZ39	UBC	Ubiquitin C	1.230	Enzyme	Cytoplasm
B4DF96	EIF2A	Eukaryotic translation initiation factor 2A, 65 kDa	1.223	Translation regulator	Cytoplasm

Q6IPX4	RPS16	Ribosomal protein S16	1.216	Other	Cytoplasm
E9PG15	YWHAQ	Tyrosine 3-monooxygenase/tryptophan 5-monooxygenase activation protein, θ	1.214	Other	Cytoplasm
F5H282	TCP1	t-Complex 1	1.210	Other	Cytoplasm
B7Z2F4	CCT4	Chaperonin containing TCP1, subunit 4 (δ)	1.208	Other	Cytoplasm
B4DQH4	CCT8	Chaperonin containing TCP1, subunit 8 (θ)	1.205	Enzyme	Cytoplasm
F8W7I9	RANGAP1	Ran GTPase activating protein 1	1.204	Other	Nucleus
A8MWI8	CCT7	Chaperonin containing TCP1, subunit 7 (η)	1.202	Other	Cytoplasm
F5GXM1	HDAC1	Histone deacetylase 1	1.194	Transcription regulator	Nucleus
E7ESE0	RPL9	Ribosomal protein L9	1.194	Other	Cytoplasm
Q5SX88	GDI2	GDP dissociation inhibitor 2	1.193	Other	Cytoplasm
D6RIH9	HNRNPH1	Heterogeneous nuclear ribonucleoprotein H1 (H)	1.187	Other	Nucleus
F8VUG2	KRT8	Keratin 8	1.186	Other	Cytoplasm
B7Z4N8	USP14	Ubiquitin specific peptidase 14 (tRNA-guanine transglycosylase)	1.185	Peptidase	Cytoplasm
E7ENZ3	CCT5	Chaperonin containing TCP1, subunit 5 (ε)	1.184	Other	Cytoplasm
Q567Q0	PPIA	Peptidylprolyl isomerase A (cyclophilin A)	1.184	Enzyme	Cytoplasm
Q96K98	SRP68	Signal recognition particle 68 kDa	1.177	Other	Nucleus
E9PPK9	DPP3	Dipeptidyl-peptidase 3	1.175	Peptidase	Cytoplasm
E7ES32	DNAJA3	DnaJ (Hsp40) homolog, subfamily A, member 3	1.174	Other	Cytoplasm
B4E3U4	RBMX	RNA binding motif protein, X-linked	1.171	Other	Nucleus
F5H2M7	WNK1	WNK lysine deficient protein kinase 1	1.169	Kinase	Cytoplasm
E9PQY2	PFDN4	Prefoldin subunit 4	1.164	Other	Cytoplasm
B3KSF1	CACYBP	Calcyclin binding protein	1.162	Other	Nucleus
A8K854	TUBB3	Tubulin, β 3 class III	1.161	Other	Cytoplasm
B8ZWD6	DBI	Diazepam binding inhibitor (GABA receptor modulator, acyl-CoA binding protein)	1.158	Other	Cytoplasm
B7ZAV5	MATR3	Matrin 3	1.158	Other	Nucleus
B4DMJ2	RPL4	Ribosomal protein L4	1.156	Enzyme	Cytoplasm
E7EMV0	DIAPH1	Diaphanous-related formin 1	1.155	Other	Plasma membrane
B4DUI3	EIF3J	Eukaryotic translation initiation factor 3, subunit J	1.152	Translation regulator	Cytoplasm
E9PN18	PUF60	Poly-U binding splicing factor 60 KDa	1.152	Other	Nucleus
Q5JR89	KIF2C	Kinesin family member 2C	1.151	Other	Nucleus
E5RHC1	PPP2CB	Protein phosphatase 2, catalytic subunit, β isozyme	1.151	Phosphatase	Cytoplasm
D6RGF4	ABCE1	ATP-binding cassette, sub-family E (OABP), member 1	1.149	Transporter	Cytoplasm
G3V576	HNRNPC	Heterogeneous nuclear ribonucleoprotein C (C1/C2)	1.148	Other	Nucleus
F8VQ14	CCT2	Chaperonin containing TCP1, subunit 2 (β)	1.147	Kinase	Cytoplasm
Q5T0R9	CAP1	CAP, adenylate cyclase-associated protein 1 (yeast)	1.145	Other	Plasma membrane
E9PCT1	SRRM1	Serine/arginine repetitive matrix 1	1.144	Other	Nucleus
G3XAN0	RPS20	Ribosomal protein S20	1.137	Other	Cytoplasm
B4DDM6	BUB3	BUB3 mitotic checkpoint protein	1.135	Other	Nucleus
B4DQR4	PSMA6	Proteasome (prosome, macropain) subunit, α type, 6	1.135	Peptidase	Cytoplasm
Q5SRQ6	CSNK2B	Casein kinase 2, β polypeptide	1.134	Kinase	Cytoplasm
E5RH77	RPS14	Ribosomal protein S14	1.132	Translation regulator	Cytoplasm

F8W1H5	RAB5C	RAB5C, member RAS oncogene family	1.131	Enzyme	Cytoplasm
C9JF79	MDH1	Malate dehydrogenase 1, NAD (soluble)	1.129	Enzyme	Cytoplasm
A8MUD9	RPL7	Ribosomal protein L7	1.129	Transcription regulator	Nucleus
B0QYA7	EIF3D	Eukaryotic translation initiation factor 3, subunit D	1.126	Other	Cytoplasm
B4E3P0	ACLY	ATP citrate lyase	1.123	Enzyme	Cytoplasm
Q9BQ02	NCL	Nucleolin	1.122	Other	Nucleus
G5E9P0	RAD23B	RAD23 homolog B (*S. cerevisiae*)	1.121	Other	Nucleus
G3V2X6	PRMT5	Protein arginine methyltransferase 5	1.119	Enzyme	Cytoplasm
Q96II6	NDUFB10	NADH dehydrogenase (ubiquinone) 1 β subcomplex, 10, 22 kDa	1.116	Enzyme	Cytoplasm
D6RDJ1	LYAR	Ly1 antibody reactive	1.113	Other	Plasma membrane
F5H4R7	KPNB1	Karyopherin (importin) β 1	1.112	Transporter	Nucleus
G3V2F7	TMEM189	Transmembrane protein 189	1.111	Other	Other
E7EQY1	FAM136A	Family with sequence similarity 136, member A	1.110	Other	Cytoplasm
A8MUS3	RPL23A	Ribosomal protein L23a	1.108	Other	Other
B4DP62	SLC25A1	Solute carrier family 25 (mitochondrial carrier; citrate transporter), member 1	1.107	Transporter	Other
B0YJC5	VIM	Vimentin	1.105	Other	Cytoplasm
E9PK25	CFL1	Cofilin 1 (non-muscle)	1.097	Other	Nucleus
B3KPQ8	NUP93	Nucleoporin 93 kDa	1.093	Other	Nucleus
E9PN81	RNASEH2C	Ribonuclease H2, subunit C	1.093	Other	Other
B4DKT0	GORASP2	Golgi reassembly stacking protein 2, 55 kDa	1.092	Other	Cytoplasm
F8VV04	SART3	Squamous cell carcinoma antigen recognized by T cells 3	1.090	Other	Nucleus
F8VZY9	KRT18	Keratin 18	1.084	Other	Cytoplasm
B3KS31	TUBB6	Tubulin, β 6 class V	1.082	Other	Cytoplasm
E9PB61	ALYREF	Aly/REF export factor	1.079	Transcription regulator	Nucleus
B7Z2F6	SAFB	Scaffold attachment factor B	1.079	Other	Nucleus
B3KSH1	EIF3F	Eukaryotic translation initiation factor 3, subunit F	1.077	Translation regulator	Cytoplasm
F5GZE5	SEPT7	Septin 7	1.072	Other	Cytoplasm
B4E3S0	CORO1C	Coronin, actin binding protein, 1C	1.071	Other	Cytoplasm
B4E335	ACTB	β-Actin	1.070	Other	Cytoplasm
G5EA30	CELF1	CUGBP, Elav-like family member 1	1.063	Translation regulator	Cytoplasm
F8VTL3	MYH10	Myosin, heavy chain 10, non-muscle	1.062	Other	Cytoplasm
B4DTG2	EEF1G	Eukaryotic translation elongation factor 1 γ	1.060	Translation regulator	Cytoplasm
C9JXA5	GNB2	Guanine nucleotide binding protein (G protein), β polypeptide 2	1.057	Enzyme	Plasma membrane
Q5W0X3	FKBP1A	FK506 binding protein 1A, 12 kDa	1.056	Enzyme	Cytoplasm
G3V4N7	CKB	Creatine kinase, brain	1.054	Kinase	Cytoplasm
E9PEB5	FUBP1	Far upstream element (FUSE) binding protein 1	1.050	Transcription regulator	Nucleus
B4DJ45	TARDBP	TAR DNA binding protein	1.050	Transcription regulator	Nucleus
Q5VSR7	PFKP	Phosphofructokinase, platelet	1.043	Kinase	Cytoplasm
B4DT72	PSMD3	Proteasome (prosome, macropain) 26 S subunit, non-ATPase, 3	1.041	Other	Cytoplasm
B4DK71	SACM1L	SAC1 suppressor of actin mutations 1-like (yeast)	1.041	Phosphatase	Cytoplasm
B4DRT2	MRPS27	Mitochondrial ribosomal protein S27	1.039	Other	Cytoplasm
F6QR24	NUP153	Nucleoporin 153 kDa	1.039	Transporter	Nucleus

Q9BTE9	NUMA1	Nuclear mitotic apparatus protein 1	1.035	Other	Nucleus
Q9C083	PFDN5	Prefoldin subunit 5	1.032	Transcription regulator	Nucleus
B4DHC4	YWHAG	Tyrosine 3-monooxygenase/tryptophan 5-monooxygenase activation protein, γ	1.030	Other	Cytoplasm
F5H018	RAN	RAN, member RAS oncogene family	1.029	Enzyme	Nucleus
B4DUI8	ACTA2	Actin, β2, smooth muscle, aorta	1.028	Other	Cytoplasm
E3W975	C11 or f58	Chromosome 11 open reading frame 58	1.024	Other	Other
B3KQ59	RUVBL2	RuvB-like AAA ATPase 2	1.021	Transcription regulator	Nucleus
E9PRB9	SPCS2	Signal peptidase complex subunit 2 homolog (*S. cerevisiae*)	1.021	Other	Cytoplasm
G3V361	CALM1 (includes others)	Calmodulin 1 (phosphorylase kinase, δ)	1.018	Other	Cytoplasm
E9PKT8	NAP1L4	Nucleosome assembly protein 1-like 4	1.015	Other	Cytoplasm
Q9BYG9	NPM1	Nucleophosmin (nucleolar phosphoprotein B23, numatrin)	1.012	Transcription regulator	Nucleus
E9PJ04	SF3B2	Splicing factor 3b, subunit 2, 145 kDa	1.010	Other	Nucleus
Q5VWC4	PSMD4	Proteasome (prosome, macropain) 26 S subunit, non-ATPase, 4	1.009	Other	Cytoplasm
B4DW94	RAP1B	RAP1B, member of RAS oncogene family	1.009	Enzyme	Cytoplasm
D6RF62	PAICS	Phosphoribosylaminoimidazole carboxylase, phosphoribosylaminoimidazole succinocarboxamide synthetase	1.008	Enzyme	Cytoplasm
E5RJD8	TBCA	Tubulin folding cofactor A	1.007	Other	Cytoplasm
A6NFX8	NUDT5	Nudix (nucleoside diphosphate linked moiety X)-type motif 5	1.006	Phosphatase	Cytoplasm
C9JYS8	NONO	Non-POU domain containing, octamer-binding	1.005	Other	Nucleus
B4DHY1	HNRNPH3	Heterogeneous nuclear ribonucleoprotein H3 (2H9)	1.002	Other	Nucleus
Q5LJA5	UCHL5	Ubiquitin carboxyl-terminal hydrolase L5	1.002	Peptidase	Cytoplasm
E9PMN9	NAT10	*N*-acetyltransferase 10 (GCN5-related)	1.001	Enzyme	Nucleus
B4E2P2	SSR3	Signal sequence receptor, γ (translocon-associated protein γ)	-1.001	Other	Cytoplasm
E7EW37	TNPO1	Transportin 1	-1.001	Transporter	Nucleus
E7ESC6	XPO7	Exportin 7	-1.002	Transporter	Nucleus
B4E3C2	RPL17	Ribosomal protein L17	-1.003	Other	Cytoplasm
B0QZ36	RAE1	Ribonucleic acid export 1	-1.004	Other	Nucleus
C9JDM3	RANBP1	RAN binding protein 1	-1.007	Other	Nucleus
Q5TCU6	TLN1	Talin 1	-1.007	Other	Plasma membrane
B4E2V4	PSMA5	Proteasome (prosome, macropain) subunit, α type, 5	-1.010	Peptidase	Cytoplasm
F5GWY2	ATIC	5-Aminoimidazole-4-carboxamide ribonucleotide formyltransferase/IMP cyclohydrolase	-1.011	Enzyme	Cytoplasm
Q8IV96	DDX6	DEAD (Asp-Glu-Ala-Asp) box helicase 6	-1.012	Enzyme	Nucleus
G3V1V4	GTSF1	Gametocyte specific factor 1	-1.012	Other	Cytoplasm
A6NLN1	PTBP1	Polypyrimidine tract binding protein 1	-1.012	Enzyme	Nucleus
C9JIG9	OXSR1	Oxidative stress responsive 1	-1.013	Kinase	Nucleus
F8WAR4	CHCHD3	Coiled-coil-helix-coiled-coil-helix domain containing 3	-1.017	Other	Cytoplasm
Q5T6W2	HNRNPK	Heterogeneous nuclear ribonucleoprotein K	-1.019	Other	Nucleus
F5H783	STIP1	Stress-induced phosphoprotein 1	-1.019	Other	Cytoplasm
G5E9R9	TROVE2	TROVE domain family, member 2	-1.020	Other	Nucleus
A8MXW0	ARHGDIA	Rho GDP dissociation inhibitor (GDI) α	-1.022	Other	Cytoplasm
B4DXP9	ACTR1A	ARP1 actin-related protein 1 homolog A, centractin α (yeast)	-1.026	Other	Cytoplasm
B1AHD1	NHP2L1	NHP2 non-histone chromosome protein 2-like 1 (S. cerevisiae)	-1.026	Other	Nucleus

E5RH18	LSM1	LSM1, U6 small nuclear RNA associated	-1.027	Other	Nucleus
E9PAW1	SF3A1	Splicing factor 3a, subunit 1, 120 kDa	-1.033	Other	Nucleus
B7TY16	ACTN1	Actinin, α1	-1.035	Other	Cytoplasm
G5E975	SMARCB1	SWI/SNF related, matrix associated, actin dependent regulator of chromatin, subfamily b, member 1	-1.038	Transcription regulator	Nucleus
Q5JUL1	PAGE5	P antigen family, member 5 (prostate associated)	-1.048	Other	Other
B4DPN6	DDX1	DEAD (Asp-Glu-Ala-Asp) box helicase 1	-1.052	Enzyme	Nucleus
B4DFG4	ILF3	Interleukin enhancer binding factor 3, 90 kDa	-1.052	Transcription regulator	Nucleus
E9PND2	CSRP1	Cysteine and glycine-rich protein 1	-1.058	Other	Nucleus
B1AMU3	EXOSC1	Exosome component 1	-1.063	Enzyme	Nucleus
B3KX72	HNRNPU	Heterogeneous nuclear ribonucleoprotein U (scaffold attachment factor A)	-1.065	Transporter	Nucleus
B4DHM5	PGK1	Phosphoglycerate kinase 1	-1.066	Kinase	Cytoplasm
B3KXH8	SNX9	Sorting nexin 9	-1.066	Transporter	Cytoplasm
E9PFH4	TNPO3	Transportin 3	-1.066	Other	Cytoplasm
E9PIM9	RNH1	Ribonuclease/angiogenin inhibitor 1	-1.068	Other	Cytoplasm
A8MU27	SUMO3	Small ubiquitin-like modifier 3	-1.070	Other	Nucleus
C9IZE4	PSMD6	Proteasome (prosome, macropain) 26 S subunit, non-ATPase, 6	-1.073	Enzyme	Cytoplasm
B4DGR0	API5	Apoptosis inhibitor 5	-1.075	Other	Cytoplasm
G3XAN9	TARS	Threonyl-tRNA synthetase	-1.075	Enzyme	Nucleus
E9PLX7	RPL27A	Ribosomal protein L27a	-1.079	Other	Nucleus
E9PCX6	ASNS	Asparagine synthetase (glutamine-hydrolyzing)	-1.085	Enzyme	Cytoplasm
Q8N5M0	DDX39A	DEAD (Asp-Glu-Ala-Asp) box polypeptide 39A	-1.085	Enzyme	Nucleus
E9PMI5	SERPINH1	Serpin peptidase inhibitor, clade H (heat shock protein 47), member 1, (collagen binding protein 1)	-1.085	Other	Extracellular space
D6RCF4	CISD2	CDGSH iron sulfur domain 2	-1.088	Other	Cytoplasm
Q567Q5	PSMA4	Proteasome (prosome, macropain) subunit, α type, 4	-1.088	Peptidase	Cytoplasm
E7ETU3	CDC42	Cell division cycle 42	-1.091	Enzyme	Cytoplasm
B4E363	FARSA	Phenylalanyl-tRNA synthetase, α subunit	-1.093	Enzyme	Cytoplasm
C9JLS9	PSMC2	Proteasome (prosome, macropain) 26 S subunit, ATPase, 2	-1.093	Peptidase	Nucleus
Q5T624	NASP	Nuclear autoantigenic sperm protein (histone-binding)	-1.096	Other	Nucleus
C9J4S4	RAB7A	RAB7A, member RAS oncogene family	-1.098	Enzyme	Cytoplasm
E9PF41	ACTR2	ARP2 actin-related protein 2 homolog (yeast)	-1.101	Other	Plasma membrane
E7ERC4	SSB	Sjogren syndrome antigen B (autoantigen La)	-1.102	Enzyme	Nucleus
E9PEG8	USP19	Ubiquitin specific peptidase 19	-1.102	Peptidase	Cytoplasm
F5H5E4	BCAT1	Branched chain amino-acid transaminase 1, cytosolic	-1.105	Enzyme	Cytoplasm
E7EQR4	EZR	Ezrin	-1.105	Other	Plasma membrane
C9JTV6	GART	Phosphoribosylglycinamide formyltransferase, phosphoribosylglycinamide synthetase, phosphoribosylaminoimidazole synthetase	-1.105	Enzyme	Cytoplasm
F5H1I8	XRCC6	X-ray repair complementing defective repair in Chinese hamster cells 6	-1.106	Enzyme	Nucleus
D6RCQ0	EEF1E1	Eukaryotic translation elongation factor 1 epsilon 1	-1.109	Translation regulator	Cytoplasm
C9J8F3	ALDOC	Aldolase C, fructose-bisphosphate	-1.110	Enzyme	Cytoplasm
B4DPJ6	TPD52L2	Tumor protein D52-like 2	-1.110	Other	Cytoplasm
B7Z9J4	CALB1	Calbindin 1, 28 kDa	-1.114	Other	Cytoplasm
E7EW44	CORO1B	Coronin, actin binding protein, 1B	-1.115	Other	Cytoplasm

B4E1K5	DHCR7	7-Dehydrocholesterol reductase	-1.121	Enzyme	Cytoplasm
E9PB24	RPL28	Ribosomal protein L28	-1.122	Other	Cytoplasm
Q5T446	UROD	Uroporphyrinogen decarboxylase	-1.122	Enzyme	Cytoplasm
Q5HY57	EMD	Emerin	-1.123	Other	Nucleus
D6RGV5	COX7A2	Cytochrome c oxidase subunit VIIa polypeptide 2 (liver)	-1.125	Enzyme	Cytoplasm
A6NIW5	PRDX2	Peroxiredoxin 2	-1.126	Enzyme	Cytoplasm
O95485	SNRPA1	Small nuclear ribonucleoprotein polypeptide A'	-1.126	Other	Nucleus
A8MX94	GSTP1	Glutathione S-transferase pi 1	-1.129	Enzyme	Cytoplasm
B1AJY5	PSMD10	Proteasome (prosome, macropain) 26 S subunit, non-ATPase, 10	-1.130	Transcription regulator	Cytoplasm
Q5JSD1	VDAC2	Voltage-dependent anion channel 2	-1.135	Ion channel	Cytoplasm
E7ETR0	RUVBL1	RuvB-like AAA ATPase 1	-1.138	Transcription regulator	Nucleus
B0YIW6	ARCN1	Archain 1	-1.139	Other	Cytoplasm
B4DKS8	HNRNPF	Heterogeneous nuclear ribonucleoprotein F	-1.142	Other	Nucleus
F5H423	ARF3	ADP-ribosylation factor 3	-1.146	Enzyme	Cytoplasm
F5H2F4	MTHFD1	Methylenetetrahydrofolate dehydrogenase (NADP+ dependent) 1, methenyltetrahydrofolate cyclohydrolase, formyltetrahydrofolate synthetase	-1.146	Enzyme	Cytoplasm
C9J0F2	PCMT1	Protein-L-isoaspartate (D-aspartate) O-methyltransferase	-1.151	Enzyme	Cytoplasm
B1AVU8	PSAP	Prosaposin	-1.153	Other	Extracellular space
F5GX11	PSMA1	Proteasome (prosome, macropain) subunit, α type, 1	-1.154	Peptidase	Cytoplasm
E7EW34	PSMD2	Proteasome (prosome, macropain) 26 S subunit, non-ATPase, 2	-1.155	Other	Cytoplasm
F8WF69	CLTA	Clathrin, light chain A	-1.157	Other	Plasma membrane
B4DDG1	UBE2L3	Ubiquitin-conjugating enzyme E2L 3	-1.157	Enzyme	Nucleus
F5HE57	HSD17B4	Hydroxysteroid (17-β) dehydrogenase 4	-1.160	Enzyme	Cytoplasm
A8K092	ATP5A1	ATP synthase, H^+ transporting, mitochondrial F1 complex, α subunit 1, cardiac muscle	-1.161	Transporter	Cytoplasm
B4E3A8	SERPINB1	Serpin peptidase inhibitor, clade B (ovalbumin), member 1	-1.161	Other	Cytoplasm
F5H7R1	FKBP5	FK506 binding protein 5	-1.162	Enzyme	Nucleus
F5H3F0	OTUB1	OTU deubiquitinase, ubiquitin aldehyde binding 1	-1.162	Enzyme	Cytoplasm
E9PKD5	PSMC3	Proteasome (prosome, macropain) 26 S subunit, ATPase, 3	-1.168	Transcription regulator	Nucleus
D6R904	TPM3	Tropomyosin 3	-1.174	Other	Cytoplasm
A2A2D0	STMN1	Stathmin 1	-1.180	Other	Cytoplasm
B4DRT4	PEBP1	Phosphatidylethanolamine binding protein 1	-1.181	Other	Cytoplasm
B7Z977	ARHGEF2	Rho/Rac guanine nucleotide exchange factor (GEF) 2	-1.185	Other	Cytoplasm
Q5TCI8	LMNA	Lamin A/C	-1.186	Other	Nucleus
E7ERS3	ZC3H18	Zinc finger CCCH-type containing 18	-1.187	Other	Nucleus
B4DHN0	MAPK1	Mitogen-activated protein kinase 1	-1.188	Kinase	Cytoplasm
E7EQL5	DYNC1I2	Dynein, cytoplasmic 1, intermediate chain 2	-1.191	Other	Cytoplasm
F5GXQ6	ZCCHC8	Zinc finger, CCHC domain containing 8	-1.191	Other	Nucleus
G3XAH0	SEPT5	Septin 5	-1.192	Enzyme	Cytoplasm
A6NDY9	FLNA	Filamin A, α	-1.198	Other	Cytoplasm
D6R9A6	HMGB2	High mobility group box 2	-1.200	Transcription regulator	Nucleus
E9PFW3	AP2M1	Adaptor-related protein complex 2, mu 1 subunit	-1.203	Transporter	Cytoplasm
E2QRM3	XPO5	Exportin 5	-1.203	Transporter	Nucleus

Q68CR9	DARS	Aspartyl-tRNA synthetase	-1.207	Enzyme	Cytoplasm
F5H456	RRP12	Ribosomal RNA processing 12 homolog (*S. cerevisiae*)	-1.207	Other	Nucleus
F8VZQ9	SARNP	SAP domain containing ribonucleoprotein	-1.210	Other	Nucleus
F5GXQ0	BROX	BRO1 domain and CAAX motif containing	-1.211	Other	Cytoplasm
F8WDZ1	PELP1	Proline, glutamate and leucine rich protein 1	-1.214	Other	Nucleus
A8K3Z3	PSMC5	Proteasome (prosome, macropain) 26 S subunit, ATPase, 5	-1.218	Transcription regulator	Nucleus
F2Z2K0	NSFL1C	NSFL1 (p97) cofactor (p47)	-1.219	Other	Cytoplasm
E5RHZ6	VDAC3	Voltage-dependent anion channel 3	-1.219	Ion channel	Cytoplasm
G3V4X1	PSMC1	Proteasome (prosome, macropain) 26 S subunit, ATPase, 1	-1.224	Peptidase	Nucleus
B1AKR6	DYNLRB1	Dynein, light chain, roadblock-type 1	-1.225	Other	Cytoplasm
C9IYI4	RPL29	Ribosomal protein L29	-1.226	Other	Cytoplasm
B3KSI4	TKT	Transketolase	-1.226	Enzyme	Cytoplasm
C9JT33	IGF2BP1	Insulin-like growth factor 2 mRNA binding protein 1	-1.227	Translation regulator	Cytoplasm
B7Z2R2	UQCRB	Ubiquinol-cytochrome c reductase binding protein	-1.232	Enzyme	Cytoplasm
B4DNK3	AIMP1	Aminoacyl tRNA synthetase complex-interacting multifunctional protein 1	-1.233	Cytokine	Extracellular space
B4DQJ1	SNRNP40	Small nuclear ribonucleoprotein 40 kDa (U5)	-1.233	Other	Nucleus
E9PBF6	LMNB1	Lamin B1	-1.234	Other	Nucleus
C9J2Q4	SEPT2	Septin 2	-1.235	Enzyme	Cytoplasm
E7EWT1	DDOST	Dolichyl-diphosphooligosaccharide–protein glycosyltransferase subunit (non-catalytic)	-1.236	Enzyme	Cytoplasm
C8KIL8	GSR	Glutathione reductase	-1.236	Enzyme	Cytoplasm
G3V1I6	ATAD3A	ATPase family, AAA domain containing 3A	-1.237	Other	Cytoplasm
B7Z8J4	NMT1	*N*-myristoyltransferase 1	-1.237	Enzyme	Cytoplasm
Q5TB19	ANP32E	Acidic (leucine-rich) nuclear phosphoprotein 32 family, member E	-1.244	Other	Nucleus
F8VV40	LTA4H	Leukotriene A4 hydrolase	-1.244	Enzyme	Cytoplasm
E7EN38	RAD50	RAD50 homolog (*S. cerevisiae*)	-1.248	Enzyme	Nucleus
A8MUF7	HBE1	Hemoglobin, epsilon 1	-1.249	Transporter	Cytoplasm
A6NEL0	HMGN1	High mobility group nucleosome binding domain 1	-1.251	Transcription regulator	Nucleus
F8VVL1	DENR	Density-regulated protein	-1.252	Other	Other
E9PMX3	NDUFV1	NADH dehydrogenase (ubiquinone) flavoprotein 1, 51 kDa	-1.252	Enzyme	Cytoplasm
E7ERW2	GOT2	Glutamic-oxaloacetic transaminase 2, mitochondrial	-1.262	Enzyme	Cytoplasm
F5H6R6	HNRNPD	Heterogeneous nuclear ribonucleoprotein D (AU-rich element RNA binding protein 1, 37 kDa)	-1.265	Transcription regulator	Nucleus
Q2L7G6	HNRNPR	Heterogeneous nuclear ribonucleoprotein R	-1.265	Other	Nucleus
B4E0P8	UBXN1	UBX domain protein 1	-1.267	Other	Cytoplasm
C9J2F8	PSMG4	Proteasome (prosome, macropain) assembly chaperone 4	-1.268	Transcription regulator	Other
C9JI87	VDAC1	Voltage-dependent anion channel 1	-1.269	Ion channel	Cytoplasm
B4DL85	HN1L	Hematological and neurological expressed 1-like	-1.273	Other	Cytoplasm
C9K0U8	SSBP1	Single-stranded DNA binding protein 1, mitochondrial	-1.273	Other	Cytoplasm
B4DGX2	PIP4K2A	Phosphatidylinositol-5-phosphate 4-kinase, type II, α	-1.277	Kinase	Cytoplasm
F8WC37	RFC2	Replication factor C (activator 1) 2, 40 kDa	-1.279	Other	Nucleus
F2Z393	TALDO1	Transaldolase 1	-1.282	Enzyme	Cytoplasm
B4DF41	MSH6	MutS homolog 6	-1.292	Enzyme	Nucleus
E7ETI0	ARPC4	Actin related protein 2/3 complex, subunit 4, 20 kDa	-1.293	Other	Cytoplasm

B8ZZ54	HSPE1	Heat shock 10 kDa protein 1	-1.295	Enzyme	Cytoplasm
F5GZQ3	HADHB	Hydroxyacyl-CoA dehydrogenase/3-ketoacyl-CoA thiolase/enoyl-CoA Hydratase (trifunctional protein), β subunit	-1.298	Enzyme	Cytoplasm
F8VXU5	VPS29	Vacuolar protein sorting 29 homolog (*S. cerevisiae*)	-1.302	Transporter	Cytoplasm
Q9NW21	FAM49B	Family with sequence similarity 49, member B	-1.308	Other	Extracellular space
B4DNJ5	RPN1	Ribophorin I	-1.308	Enzyme	Cytoplasm
B5MCC7	ACP1	Acid phosphatase 1, soluble	-1.315	Phosphatase	Cytoplasm
G3V1N8	VPS26A	Vacuolar protein sorting 26 homolog A (*S. pombe*)	-1.319	Transporter	Cytoplasm
E9PIE4	MTCH2	Mitochondrial carrier 2	-1.323	Other	Cytoplasm
F8WCA0	VAMP2	Vesicle-associated membrane protein 2 (synaptobrevin 2)	-1.328	Other	Plasma membrane
F8W079	ATP5B	ATP synthase, H^+ transporting, mitochondrial F1 complex, β polypeptide	-1.329	Transporter	Cytoplasm
F5H1N1	DNAJC11	DnaJ (Hsp40) homolog, subfamily C, member 11	-1.330	Other	Cytoplasm
B4DP75	PHB2	Prohibitin 2	-1.331	Transcription regulator	Cytoplasm
E9PCW0	PHB	Prohibitin	-1.333	Transcription regulator	Nucleus
F8W950	AIMP2	Aminoacyl tRNA synthetase complex-interacting multifunctional protein 2	-1.338	Other	Plasma membrane
A6NIT8	HNRNPL	Heterogeneous nuclear ribonucleoprotein L	-1.344	Other	Nucleus
B7Z5W8	DLST	Dihydrolipoamide S-succinyltransferase (E2 component of 2-oxo-glutarate complex)	-1.347	Enzyme	Cytoplasm
A8MUH2	ATP5J	ATP synthase, H^+ transporting, mitochondrial Fo complex, subunit F6	-1.348	Transporter	Cytoplasm
C9JNV2	BUD31	BUD31 homolog (*S. cerevisiae*)	-1.350	Transcription regulator	Nucleus
E7EQD5	STXBP2	Syntaxin binding protein 2	-1.350	Transporter	Plasma membrane
G3XAL0	MDH2	Malate dehydrogenase 2, NAD (mitochondrial)	-1.353	Enzyme	Cytoplasm
Q5T0H9	GSN	Gelsolin	-1.355	Other	Extracellular space
Q8WXC9	NDUFA10	NADH dehydrogenase (ubiquinone) 1 α subcomplex, 10, 42 kDa	-1.357	Transporter	Cytoplasm
A8MUW5	FAM98B	Family with sequence similarity 98, member B	-1.361	Other	Other
Q5T5C7	SARS	Seryl-tRNA synthetase	-1.369	Enzyme	Cytoplasm
B4DZT4	SEC24C	SEC24 family member C	-1.371	Transporter	Cytoplasm
C9JIF9	APEH	Acylaminoacyl-peptide hydrolase	-1.374	Peptidase	Cytoplasm
F5H2L4	ACOT13	Acyl-CoA thioesterase 13	-1.378	Enzyme	Cytoplasm
Q5T6H2	XPNPEP1	X-prolyl aminopeptidase (aminopeptidase P) 1, soluble	-1.386	Peptidase	Cytoplasm
E9PKH6	NDUFS8	NADH dehydrogenase (ubiquinone) Fe-S protein 8, 23 kDa (NADH-coenzyme Q reductase)	-1.393	Enzyme	Cytoplasm
F2Z2W7	TRMT2A	tRNA methyltransferase 2 homolog A (*S. cerevisiae*)	-1.397	Kinase	Other
Q1W5D8	RAB6A	RAB6A, member RAS oncogene family	-1.402	Enzyme	Cytoplasm
B4E2T8	CANX	Calnexin	-1.405	Other	Cytoplasm
C9IZ08	GAPVD1	GTPase activating protein and VPS9 domains 1	-1.408	Other	Cytoplasm
C9J9J4	MPP1	Membrane protein, palmitoylated 1, 55 kDa	-1.411	Kinase	Plasma membrane
C9JMA6	CBS/LOC102724560	Cystathionine-β-synthase	-1.413	Enzyme	Cytoplasm
B4DW08	ACO2	Aconitase 2, mitochondrial	-1.421	Enzyme	Cytoplasm
B4DHQ6	SRI	Sorcin	-1.424	Transporter	Cytoplasm
F5H698	LARS	Leucyl-tRNA synthetase	-1.428	Enzyme	Cytoplasm
A8MRB2	TFAM	Transcription factor A, mitochondrial	-1.428	Transcription regulator	Cytoplasm
B4DN60	NARS	Asparaginyl-tRNA synthetase	-1.430	Enzyme	Cytoplasm
A4D2A2	MCM7	Minichromosome maintenance complex component 7	-1.435	Enzyme	Nucleus
B9A067	IMMT	Inner membrane protein, mitochondrial	-1.437	Other	Cytoplasm

Q6NX52	ARHGEF1	Rho guanine nucleotide exchange factor (GEF) 1	-1.440	Other	Cytoplasm
B2BCH7	ITPA	Inosine triphosphatase (nucleoside triphosphate pyrophosphatase)	-1.441	Enzyme	Cytoplasm
B3KVK7	MARS	Methionyl-tRNA synthetase	-1.442	Enzyme	Cytoplasm
D6RFI0	SFXN1	Sideroflexin 1	-1.444	Transporter	Cytoplasm
G3V4W5	SHMT2	Serine hydroxymethyltransferase 2 (mitochondrial)	-1.450	Enzyme	Cytoplasm
B4DTC1	SRSF11	Serine/arginine-rich splicing factor 11	-1.451	Other	Nucleus
F8VY02	ERP29	Endoplasmic reticulum protein 29	-1.454	Transporter	Cytoplasm
E7EPW6	PDCD6	Programmed cell death 6	-1.457	Other	Cytoplasm
F8VXC8	SMARCC2	SWI/SNF related, matrix associated, actin dependent regulator of chromatin, subfamily c, member 2	-1.462	Transcription regulator	Nucleus
A6NFA8	H2AFV	H2A histone family, member V	-1.465	Other	Nucleus
G3V2K7	TMED10	Transmembrane emp24-like trafficking protein 10 (yeast)	-1.465	Transporter	Cytoplasm
E9PF31	ALDH1A2	Aldehyde dehydrogenase 1 family, member A2	-1.471	Enzyme	Cytoplasm
B4DUA5	P4HB	Prolyl 4-hydroxylase, β polypeptide	-1.474	Enzyme	Cytoplasm
F8VWL5	COPZ1	Coatomer protein complex, subunit ζ 1	-1.478	Transporter	Cytoplasm
F5H8B1	PCYT2	Phosphate cytidylyltransferase 2, ethanolamine	-1.482	Enzyme	Cytoplasm
E9PCX7	NNT	Nicotinamide nucleotide transhydrogenase	-1.487	Enzyme	Cytoplasm
E9PBW4	HBG2	Hemoglobin, γ G	-1.494	Other	Cytoplasm
E9PKU7	GANAB	α-Glucosidase, neutral AB	-1.500	Enzyme	Cytoplasm
B0QYN7	UBE2I	Ubiquitin-conjugating enzyme E2I	-1.500	Enzyme	Nucleus
B4DHX4	GDI1	GDP dissociation inhibitor 1	-1.509	Other	Cytoplasm
G5E977	NAPRT	Nicotinate phosphoribosyltransferase	-1.513	Enzyme	Cytoplasm
E7EPT4	NDUFV2	NADH dehydrogenase (ubiquinone) flavoprotein 2, 24 kDa	-1.519	Enzyme	Cytoplasm
E7ERK9	EIF2B4	Eukaryotic translation initiation factor 2B, subunit 4 δ, 67 kDa	-1.520	Other	Cytoplasm
B7Z1I2	GOT1	Glutamic-oxaloacetic transaminase 1, soluble	-1.522	Enzyme	Cytoplasm
E9PEX6	DLD	Dihydrolipoamide dehydrogenase	-1.529	Enzyme	Cytoplasm
G3V5D9	APEX1	APEX nuclease (multifunctional DNA repair enzyme) 1	-1.533	Enzyme	Nucleus
B4DTQ6	UNC13D	Unc-13 homolog D (*C. elegans*)	-1.540	Other	Cytoplasm
A8MVQ3	CARS	Cysteinyl-tRNA synthetase	-1.542	Enzyme	Cytoplasm
B4DDC7	SNRPA	Small nuclear ribonucleoprotein polypeptide A	-1.543	Other	Nucleus
F8WE76	PTCD3	Pentatricopeptide repeat domain 3	-1.544	Other	Cytoplasm
Q5QPE2	SEC23B	Sec23 homolog B (*S. cerevisiae*)	-1.554	Transporter	Extracellular space
B3KY56	ESYT1	Extended synaptotagmin-like protein 1	-1.556	Other	Cytoplasm
B8ZZ75	GALM	Galactose mutarotase (aldose 1-epimerase)	-1.558	Enzyme	Cytoplasm
E9PPU0	EPPK1	Epiplakin 1	-1.569	Other	Cytoplasm
B8ZZN6	SUMO1	Small ubiquitin-like modifier 1	-1.574	Enzyme	Nucleus
F8WDU6	XPOT	Exportin, tRNA	-1.585	Other	Nucleus
B4E0Y9	STK26	Serine/threonine protein kinase 26	-1.597	Kinase	Nucleus
E9PPD9	EPB41L2	Erythrocyte membrane protein band 4.1-like 2	-1.602	Other	Plasma membrane
B4DT43	ETFA	Electron-transfer-flavoprotein, α polypeptide	-1.606	Transporter	Cytoplasm
E9PPN1	TSEN15	TSEN15 tRNA splicing endonuclease subunit	-1.612	Enzyme	Nucleus
E7EVD1	PRPF3	Pre-mRNA processing factor 3	-1.625	Other	Nucleus
B7Z525	HDGF	Hepatoma-derived growth factor	-1.628	Growth factor	Extracellular space

B4DJE7	ACADM	Acyl-CoA dehydrogenase, C-4 to C-12 straight chain	-1.635	Enzyme	Cytoplasm
B4E358	CTTN	Cortactin	-1.666	Other	Plasma membrane
F5H6P0	TGM2	Transglutaminase 2	-1.670	Enzyme	Cytoplasm
C9JWI7	TACC3	Transforming, acidic coiled-coil containing protein 3	-1.682	Other	Nucleus
Q5QPH3	ACSS2	Acyl-CoA synthetase short-chain family member 2	-1.689	Enzyme	Cytoplasm
C9JZI1	RFC4	Replication factor C (activator 1) 4, 37 kDa	-1.693	Other	Nucleus
C9JH19	CTSD	Cathepsin D	-1.696	Peptidase	Cytoplasm
G3V1N2	HBA1/HBA2	Hemoglobin, α1	-1.696	Transporter	Extracellular space
A8MTM1	CBR1	Carbonyl reductase 1	-1.707	Enzyme	Cytoplasm
E9PCR7	OGDH	Oxoglutarate (α-ketoglutarate) dehydrogenase (lipoamide)	-1.733	Enzyme	Cytoplasm
F8WEA9	KSR1	Kinase suppressor of ras 1	-1.739	Kinase	Cytoplasm
E9PP73	COPB1	Coatomer protein complex, subunit β 1	-1.794	Transporter	Cytoplasm
D3YLG5	BSG	Basigin (Ok blood group)	-1.797	Transporter	Plasma membrane
Q5TD05	NQO2	NAD(P)H dehydrogenase, quinone 2	-1.797	Enzyme	Cytoplasm
Q9P0H9	RER1	Retention in endoplasmic reticulum sorting receptor 1	-1.808	Other	Cytoplasm
B7Z4S1	TCEA1	Transcription elongation factor A (SII), 1	-1.809	Transcription regulator	Nucleus
E9PF49	NDUFB9	NADH dehydrogenase (ubiquinone) 1 β subcomplex, 9, 22 kDa	-1.841	Enzyme	Cytoplasm
C9JJP5	TFG	TRK-fused gene	-1.843	Other	Cytoplasm
D6REQ8	HEXB	Hexosaminidase B (β polypeptide)	-1.855	Enzyme	Cytoplasm
E9PEJ4	DLAT	Dihydrolipoamide S-acetyltransferase	-1.861	Enzyme	Cytoplasm
D6RBL5	ANXA5	Annexin A5	-1.872	Other	Plasma membrane
E2QRB3	PYCR1	Pyrroline-5-carboxylate reductase 1	-1.874	Enzyme	Cytoplasm
D3DRA3	GSTO1	Glutathione S-transferase ω 1	-1.903	Enzyme	Cytoplasm
A2AB09	FLOT1	Flotillin 1	-1.932	Other	Plasma membrane
E9PEW9	EPB41	Erythrocyte membrane protein band 4.1	-1.939	Other	Plasma membrane
B7Z2C3	PPM1F	Protein phosphatase, Mg^{2+}/Mn^{2+} dependent, 1F	-1.986	Phosphatase	Cytoplasm
D6RDU5	SEPT11	Septin 11	-2.045	Other	Nucleus
B4E2Y9	CALR	Calreticulin	-2.086	Transcription regulator	Cytoplasm
A6PVS0	CLIC2	Chloride intracellular channel 2	-2.096	Ion channel	Cytoplasm
A8MV58	DBN1	Drebrin 1	-2.106	Other	Cytoplasm
E9PF86	PGM3	Phosphoglucomutase 3	-2.131	Enzyme	Cytoplasm
E9PDV0	CTH	Cystathionine γ-lyase	-2.179	Enzyme	Cytoplasm
B4DHX5	FDXR	Ferredoxin reductase	-2.189	Enzyme	Cytoplasm
E7ETR5	ACSM3	Acyl-CoA synthetase medium-chain family member 3	-2.190	Enzyme	Cytoplasm
A6NC19	PRDX5	Peroxiredoxin 5	-2.217	Enzyme	Cytoplasm
B3KUF8	VAT1	Vesicle amine transport 1	-2.255	Transporter	Plasma membrane
E7EWR4	CSTF2	Cleavage stimulation factor, 3' pre-RNA, subunit 2, 64 kDa	-2.344	Other	Nucleus
B4DEF7	HSPA5	Heat shock 70 kDa protein 5 (glucose-regulated protein, 78 kDa)	-2.390	Enzyme	Cytoplasm
F8W914	RTN4	Reticulon 4	-2.432	Other	Cytoplasm
B7Z7L3	CYB5R3	Cytochrome b5 reductase 3	-2.494	Enzyme	Cytoplasm
C9J8T6	COX17	COX17 cytochrome c oxidase copper chaperone	-2.506	Enzyme	Cytoplasm
B7Z3I2	EML2	Echinoderm microtubule associated protein like 2	-2.531	Other	Cytoplasm

D6RBW1	EIF4E	Eukaryotic translation initiation factor 4E	-2.599	Translation regulator	Cytoplasm
E9PHK9	TCOF1	Treacher Collins-Franceschetti syndrome 1	-2.735	Transporter	Nucleus
A6NJG9	PSME1	Proteasome (prosome, macropain) activator subunit 1 (PA28 α)	-2.759	Other	Cytoplasm
F8W930	IGF2BP2	Insulin-like growth factor 2 mRNA binding protein 2	-3.261	Translation regulator	Cytoplasm

Table S4. The networks of potential molecular targets regulated by ALS in k562 cells

ID	Molecules in network	Score	Focus molecules	Top diseases and functions
1	ANP32E, APEH, BROX, BUD31, C7orf55, CARS, CISD2, CYB5R3, DDX19A, DENR, EIF3CL, EML2, FAM136A, FAM49B, FAM98B, GTSF1, HBS1L, HN1L, ITPA, MRPL21, NAPRT, NMT1, NNT, PSMG4, RNASEH2C, SEPT2, SEPT5, SEPT7, SEPT11, Septin, TMEM189, TSEN15, UBC, UROD, XPNPEP1	59	34	Cell morphology, cellular compromise, hereditary disorder
2	APEX1, Basc, BUB3, CHCHD3, CLTA, CSTF2, DDX1, DNAJC11, EIF3D, EIF3L, HDGF, HMGN1, HNRNPL, ILF3, IMMT, KIF2C, MRPS27, MSH6, NACA, NDRG2, NOP2, RAD50, RAE1, RER1, RFC2, RFC4, Rnr, RPS2, Secretase γ, SRP68, TACC3, TARDBP, TCOF1, Vegf, XRCC6	51	31	Cell morphology, cellular function and maintenance, DNA replication, recombination, and repair
3	60S ribosomal subunit, AP-3, CALB1, CNBP, DDOST, DPP3, Fascin, GSR, IGF2BP1, IGF2BP2, LUC7L3, LYAR, NAT10, NFkB (complex), OTUB1, PHF6, PUF60, RPL4, RPL7, RPL9, RPL13, RPL15, RPL17, RPL28, RPL29, RPL31, RPL32, RPL13A, RPL23A, RPL27A, RPL7A, SRSF11, TROVE2, UBE2, ZC3H18	48	30	Hematological disease, organismal injury and abnormalities, gene expression
4	ACTR1A, AHCY, ATAD3A, ATIC, CACYBP, Calcineurin A, CALM1 (includes others), CAPZA2, CBR1, CLNS1A, Cytoplasmic Dynein, DCTN2, DYNC1I2, Dynein, DYNLRB1, EPB41, EPB41L2, FKBP5, FKBP1A, GART, Lamin b, LUC7L, MPP1, NUMA1, PAICS, peptidylprolyl isomerase, Pkc(s), PPIA, PTGES3, RTN4, SARS, STIP1, TPD52L2, TRMT112, YWHAQ	46	29	Amino acid metabolism, small molecule biochemistry, vitamin and mineral metabolism
5	2-ketoglutarate dehydrogenase, α-actin, ATPase, DLD, DLST, EMD, HNRNPD, HNRNPF, HNRNPH1, HNRNPH3, HNRNPK, HNRNPU, Immunoproteasome Pa28/20 s, MYH10, NAP1L1, NARS, NHP2L1, OGDH, P38 MAPK, PABPC1, PSMA6, PSMC1, PSMC3, PSMD4, PSME1, PSME3, PTCD3, RAD23B, RBMX, RNH1, RPN1, RRP12, SAFB, TPM3, Tropomyosin	46	29	RNA post-transcriptional modification, infectious disease, nucleic acid metabolism
6	ALYREF, CD3, CDC42, COX7A2, CSNK2B, DDX39A, DDX3Y, DLAT, EEF1G, FLNA, G protein βγ, GSTO1, HEXB, HSD17B4, LMNA, LMNB1, NADPH oxidase, NASP, NCL, p70 S6k, p85 (pik3r), PDGF BB, Rac, RPLP0, RPS6, RPS8, RPS13, RPS14, RPS16, RPS21, SARNP, SFXN1, SLC25A1, SSB, SUMO1	43	28	Cell morphology, cell cycle, skeletal and muscular system development and function
7	ACO2, ACP1, ACTA2, C11 or f58, DBI, DDB1, Fibrin, FLOT1, Focal adhesion kinase, Gcn5l, GPI, HNRNPC, KRT8, KRT18, Lh, LSM1, mediator, Mlc, NONO, NSFL1C, PRPF3, PTBP1, RBM17, SART3, SF3A1, SF3B2, SMARCB1, SMARCC2, snRNP, SNRPA, Sod, STRAP, SUMO3, UBXN1, USP15	41	27	RNA post-transcriptional modification, cell morphology, cellular assembly and organization
8	AHSA1, AIMP1, AIMP2, ARHGDIA, ARHGEF, atypical protein kinase C, CAPRIN1, DARS, EEF1E1, ERK1/2, Erm, EZR, FUBP1, GAPVD1, GC-GCR dimer, GDI1, GDI2, GORASP2, GSN, LARS, MARS, NQO2, Pak, Rab5, RAB7, RAB2A, RAB5C, RAB6A, RAB7A, RDX, Rho gdi, TRMT2A, VAT1, VPS29, VPS26A	39	26	Cellular assembly and organization, cell signaling, post-translational modification
9	19S proteasome, 20 s proteasome, CD59, COX17, CTSD, DUB, Ephb, EPPK1, FDXR, H2AFV, HBA1/HBA2, HBE1, HBG2, hemoglobin, HSPE1, KIAA0368, MAPK1, MDH2, PRDX2, Proteasome PA700/20 s, PSAP, PSMA1, PSMA4, PSMA5, PSMC, PSMC2, PSMD, PSMD2, PSMD3, PSMD6, PSMD10, tubulin (family), UCHL5, USP14, USP19	39	26	Connective tissue disorders, hematological disease, organismal injury and abnormalities
10	ACADM, adenosine-tetraphosphatase, Akt, α-tubulin, ATP synthase, ATP5A1, ATP5J, β-tubulin, CLINT1, Cytochrome bc1, cytochrome C, cytochrome-c oxidase, ELOVL5, ETFA, GAPDH, GOT2, GSS, Mitochondrial complex 1, NADH dehydrogenase, NDUFA10, NDUFB9, NDUFB10, NDUFS8, NDUFV1, NDUFV2, PFDN4, PFDN5, PHB, TBCA, TFAM, UQCRB, Vdac, VDAC1, VDAC2, VDAC3	34	24	Developmental disorder, hereditary disorder, metabolic disease
11	ACLY, ACSS2, ALDH1A2, API5, BPNT1, chymotrypsin, CTH, ERK, ERP29, GOT, GOT1, Histone H1, Importin α/β, Importin β, KPNB1, MST4, NUP153, PDCD10, PEBP1, Pias, Ppp2c, RAN, RANBP1, RANGAP1, RPS6KA, Rsk, SERPINB1, SLC2A1, Srebp, TNPO1, TNPO3, Transportin, XPO5, XPO7, XPOT	32	23	Molecular transport, RNA trafficking, protein trafficking
12	ARCN1, Cbp/p300, CBS/LOC102724560, CCT7, COP I, COPB1, COPZ1, Hat, histone deacetylase, Holo RNA polymerase II, Jnk, N-cor, NFAT (complex), NUP93, POLR2H, PRPF19, PSMA, PSMC5, Rar, Rxr, SACM1L, SEC23B, SEC24C, SLIRP, SNRNP40, SNRPA1, SNW1, SRRM1, SSBP1, TCEA1, TCEB2, TFIIH, thymidine kinase, thyroid hormone receptor, TMED10	28	21	Infectious disease, cell death and survival, carbohydrate metabolism
13	ACTB, ACTR2, Arf, ARHGEF2, Arp2/3, CAP1, CCT2, CCT4, CCT5, CCT8, CCT6A, CFL1, Cofilin, CORO1B, Cytokeratin, Eif2, EIF2A, EIF2B4, G-Actin, Gef, GTPase, KSR1, MTCH2, NCK, NWASP, OXSR1, PI3K (complex), PP1-C, PPP2CB, Profilin, Ribosomal 40s subunit, STMN1, TCP1, TUBB3, TUBB6	28	21	Cell death and survival, cellular assembly and organization, cellular compromise

14	ACOT1, ACOT13, CEP78, CLIC2, DDX60, ESYT1, ESYT2, EXOSC1, GANAB, GANC, GPX8, LTA4H, MGAM, NAP1L2, NAP1L4, PGM2, PGM3, PYCR1, PYCRL, RPS21, RPS24, RPS4Y2, SEC11C, SHMT2, SPCS1, SPCS2, SPCS3, SSR3, TALDO1, TEFM, TKT, TTLL4, UBC, ZCCHC8, ZNF143	22	18	Carbohydrate metabolism, nucleic acid metabolism, small molecule biochemistry
15	Actin, ACTN1, α-actinin, α-catenin, ARF3, ARPC4, calpain, CKB, CSRP1, CTTN, DBN1, DHCR7, DIAPH1, Eif4g, F Actin, Fibrinogen, Growth hormone, IgG, Integrin, Laminin, Laminin1, Ldh (complex), LDHB, PDCD6IP, Pde, PGK1, Pka, Pld, Rap1, RAP1B, STXBP2, TARS, TLN1, TSH, VAMP2	21	17	Cardiovascular system development and function, cell morphology, cell-to-cell signaling and interaction
16	Adaptor protein 2, ADCY, ADRB, AP2M1, CAPZB, Ck2, Clathrin, CORO1C, Creb, DDX6, DNAJA3, Dynamin, Gsk3, HMGB2, HSP, Hsp27, Hsp70, Hsp90, HSPA8, NPM1, NUDT5, PCMT1, PCYT2, phosphatase, PIP4K2A, PP1 protein complex group, PP2A, PPM1F, Proinsulin, Rock, RUVBL2, SUGT1, TFRC, tyrosine kinase, UNC13D	21	17	Molecular transport, cellular function and maintenance, post-translational modification
17	26 s Proteasome, Ap1, ARHGEF1, CDK1, Collagen type I, Collagen(s), Cyclin B, DDX5, GSTP1, HDAC1, HISTONE, Histone h3, Histone h4, IFN β, Igm, IL12 (complex), Immunoglobulin, LDL, Nos, NuRD, Pdgfr, PHB2, PRDX5, PRMT5, Ras homolog, RBBP7, RNA polymerase II, RUVBL1, SERPINH1, SRI, STAT5a/b, TGF-β, TGM2, UBE2I, VIM	17	15	Gene expression, DNA replication, recombination, and repair, energy production
18	ABCE1, AChR, aldo, ALDOC, ASNS, BCR (complex), Cdc2, Collagen type IV, Cyclin A, Cyclin D, Cyclin E, E2f, EIF3, EIF3B, EIF3F, EIF3J, EIF4A, EIF4E, EIF4F, EIF4G1, GTF2I, Mapk, MCM7, Mek, MTHFD1, Pdgf (complex), PDGF-AA, PELP1, Pkg, PLCγ, Rb, Smad, SNX9, Sos, VAV	14	13	Gene expression, protein synthesis, cell cycle
19	14-3-3, ANXA1, ANXA5, BSG, Calcineurin protein(s), CALR, CaMKII, CANX, caspase, Cd1, CELF1, CK1, EIF4B, ENaC, FARSA, HNRNPR, Ifn γ, ITPR, Lamin, MAP2K1/2, MATR3, MHC Class I (complex), MTORC2, Nfat (family), NFkB (family), P4HB, PDGF (family), PFKP, Raf, Ras, Sapk, Tap, TCR, trypsin, WNK1	14	13	Developmental disorder, hereditary disorder, skeletal and muscular disorders
20	AMPK, ATP5B, BCAT1, Calmodulin, Cg, estrogen receptor, Fgf, FSH, G-protein β, GNB2, GNB2L1, GNRH, HSP90AA1, HSPA5, Ifn, Ige, Ikb, IKK (complex), IL1, Insulin, Interferon α, MDH1, Mmp, PARP, PDCD6, PLC, Pro-inflammatory Cytokine, Shc, SRC (family), TFG, tubulin (complex), UBE2L3, Ubiquitin, voltage-gated calcium channel, YWHAG	11	11	Nucleic acid metabolism, small molecule biochemistry, hereditary disorder
21	ACSM3, ACTR1B, ADRB2, ATP13A3, β-arrestin, CAPN15, EMR2, FAM127C, FASTKD1, FCRLB, GALM, GIN1, GMPR2, GPR107, GPR115, GPR155, GPR89A/GPR89B, HADHB, IgG1, MTORC1, NFKB2, NIPA2, OARD1, Olfr1508, RPS10, RPS20, RPS4Y2, SLC13A3, SLC26A11, SLC2A6, SLC35A5, TGFB1, TM9SF3, TMEM184B, UBC	5	6	Cardiovascular disease, gastrointestinal disease, hepatic system disease
22	PAGE5, POT1	1	1	Cellular assembly and organization, DNA replication, recombination, and repair, cell cycle

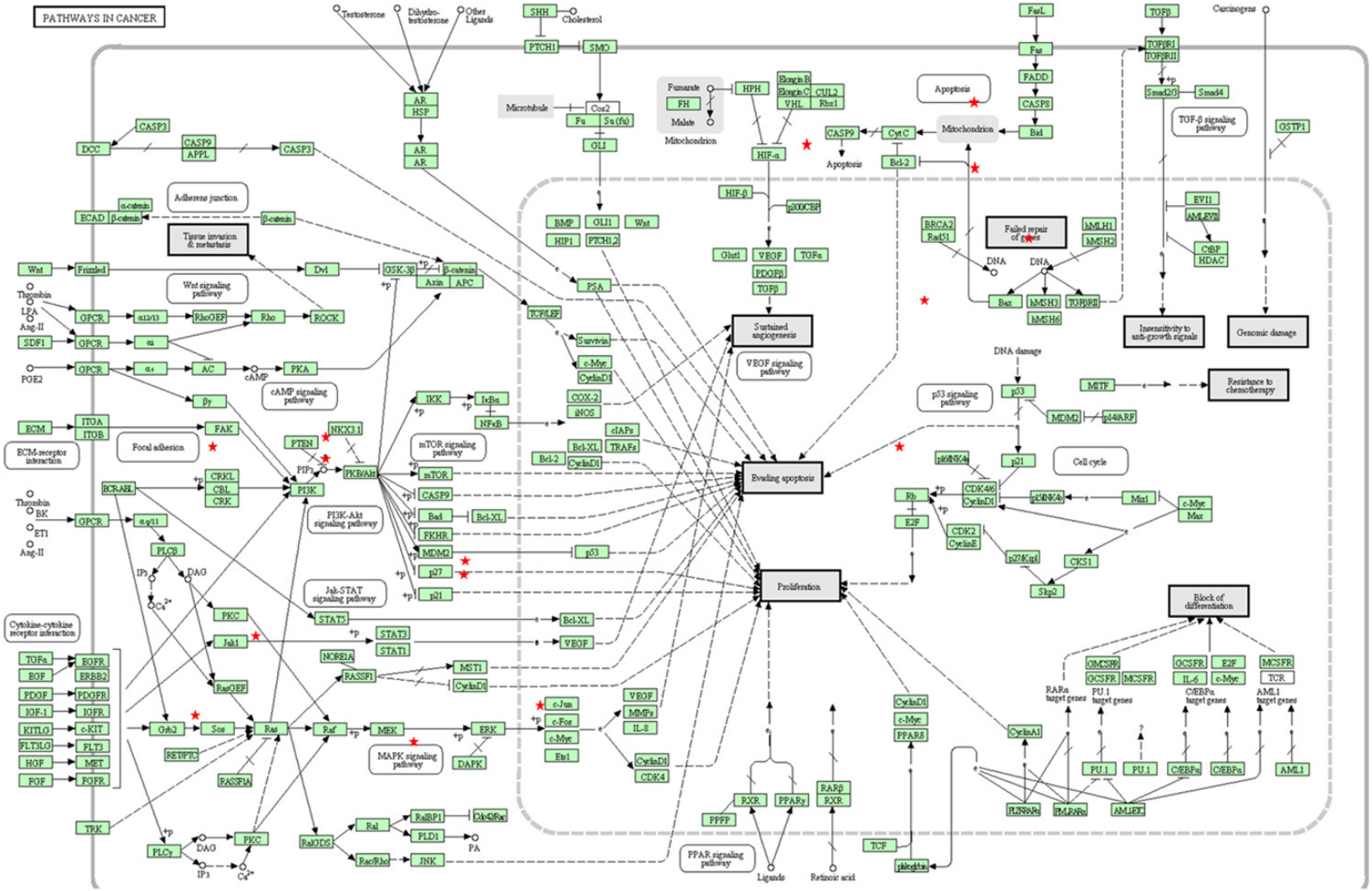

Figure S1. Pathways responding to ALS incubation in K562 cells analyzed by DAVID. K562 cells were treated with 1 μM ALS for 24 h and analyzed following the SILAC-based proteomic approach. The proteins was identified and subject to DAVID analysis. The KEGG pathways was selected to evaluate the signaling pathways responding to ALS treatment.

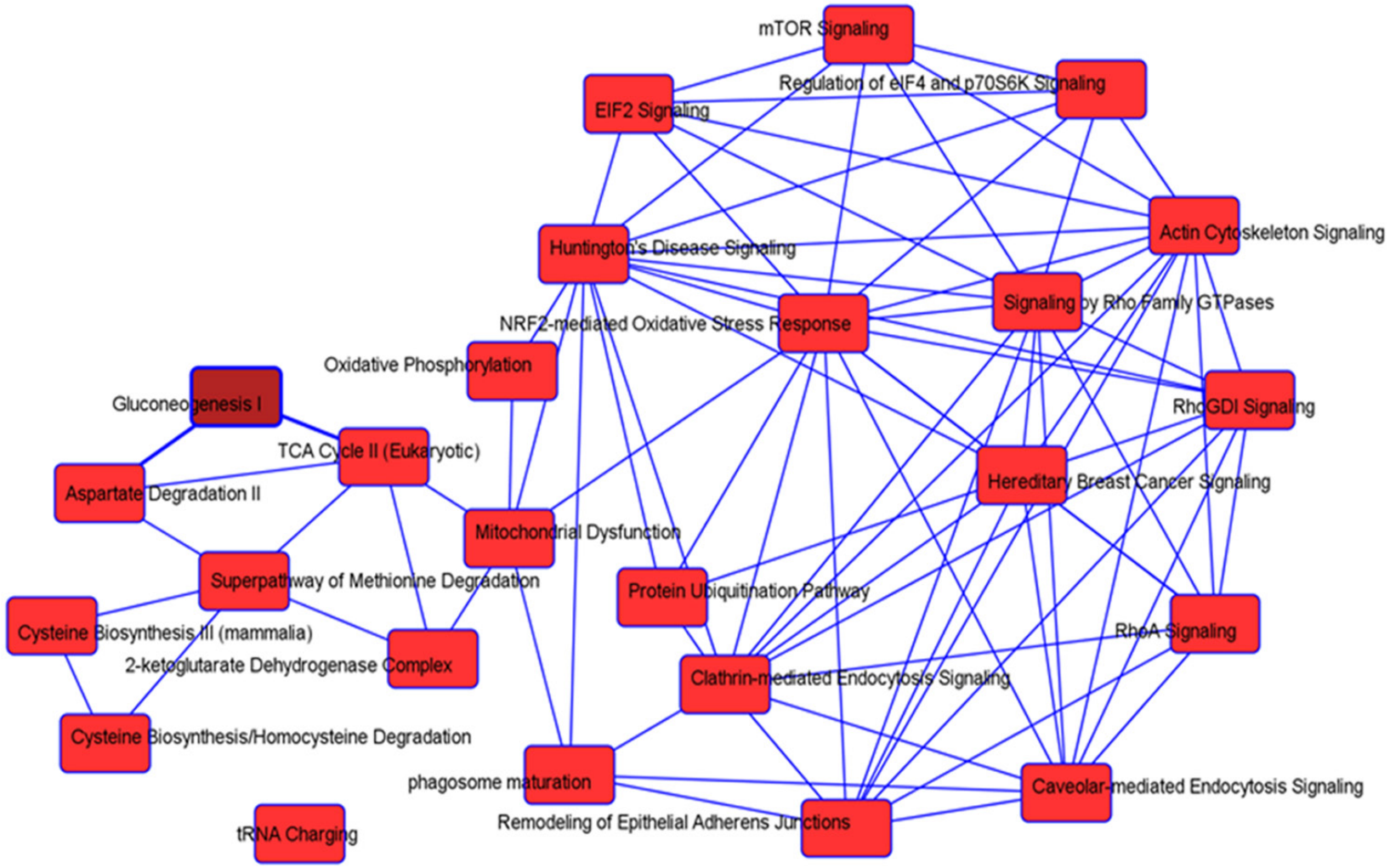

Figure S2. Network of signaling pathway analyzed by IPA. K562 cells were treated with 1 μM ALS for 24 h and analyzed following the SILAC-based proteomic approach. The proteins was identified and subject to IPA analysis.

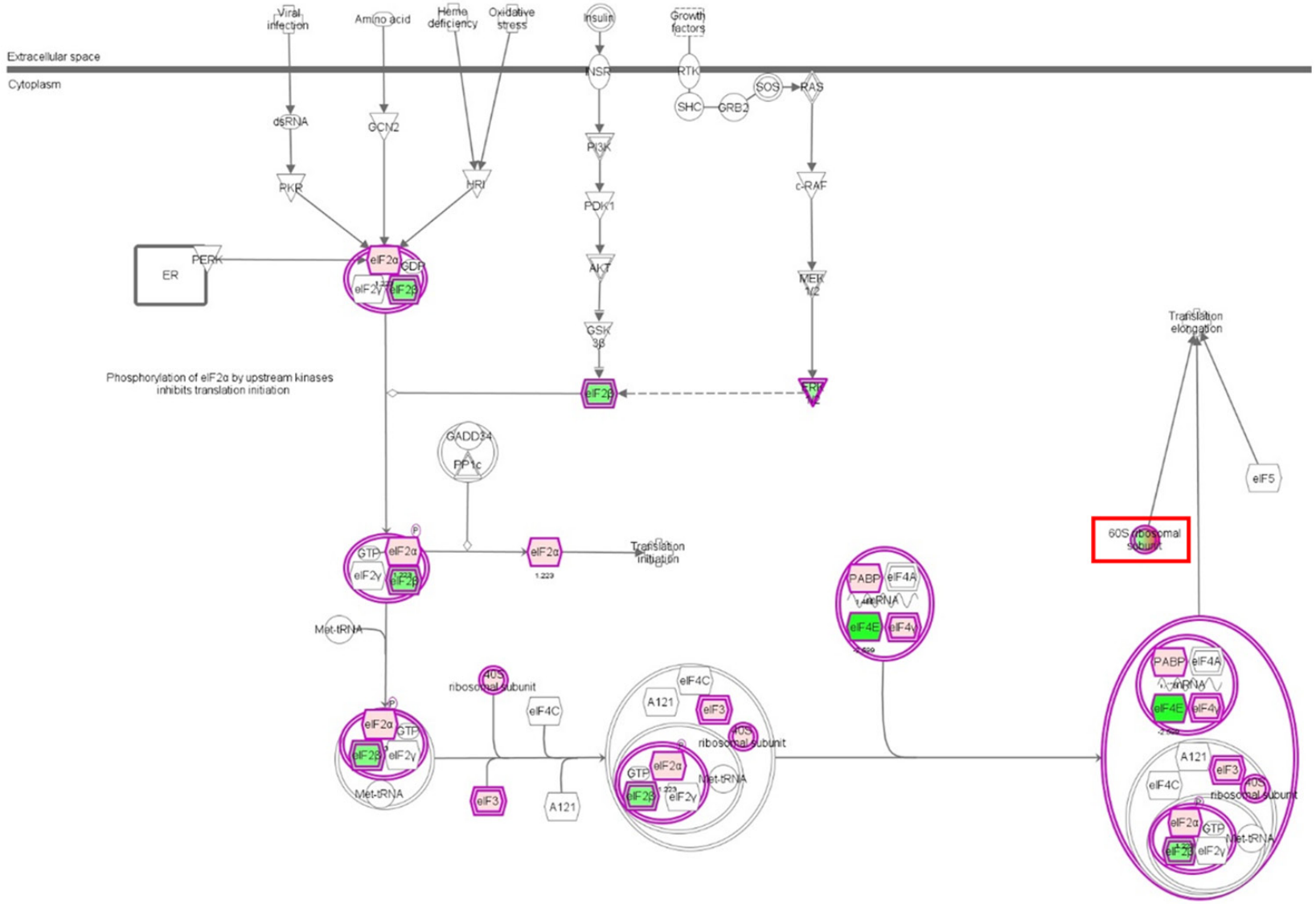

Figure S3. EIF2 signaling pathway was regulated by ALS in K562 cells. K562 cells were treated with 1 μM ALS for 24 h and analyzed following the SILAC-based proteomic approach. The proteins was identified and subject to IPA analysis. Red indicates an up-regulation and green indicates a down-regulation. The intensity of green and red molecule colors indicates the degree of down or up-regulation, respectively. Solid arrow indicates direct interaction and dashed arrow indicates indirect interaction.

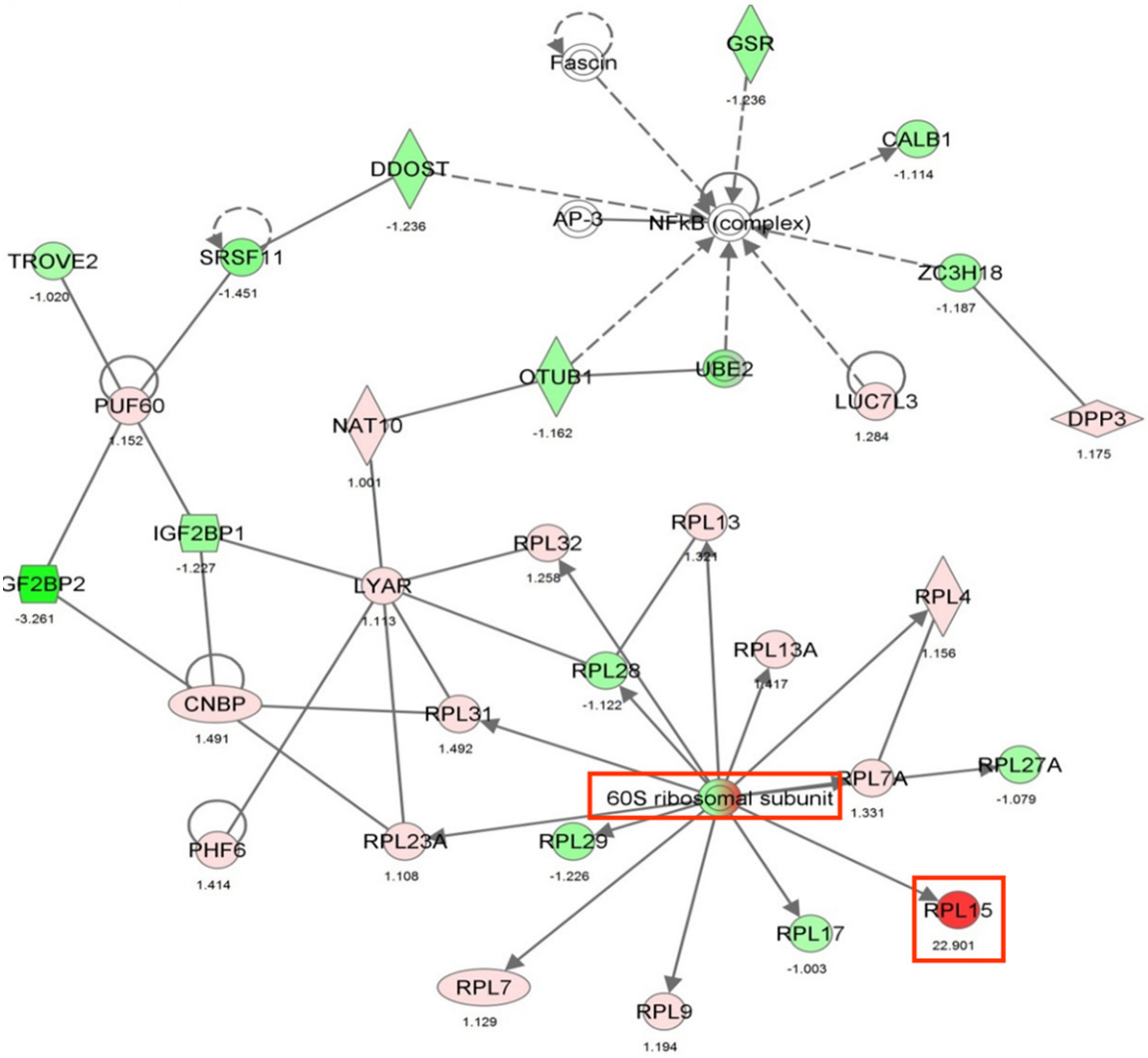

Figure S4. ALS regulates a network of NF-κB and ribosome in K562 cells. K562 cells were treated with 1 μM ALS for 24 h and analyzed following the SILAC-based proteomic approach. The proteins was identified and subject to IPA analysis. Red indicates an up-regulation and green indicates a down-regulation. The intensity of green and red molecule colors indicates the degree of down or up-regulation, respectively. Solid arrow indicates direct interaction and dashed arrow indicates indirect interaction.

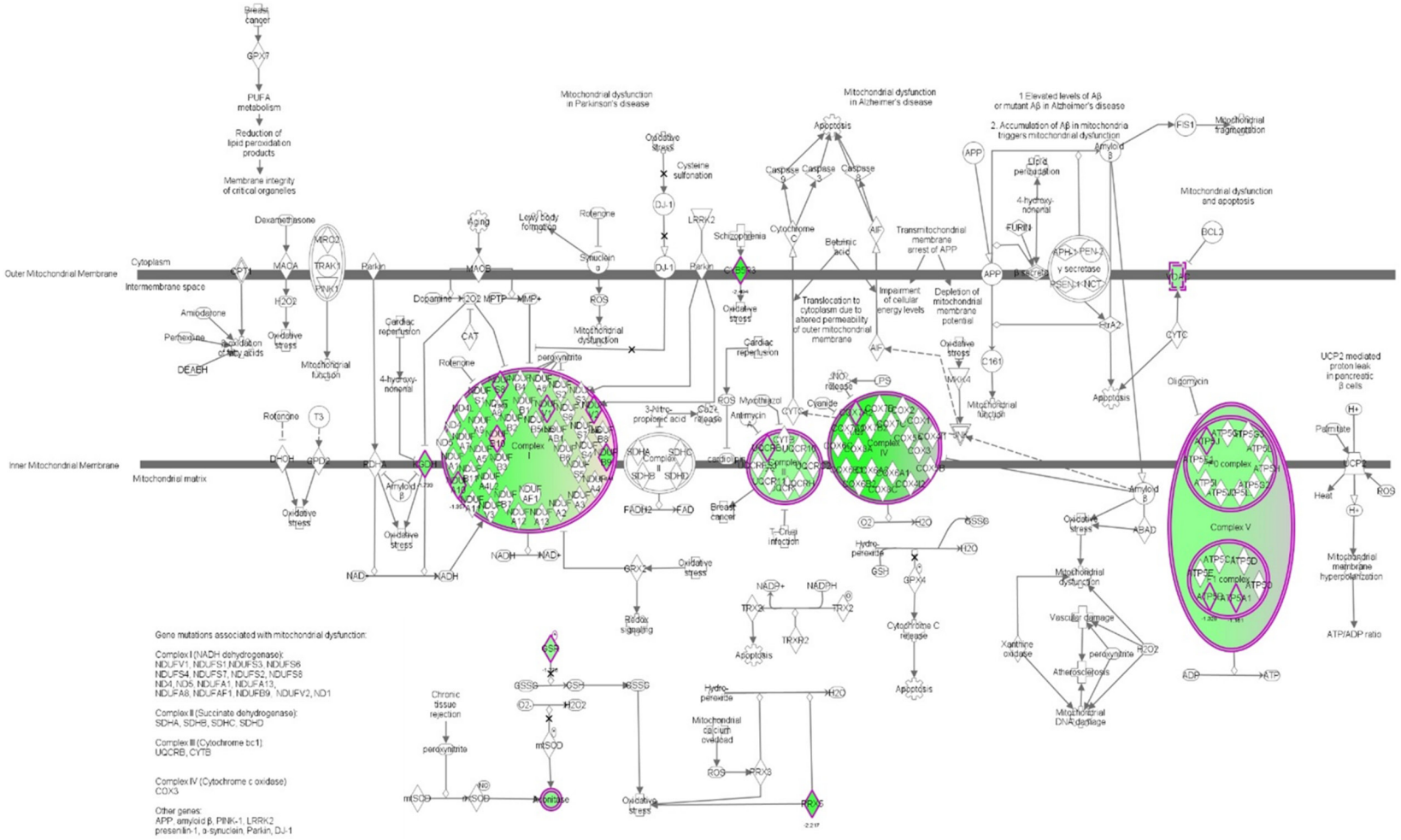

Figure S5. ALS regulates mitochondria function in K562 cells. K562 cells were treated with 1 μM ALS for 24 h and analyzed following the SILAC-based proteomic approach. The proteins was identified and subject to IPA analysis. Red indicates an up-regulation and green indicates a down-regulation. The intensity of green and red molecule colors indicates the degree of down or up-regulation, respectively. Solid arrow indicates direct interaction and dashed arrow indicates indirect interaction.

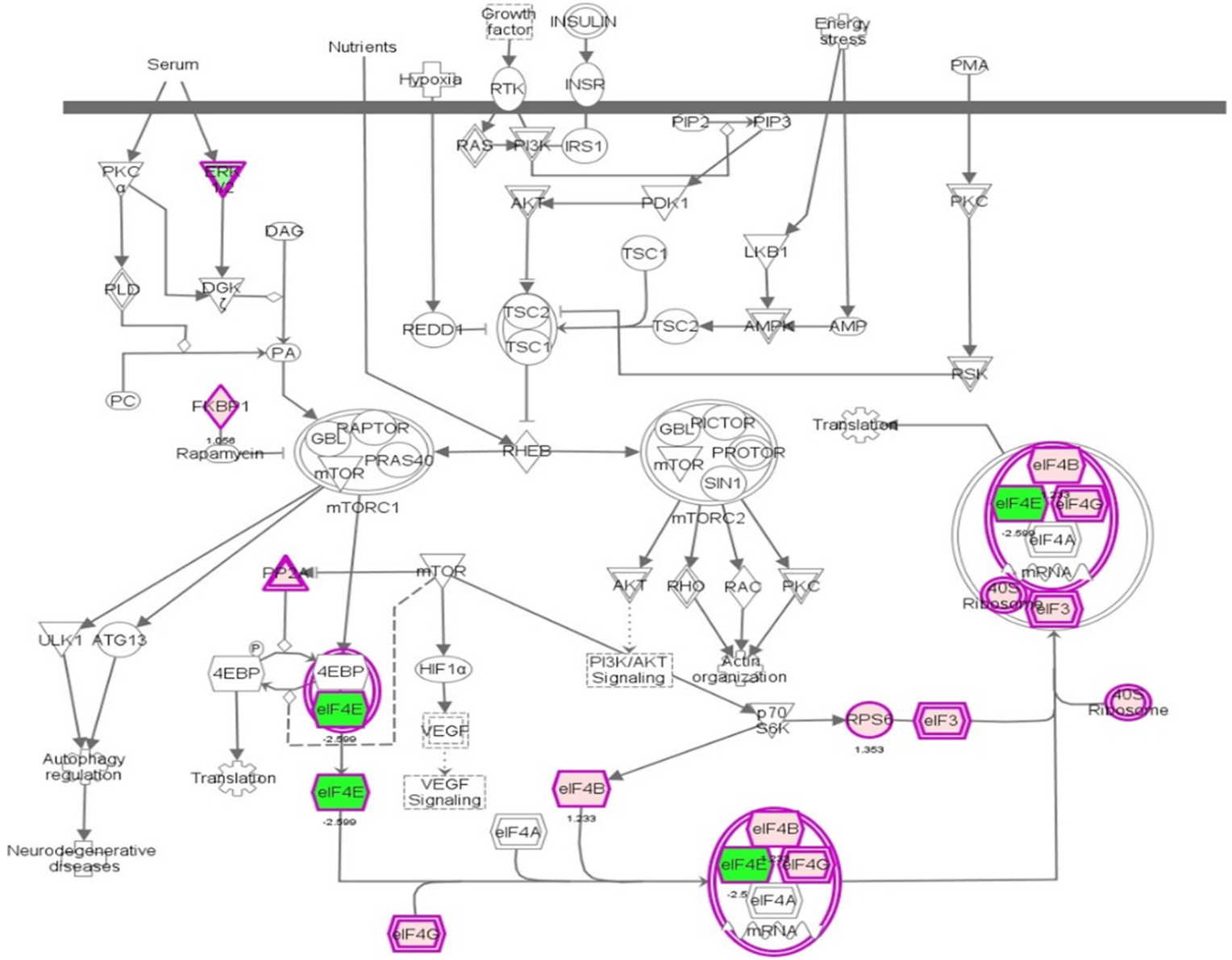

Figure S6. ALS regulates mTOR signaling pathway in K562 cells. K562 cells were treated with 1 μM ALS for 24 h and analyzed following the SILAC-based proteomic approach. The proteins was identified and subject to IPA analysis. Red indicates an up-regulation and green indicates a down-regulation. The intensity of green and red molecule colors indicates the degree of down or up-regulation, respectively. Solid arrow indicates direct interaction and dashed arrow indicates indirect interaction.

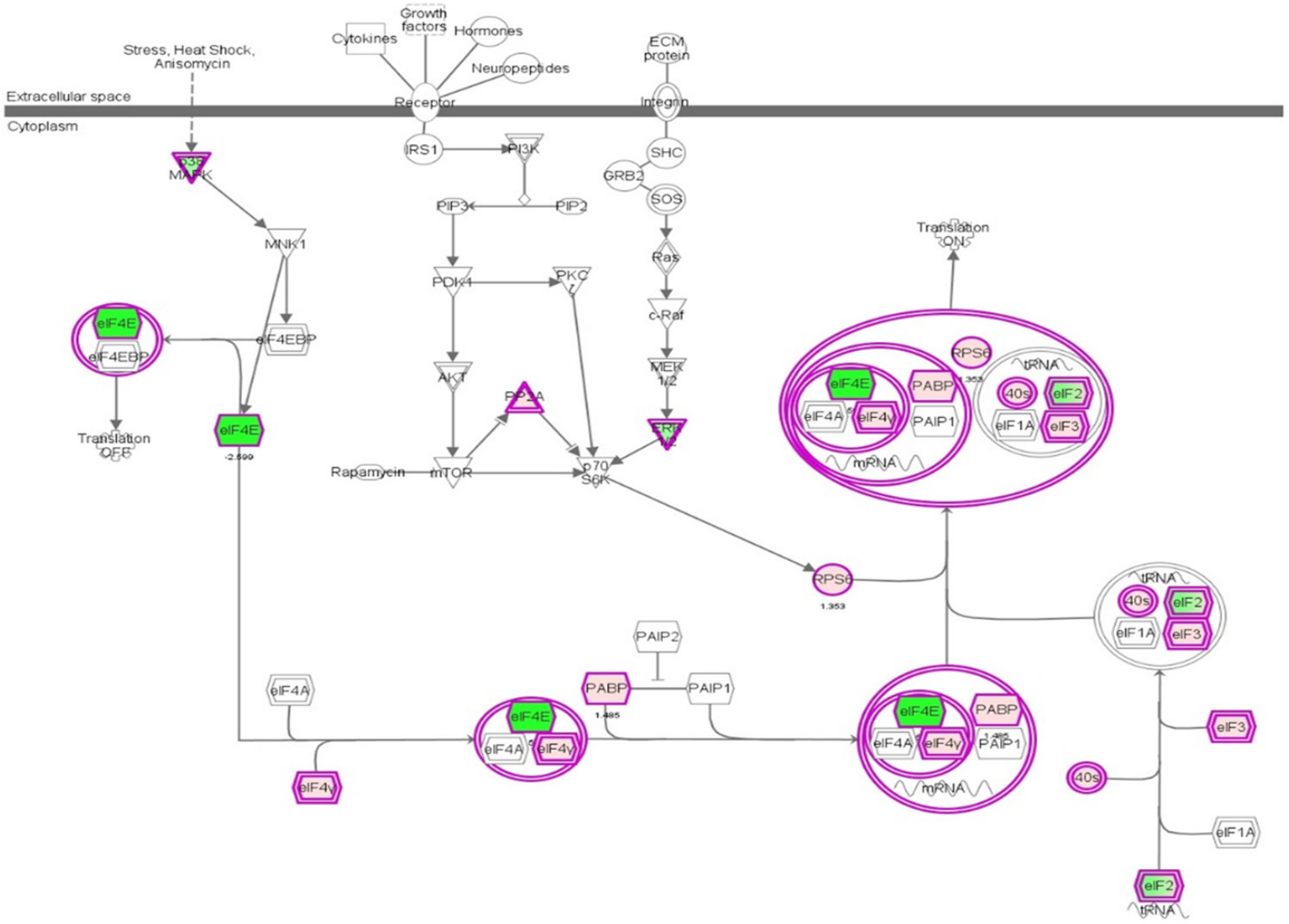

Figure S7. ALS regulates eIF4E and p70S6K signaling pathway in K562 cells. K562 cells were treated with 1 μM ALS for 24 h and analyzed following the SILAC-based proteomic approach. The proteins was identified and subject to IPA analysis. Red indicates an up-regulation and green indicates a down-regulation. The intensity of green and red molecule colors indicates the degree of down or up-regulation, respectively. Solid arrow indicates direct interaction and dashed arrow indicates indirect interaction.

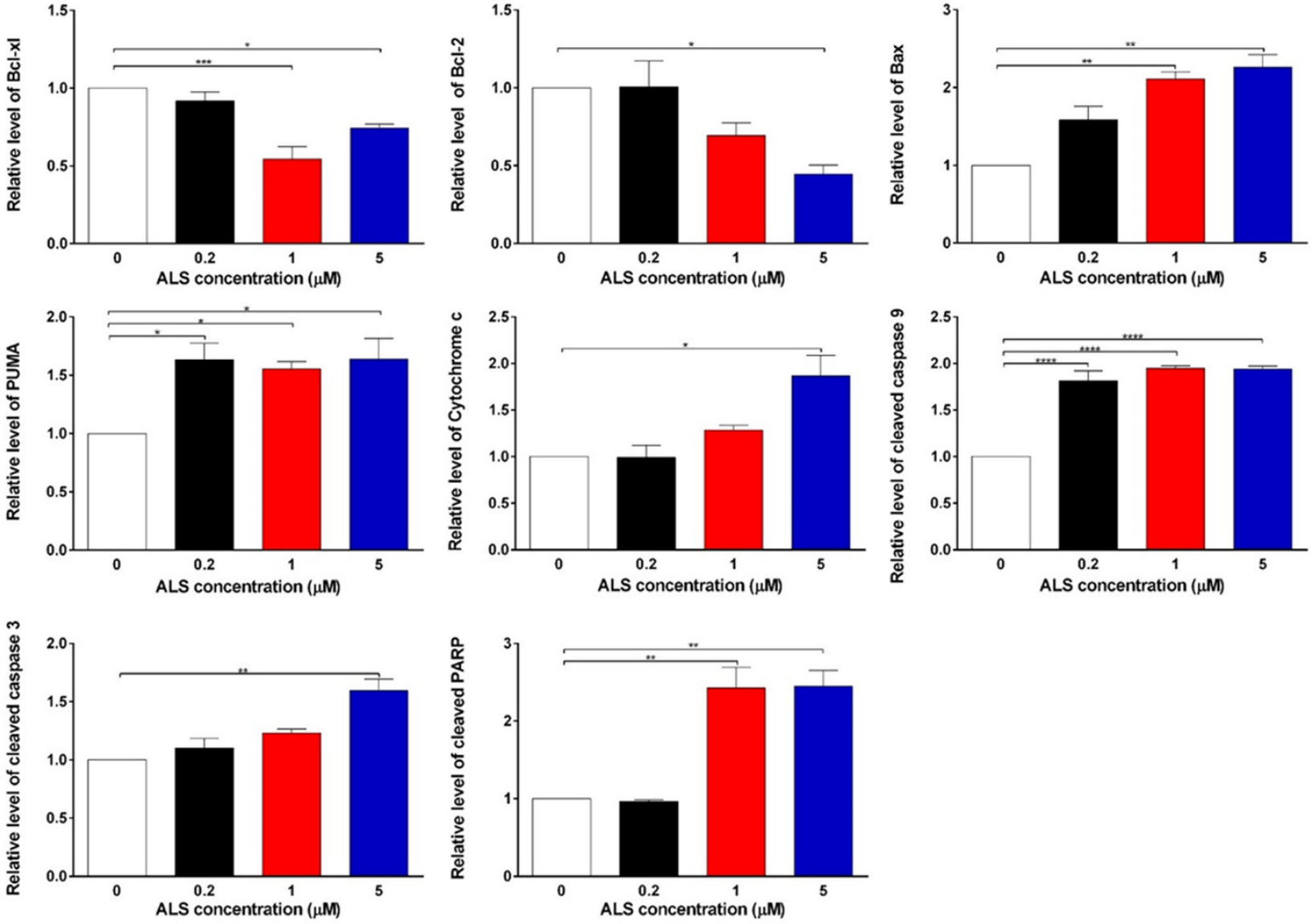

Figure S8. ALS alters the expression of pro-apoptotic and anti-apoptotic proteins in K562 cells. K562 cells were treated with ALS at 0.2, 1, and 5 μM for 24 h and the expression level of Bcl-xl, Bcl-2, Bax, PUMA, cytochrome c, cleaved caspase 9, cleaved caspase 3, and cleaved PARP was determined by Western blotting assay. Relative level of Bcl-xl, Bcl-2, Bax, PUMA, cytochrome c, cleaved caspase 9, cleaved caspase 3, and cleaved PARP. β-actin functions as the internal control. Data are expressed as mean ± SD of three independent experiments. *P<0.05; **P<0.01; ***P<0.001; and ****P<0.0001 by one-way ANOVA.

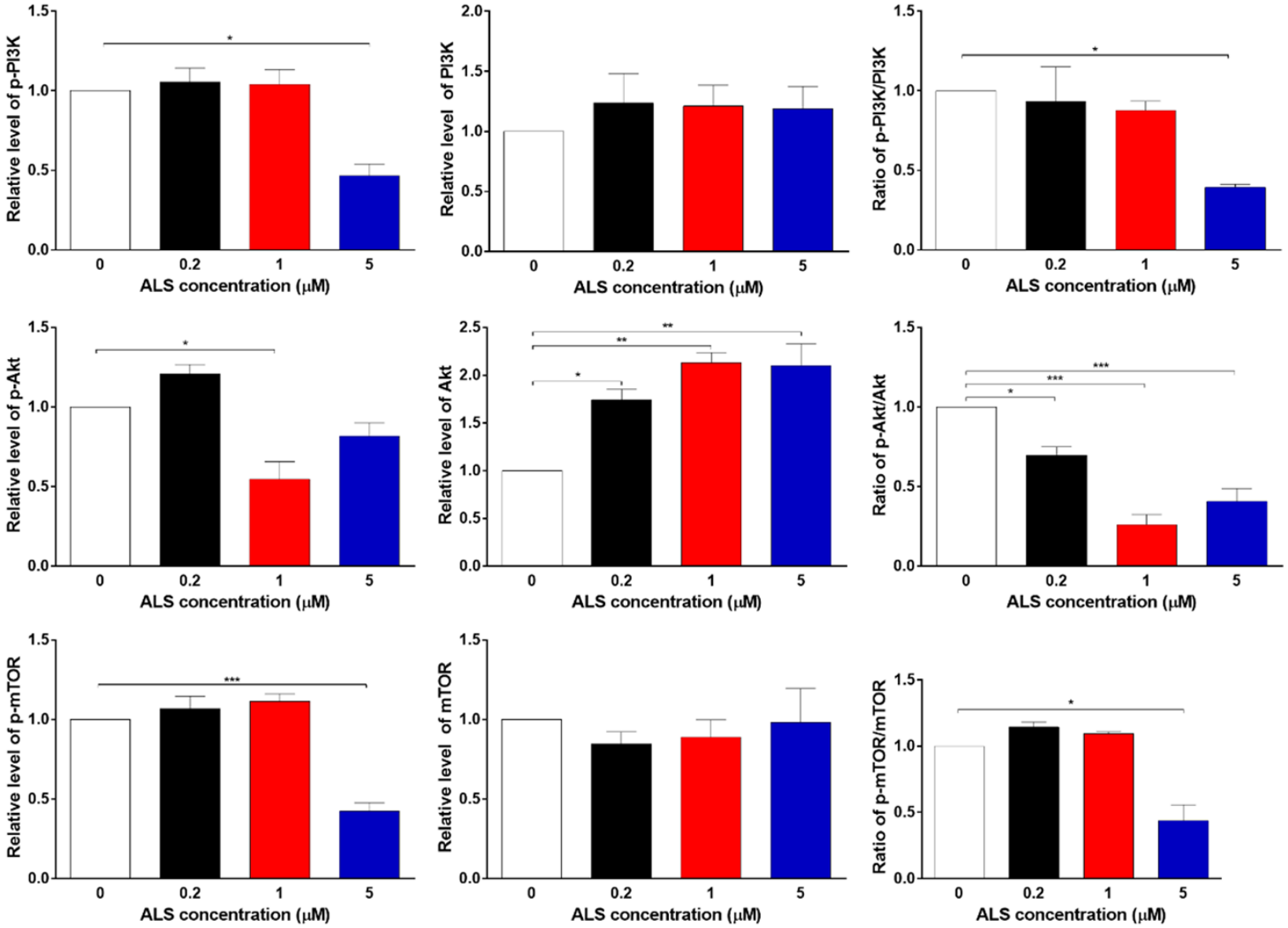

Figure S9. Relative level of p-PI3K, PI3K, p-Akt, Akt, p-mTOR, mTOR; and the ratio of p-PI3K/PI3K, p-Akt/Akt, and p-mTOR/mTOR. β-actin functions as the internal control. Data are expressed as mean ± SD of three independent experiments. **P*<0.05; ***P*<0.01; ****P*<0.001 by one-way ANOVA.

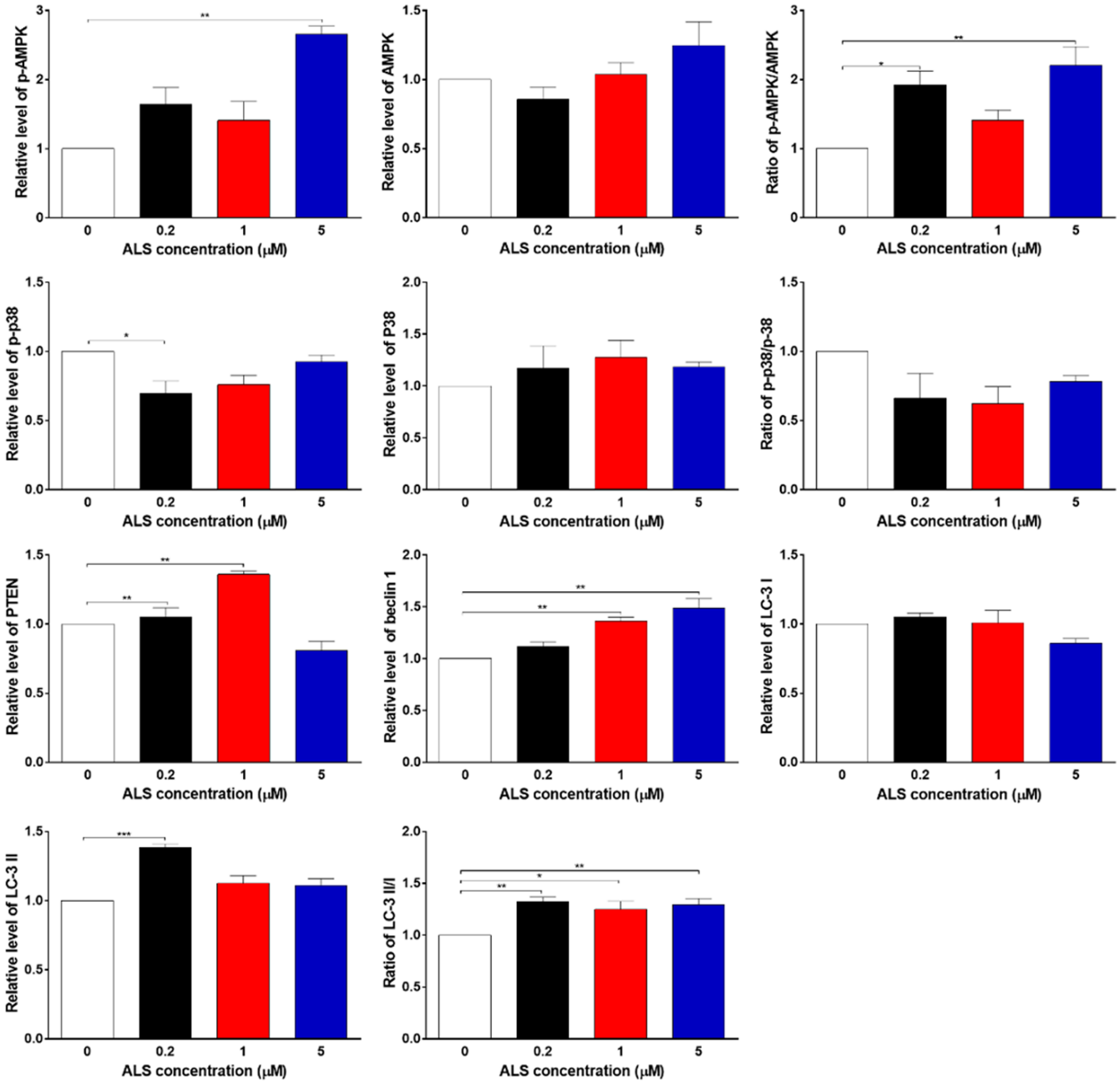

Figure S10 Relative level of p-AMPK, AMPK, p-p38 MAPK, p38 MAPK, PTEN, beclin 1, LC3-I, and LC3-II; and the ratio of p-AMPK/AMPK and p-p38 MAPK/p38 MAPK. β-actin functions as the internal control. Data are expressed as mean ± SD of three independent experiments. *P<0.05; **P< 0.01; and ***P<0.001 by one-way ANOVA.